AN ELECTROACOUSTIC ANALYSIS OF TRANSMISSION LINE LOUDSPEAKERS

A Dissertation
Presented to
The Academic Faculty

by

Robert Allen Robinson, Jr.

In Partial Fulfillment
of the Requirements for the Degree
Doctor of Philosophy in Electrical Engineering

School of Electrical and Computer Engineering
Georgia Institute of Technology
May 2007

AN ELECTROACOUSTIC ANALYSIS OF TRANSMISSION LINE LOUDSPEAKERS

Approved by:

Dr. W. Marshall Leach, Jr., Advisor
Professor, School of Electrical and Computer Engineering
Georgia Institute of Technology

Dr. Aaron D. Lanterman
Associate Professor, School of Electrical and Computer Engineering
Georgia Institute of Technology

Dr. W. Russell Callen, Jr.
Professor, School of Electrical and Computer Engineering
Georgia Institute of Technology

Dr. Glenn S. Smith
Professor, School of Electrical and Computer Engineering
Georgia Institute of Technology

Dr. Kenneth A. Cunefare
Professor, School of Mechanical Engineering
Georgia Institute of Technology

Date Approved: April 9, 2007

ACKNOWLEDGEMENTS

I must thank my advisor, Dr. Marshall Leach, for teaching me so much while I was an undergraduate and a graduate student. I am fortunate that he agreed to be my advisor. Without his help and encouragement, I could not have completed this dissertation.

In addition, I must thank Dr. Thomas Brewer for continuously urging me to complete this dissertation. He made sure that I knew of every approaching deadline and prodded me when he thought I was not making enough progress. I must also thank Dr. Russell Callen and Dr. Glenn Smith for serving on the reading committee and for helping me to improve this dissertation. My thanks also go to Dr. Aaron Lanterman and Dr. Kenneth Cunefare for serving on the oral defense committee. Also, I must thank Dr. John Dorsey, Dr. Whit Smith, and Dr. David Hertling for their advice and encouragement.

Finally, I must thank my parents, Robert A. and Elizabeth S. Robinson, and Miss Bing Liao for their patience and support.

TABLE OF CONTENTS

LIST OF TABLES

LIST OF FIGURES

LIST OF SYMBOLS

a_f radius of fibers (m)

α real part of γ $\left(\mathrm{m}^{-1}\right)$

a_T radius of tube (m)

a_D radius of loudspeaker diaphragm (m)

B magnetic flux density (T)

β imaginary part of γ $\left(\mathrm{m}^{-1}\right)$

c velocity of sound $\left(\mathrm{m\,s}^{-1}\right)$

C_A acoustical compliance $\left(\mathrm{m}^5\,\mathrm{N}^{-1}\right)$

c_{a1} total acoustical compliance in a unit length $\left(\mathrm{m}^5\,\mathrm{N}^{-1}\right)$

c_{aa} acoustical compliance per unit length $\left(\mathrm{m}^4\,\mathrm{N}^{-1}\right)$

c_{af} acoustical compliance per unit length associated with c_{mf} $\left(\mathrm{m}^4\,\mathrm{N}^{-1}\right)$

C_{AS} acoustical compliance associated with C_{MS} $\left(\mathrm{m}^5\,\mathrm{N}^{-1}\right)$

C_{AT} total acoustical compliance of loudspeaker and box $\left(\mathrm{m}^5\,\mathrm{N}^{-1}\right)$

C_M mechanical compliance $\left(\mathrm{m\,N}^{-1}\right)$

c_{m1} total mechanical mass in a unit length $\left(\mathrm{m\,N}^{-1}\right)$

c_{ma} mechanical compliance of air per unit length $\left(\mathrm{N}^{-1}\right)$

C_{MES} electrical capacitance associated with M_{AS} (F)

c_{mf} mechanical compliance of fibers per unit length $\left(\mathrm{N}^{-1}\right)$

$c_{mf\ell}$ mechanical coupling compliance among fibers per unit length $\left(\mathrm{N}^{-1}\right)$

C_{MS} mechanical compliance of diaphragm suspension $\left(\mathrm{m\,N}^{-1}\right)$

C_T acoustical compliance of test box $\left(\mathrm{m}^5\,\mathrm{N}^{-1}\right)$

d volume concentration of fibers (dimensionless)

e electrical voltage (V)

e_c back EMF in coil (V)

e_g generator voltage (V)

f force (N)

f frequency (Hz)

f_a mechanical force generated by acoustic pressure (N)

f_{CT} velocity resonance frequency of loudspeaker on closed box (Hz)

f_D mechanical force on diaphragm (N)

f_f mechanical force on fibers (N)

f_s diaphragm velocity resonance frequency (Hz)

$\gamma = \alpha + j\beta$ complex propagation constant $\left(\mathrm{m}^{-1}\right)$

γ_1, γ_2 propagation constants in filled tube $\left(\mathrm{m}^{-1}\right)$

γ_a ratio of specific heat of air at constant pressure to that at constant volume

$H_{TL}(j\omega)$ transfer function for total acoustical volume velocity output of TL system

i electrical current (A)

i_c electrical voice-coil current (A)

$j = \sqrt{-1}$

k wavenumber $\left(\mathrm{m}^{-1}\right)$

ℓ length, length of voice-coil wire (m)

L_{CES} electrical inductance associated with C_{AS} (H)

L_e lossy inductor parameter

$L_{E1}(\omega)$ voice coil lossy inductance (H)

L_{E2} voice coil lossless inductance (H)

ℓ_s length of sample (m)

L_T length of transmission line (m)

L_{uf} end correction for air mass outside of tube (m)

M_A acoustical mass $\left(\mathrm{N\,s^2\,m^{-5}}\right)$

M_{A1} acoustical mass part of Z_{AL} $\left(\mathrm{N\,s^2\,m^{-5}}\right)$

m_{a1} total acoustical mass in a unit length $\left(\mathrm{N\,s^2\,m^{-5}}\right)$

m_{aa} acoustical mass of air per unit length $\left(\mathrm{N\,s^2\,m^{-6}}\right)$

m_{aa2} additional acoustical mass of air per unit length resulting from fibers $\left(\mathrm{N\,s^2\,m^{-6}}\right)$

m_{af} acoustical mass per unit length associated with m_{mf} $\left(\mathrm{N\,s^2\,m^{-6}}\right)$

M_{AFS} total acoustical mass for infinite-baffle system $\left(\mathrm{N\,s^2\,m^{-5}}\right)$

m_{m1} total mechanical mass in a unit length $\left(\mathrm{N\,s^2\,m^{-5}}\right)$

m_{ma} mechanical mass of air per unit length $\left(\mathrm{N\,s^2\,m^{-1}}\right)$

M_{MD} mechanical mass of diaphragm $\left(\mathrm{N\,s^2\,m^{-1}}\right)$

m_{mf} mechanical mass of fibers per unit length $\left(\mathrm{N\,s^2\,m^{-1}}\right)$

M_M mechanical mass $\left(\mathrm{N\,s^2\,m^{-1}}\right)$

m_{ms} mechanical mass of fiber sample $\left(\mathrm{N\,s^2\,m^{-1}}\right)$

μ_u coefficient of viscosity of air $\left(\mathrm{kg\,m^{-1}\,s^{-1}}\right)$

n_e lossy inductor parameter (dimensionless)

ω angular frequency $\left(\mathrm{rad\,s^{-1}}\right)$

p, p_a acoustic pressure $\left(\mathrm{N\,m^{-2}}\right)$

P_0 static air pressure $\left(\mathrm{N\,m^{-2}}\right)$

p_a acoustic pressure $\left(\mathrm{N\,m^{-2}}\right)$

p_D acoustic pressure drop across diaphragm $\left(\mathrm{N\,m^{-2}}\right)$

P_D packing density $\left(\mathrm{kg\,m^{-3}}\right)$

p_s pressure drop across sample $\left(\mathrm{N\,m^{-2}}\right)$

Q_{ECT} electrical quality factor of loudspeaker on closed box (dimensionless)

Q_{ES} electrical quality factor of loudspeaker (dimensionless)

Q_{MS} mechanical quality factor of loudspeaker (dimensionless)

Q_{TS} total quality factor of loudspeaker (dimensionless)

R_A acoustical resistance (Ω)

r_a acoustical resistance associated with R_f $\left(\mathrm{N\,s\,m^{-5}}\right)$

R_{AE} acoustical resistance associated with R_E $\left(\mathrm{N\,s\,m^{-5}}\right)$

r_{afr} acoustical resistance associated with r_{fr} $\left(\mathrm{N\,s\,m^{-5}}\right)$

R_{AS} acoustical resistance associated with R_{MS} $\left(\mathrm{N\,s\,m^{-5}}\right)$

R_E voice coil electrical resistance (Ω)

R_{ES} electrical resistance associated with R_{AS} (Ω)

R_f flow resistance $\left(\mathrm{N\,s\,m^{-4}}\right)$

r_{fr} mechanical loss resistance of fibers per unit length $\left(\mathrm{N\,s\,m^{-1}}\right)$

ρ_0 density of air $\left(\mathrm{kg\,m^{-3}}\right)$

ρ_f bulk density of fibrous material $\left(\mathrm{kg\,m^{-3}}\right)$

ρ_{sf} surface density of fibers $\left(\mathrm{kg\,m^{-2}}\right)$

r_{aa2} acoustical resistance per unit length that models losses in m_{aa2} $\left(\mathrm{N\,s\,m^{-2}}\right)$

R_M mechanical resistance $\left(\mathrm{N\,s\,m^{-1}}\right)$

r_m mechanical resistance per unit length associated with R_f $\left(\mathrm{N\,s\,m^{-2}}\right)$

R_{MS} mechanical resistance of diaphragm suspension $\left(\mathrm{N\,s\,m^{-1}}\right)$

S area $\left(\mathrm{m^2}\right)$

S_D area of diaphragm $\left(\mathrm{m^2}\right)$

S_T area of tube $\left(\mathrm{m^2}\right)$

SPL_{total} total sound pressure level of a system (dB)

t time (s)

U acoustical volume velocity $\left(\mathrm{m^3\,s^{-1}}\right)$

u mechanical velocity $\left(\mathrm{m\,s^{-1}}\right)$

u_a mechanical velocity of air particles $\left(\mathrm{m\,s^{-1}}\right)$

u_D mechanical velocity of diaphragm $\left(\mathrm{m\,s^{-1}}\right)$

U_D acoustical volume velocity emitted by front of diaphragm $\left(\mathrm{m^3\,s^{-1}}\right)$

u_f mechanical velocity of fibers $\left(\mathrm{m\,s^{-1}}\right)$

U_T acoustical volume velocity input to tube $\left(\mathrm{m^3\,s^{-1}}\right)$

U_{total} total acoustical volume velocity of a system $\left(\mathrm{m^3\,s^{-1}}\right)$

U_{tube} acoustical volume velocity output of tube $\left(\mathrm{m^3\,s^{-1}}\right)$

V volume $\left(\mathrm{m^3}\right)$

V_{AS} volume compliance of loudspeaker suspension $\left(\mathrm{m^3}\right)$

V_T volume of test box $\left(\mathrm{m}^3\right)$

Z_A acoustical impedance $\left(\mathrm{N\,s\,m}^{-5}\right)$

z_a acoustical impedance associated with m_{aa} $\left(\mathrm{N\,s\,m}^{-5}\right)$

Z_{AB} acoustical impedance on back of diaphragm $\left(\mathrm{N\,s\,m}^{-5}\right)$

Z_{AD} mechanical mass associated with Z_{MD} $\left(\mathrm{N\,s\,m}^{-5}\right)$

Z_{AF} acoustical impedance on front of diaphragm $\left(\mathrm{N\,s\,m}^{-5}\right)$

Z_{AL} acoustical impedance of air load $\left(\mathrm{N\,s\,m}^{-5}\right)$

Z_{AQ} equivalent acoustical impedance for calculating output of a system $\left(\mathrm{N\,s\,m}^{-5}\right)$

Z_{AS} acoustical impedance associated with M_{AFS}, R_{AE}, R_{AS}, and C_{AS} $\left(\mathrm{N\,s\,m}^{-5}\right)$

Z_{AT} acoustical input impedance to tube $\left(\mathrm{N\,s\,m}^{-5}\right)$

Z_C characteristic acoustical impedance of transmission line $\left(\mathrm{N\,s\,m}^{-5}\right)$

z_{caa} acoustical impedance associated with c_{aa} $\left(\mathrm{N\,s\,m}^{-5}\right)$

$z_{cmf\ell}$ mechanical impedance associated with $c_{mf\ell}$ $\left(\mathrm{N\,s\,m}^{-1}\right)$

Z_E electrical impedance (Ω)

Z_M, Z_{MD} mechanical impedance $\left(\mathrm{N\,s\,m}^{-1}\right)$

z_m mechanical impedance associated with m_{mf}, r_{fr}, and c_{mf} $\left(\mathrm{N\,s\,m}^{-1}\right)$

Z_{VC} electrical input impedance of driver voice coil (Ω)

SUMMARY

The concept of mounting a loudspeaker on one end of a sound-absorbing tube has existed since at least 1936. Surprisingly, a detailed mathematical analysis of the configuration has not been performed, nor has a design method been established. This configuration, known as a transmission line loudspeaker, has received little consideration in the reviewed literature. Instead, it has become frequently featured in magazines for audio hobbyists, where it is experimentally designed with rules seemingly derived from hearsay and described with terms of high praise. In this dissertation, an electro-acoustical model of a fiberglass-filled transmission line is presented. This model represents the transmission line as two separate lines – a mechanical line that models the mechanical motion of the fiberglass and an acoustical line that models the motion of the air. The lines are linked by the flow resistance of the fiberglass. From the model, solutions for the acoustic pressure, acoustical volume velocity of the air, mechanical velocity of the fiberglass fibers, and mechanical force on the fiberglass in the line are obtained. The fiberglass is characterized, and empirical formulas that describe its characteristics are found. It is shown that the modeled input impedance to the transmission line is a good fit to measured data. The performance of the system is assessed by comparing it with the performances of typical loudspeaker mountings, i.e., the infinite baffle, the closed box, and the vented box. Finally, an example is shown of how the equations derived from the model can be used to evaluate the design of a transmission line loudspeaker system.

CHAPTER 1

INTRODUCTION

The concept of mounting a loudspeaker on one end of a sound-absorbing tube has existed since at least 1936 [1]. Surprisingly, a detailed mathematical analysis of the configuration has not been performed, nor has a design method been established. This configuration, also known as a transmission line loudspeaker, has received little consideration in the reviewed literature. Instead, it has become frequently featured in magazines for audio hobbyists, where it is experimentally designed with rules seemingly derived from hearsay and described with terms of high praise [2].

The goal of this research is to perform an electro-acoustical analysis of the transmission line loudspeaker. An electro-acoustical model is presented, which allows the relationships among the numerous parameters of the system and their effects on the system output to be determined. The performance of the system is assessed by comparing it with the performances of typical loudspeaker mountings, i.e., the infinite baffle [3], the closed box [4], and the vented box [5], [6].

1.1 Origin and History of the Problem

The few articles pertaining directly to transmission line loudspeakers that do exist in the reviewed literature are not complete. Chronologically, the first three articles [1], [7], [8] describe designs, but present no design equations. The next [9] concentrates on the properties of sound-absorbing materials, presenting a hypothesis, but not verifying it. The final paper [10], by presenting a circuit model of a transmission line system, is the only one to present a design tool, but it lacks descriptive equations and requires repeated use of circuit simulation software to be of use. These works are summarized and discussed in the following.

1.1.1 The Acoustic Labyrinth

In an effort to improve the low frequency response of loudspeakers mounted on open-backed radio receiver cabinets, Olney [1] in 1936 developed what he called an acoustical labyrinth: a folded acoustical path that had walls lined with sound-absorbing material. The loudspeaker was placed at one end of the labyrinth and was coupled to it both directly and by means of chambers on either side of the electromagnet. The far end of the path was open and faced the floor. A diagram illustrating the cross-section of the structure is shown in Figure 1.

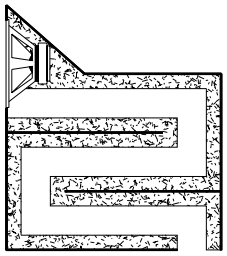

Figure 1. Cross-section of Olney's acoustic labyrinth.

Olney noted numerous undesirable characteristics of loudspeakers mounted on typical open-backed cabinets. He noted that their responses possessed peaks because of cavity resonances resulting from the open-backed cabinet and its usual placement close to a wall. Their low-frequency extension was poor, because the small path length between the front and back of the loudspeaker provided little phase shift and thus allowed for sound cancellation. The lack of resistive damping in the cabinet created sharp mechanical resonances between the cabinet air mass and the loudspeaker suspension. The electrical impedance variations around the mechanical resonance frequency could induce distortions when the loudspeaker was driven by load-sensitive amplifiers. By entirely eliminating the cabinet and replacing it with the acoustical labyrinth structure, Olney hoped to correct these problems.

Olney noted that a complete analysis of the lined tube would be involved and difficult,

so he explained the operation of the labyrinth as if it were a modified unlined tube. For an unlined tube, the acoustical impedance seen by the back of the loudspeaker is given by

$$Z_A = \frac{\rho_0 c}{S} \frac{Z_{AL} \cos(kL_T) + j\frac{\rho_0 c}{S} \sin(kL_T)}{\frac{\rho_0 c}{S} \cos(kL_T) + j Z_{AL} \sin(kL_T)} \tag{1}$$

where Z_{AL} is the acoustical impedance in $\mathrm{N\,s\,m^{-5}}$ at the open end of the tube, L_T is the length of the tube in m, ρ_0 is the density of air in $\mathrm{kg\,m^{-3}}$, c is the velocity of sound in air in $\mathrm{m\,s^{-1}}$, and k is the wavenumber which expressed in terms of the radian frequency is given by $k = \omega/c$.

Because the acoustical waves emitted from the front and back of the loudspeaker diaphragm are 180° out of phase, the tube output and the loudspeaker output are in phase when L_T is an odd number of half-wavelengths. At the frequency when this condition occurs, the tube output adds to the loudspeaker output to extend the low-frequency response. Olney chose L_T to be one half of a wavelength at the lowest frequency of interest so that the tube output would boost the system response at this frequency. He assumed that the damping material in the tube increasingly attenuated the sound waves as the frequency increased and, therefore, damped out any higher-frequency peaks in the tube output.

Olney made measurements to show that the resonance peaks were reduced and that the response at low frequencies was extended by use of the labyrinth. He showed that the higher-frequency resonances of the tube were reduced by the damping material, and he noted that the increased mass reactance of the labyrinth reduced the amplitude of the mechanical resonance and shifted it to a lower frequency. Though his results were chiefly experimental and based on qualitative reasoning, Olney achieved his purpose of illustrating that the acoustical labyrinth was an improvement over the open-backed loudspeaker cabinet.

1.1.2 The Filled Acoustic Transmission Line

In 1965, Bailey [7] presented a design for what he termed a non-resonant loudspeaker enclosure. He further refined the design in 1972 [8]. Like Olney, his intention was to eliminate

resonance effects. But Bailey was concerned with the resonances of bass-reflex cabinets rather than those of open-backed cabinets. Mounting a loudspeaker such that its back radiation is emitted into a bass-reflex cabinet was at the time, and still is, a widely popular method of improving the low-frequency response of a loudspeaker. However, Bailey believed that this mounting method unnecessarily distorted the sound output of a loudspeaker.

By performing impulse response tests on bass reflex cabinets, Bailey showed that sound was emitted from the cabinet for a significant time after the impulse excitation. This phenomenon was caused by a lack of damping within the cabinet and the inherent resonance effects of both the cabinet and the port. In addition, he found that ringing on bass transients near the system corner frequency was introduced because of the steep slope of the system response below the lower cutoff frequency.

Bailey's enclosure, effectively a modified version of Olney's design, did not possess a rear cabinet and, therefore, did not color the sound as did the bass-reflex enclosure. His design consisted of a loudspeaker mounted at one end of a folded tube that was entirely filled with an acoustical damping material, rather than just lined. The end of the tube opposite the loudspeaker was open and in the same plane as the loudspeaker. The sound output from the tube combined with that of the loudspeaker to produce the total output of the configuration.

The tube acted as a low-pass acoustical transmission line. At low frequencies, the sound wave was only lightly damped and added in phase to the loudspeaker output to boost the low-frequency response. At higher frequencies, the sound waves emitted by the loudspeaker into the tube were greatly damped by the absorbent filling. This resulted in little sound output from the tube. After experimenting with damping materials, Bailey chose to use long-fibered wool as the filling for his enclosure. He also tested short-fibered wool and fiberglass, but found that long-fibered wool best attenuated the sound waves and did so down to low frequencies.

Bailey stated that the velocity of sound in the tube was affected by the damping material and that the tube output could be altered by varying the length of the tube. He gave some practical construction considerations, but he did not present any experimental design method or any design equations. Without equations, the length and diameter of the tube and the packing density of the damping material must be determined by trial and error to create an effective transmission line for an arbitrary loudspeaker. Bailey did not determine what characteristics would be appropriate for a loudspeaker mounted on a transmission line.

1.1.3 Fibrous Filling Materials

Apparently intrigued by Bailey's conclusion that long-fibered wool was the best filling material, Bradbury [9] in 1976 investigated fibrous damping materials with some thought toward their use in loudspeaker enclosures. He believed that fibrous materials could be used not only to attenuate high-frequency resonances in a transmission line, but also they could be used to reduce the length of labyrinth and horn-loaded loudspeakers because the materials reduce the velocity of sound waves traveling through them.

Bradbury particularly wanted to understand why long-fibered wool had properties that made it extremely suitable for use in transmission line loudspeaker systems. He noted that if the wool is packed into the line at a packing density of $8\,\mathrm{kg\,m^{-3}}$, it highly attenuates the sound waves at frequencies greater than about 100 Hz. Simultaneously, it presents an an acoustical impedance to the rear of the loudspeaker diaphragm that is close to that of air. For these reasons, he noted that the fiber-filled tube does not affect the acoustical load on the loudspeaker but it dampens high-frequency resonances in the tube.

The tube output and the loudspeaker front diaphragm output add constructively to boost the system output at the frequency where the length of the tube is equal to a half-wavelength. This frequency is given by

$$f_{\text{boost}} = \frac{c}{2L_T} \tag{2}$$

where c is the velocity of sound and L_T is the length of the tube. At lower frequencies,

he found that the wool filling approximately halves the velocity of sound. Therefore, for a desired boost frequency, the filled transmission line would be about one-half as long as an unfilled one.

Bradbury thought that the above characteristics of the wool could be explained by the fibrous damping materials not being stationary in the tube. He believed that the fibers were moved by the air flow generated by the loudspeaker. In addition, he knew that the fibers impeded the flow of air through them by means of an aerodynamic drag that was proportional to the velocity of the air relative to the fibers. He combined the two above beliefs into the following equation of motion for the fibers:

$$P_D \frac{du_f}{dt} = R_f \left(u_a - u_f\right) \tag{3}$$

where P_D is the packing density of the fibrous material in $\mathrm{kg\,m^{-3}}$, u_f is the velocity of the fibers in $\mathrm{m\,s^{-1}}$, u_a is the velocity of the air in $\mathrm{m\,s^{-1}}$, and R_f is a quantity that Bradbury referred to as an aerodynamic drag parameter. It is more commonly known as flow resistance which has the units $\mathrm{N\,s\,m^{-4}}$.

The above equation assumes that the fibers are able to move freely. They are not restrained by each other or by the tube so the only force on them is aerodynamic drag induced by the air flow. This can be seen by noting that if the fiber velocity u_f is zero in Equation (3), then then the air particle velocity u_a must also equal zero. That is, the fibers cannot be stationary unless no source of air flow is present. In contrast, if a stabilizing force were present, the fibers could remain stationary in the presence of an air flow. An example of this might occur when the fiber motion is constrained by the walls of the tube.

Under these conditions, Bradbury found that the phasor equation for the acoustic pressure in a simple harmonic sound wave traveling down the filled transmission line could be written

$$\begin{aligned} p(x) &= p_0 e^{-\gamma x} \\ &= p_0 e^{-\alpha x} e^{-j\beta x} \end{aligned} \tag{4}$$

where p_0 is the phasor amplitude of the wave and $\omega = 2\pi f$ is the radian frequency. The quantity γ is called the complex propagation constant. It is given by

$$\begin{aligned} \gamma &= \alpha + j\beta \\ &= j\frac{\omega}{c}\sqrt{\frac{\left(1 + P_D/\rho_0\right) + j\omega P_D/R_f}{1 + j\omega P_D/R_f}}. \end{aligned} \tag{5}$$

In order to keep the notation consistent with that used in the following, some of the parameters in Equations (4) and (5) have been renamed and the expressions rearranged from the original forms presented by Bradbury.

If the real part of γ in Equation (5) is zero, then $\gamma = j\beta$ and the wave propagates unattenuated in the tube with a phase velocity given by $v_p = \omega/\beta$. The high frequency limit to Bradbury's equation predicts that $\gamma = j\omega/c$ so that the phase velocity at high frequencies is $v_p = c$, i.e. the phase velocity of an adiabatic acoustical wave. It is given by

$$c = \sqrt{\frac{\gamma_a P_0}{\rho_0}} \tag{6}$$

where γ_a is the ratio of the specific heat of air at constant pressure to the specific heat of air at constant volume, P_0 is the static air pressure in $\mathrm{N\,m^{-2}}$. The low-frequency limit to Equation (5) also predicts that the real part of γ is zero so that the wave propagates unattenuated. In this case, the phase velocity becomes

$$v_p = \sqrt{\frac{\gamma_a P_0}{\rho_0 + P_D}}. \tag{7}$$

This can be interpreted as the phase velocity of an adiabatic wave in a gas having the effective density $\rho_0 + P_D$.

The basic assumption of Bradbury in arriving at Equation (5) was that the time period at low frequencies is so long that the fibers move with almost the same velocity of the air particles in the acoustical wave. Bradbury assumed that the low-frequency wave propagates unattenuated because the fibers move at approximately the same velocity as the air particles so that the drag forces between the fibers can be neglected.

As the frequency is increased, the fibers are no longer able to keep up with the rapid fluctuations in direction of the air flow because of their inertia. In this case, the fibers move with a retarded velocity. With further increases in frequency, they do not move at all. The stationary fibers at high frequencies highly attenuate the air flow because the drag forces are large. However, because the fibers are not coupled with the air at these higher frequencies, the velocity of sound through the fibrous material remains nearly the same as the velocity of sound in free air.

By assuming a perfect piston in harmonic motion at the source end of the transmission line, Bradbury was able to plot the real and imaginary parts of the phasor velocity at the end of a tube with a length of 2 m for several values of packing density P_D. He also plotted the real and imaginary parts of the impedance seen by the source for both wool and fiberglass filled tubes. Continuing to concentrate on the characteristics of the fibrous materials, he determined that wool was indeed the better filling material. He noted that the reactive impedance of wool approaches zero more rapidly than it does for fiberglass. In addition, he found that the real part of the acoustical impedance with wool was less than that with fiberglass.

Bradbury ended his analysis with several conclusions. He stated that his results were not practically useful until the mechanical impedances of the loudspeaker were included. He did not experimentally verify his equations, but he did achieve his purpose of showing that loudspeaker enclosures could perhaps be improved by understanding and utilizing the characteristics of fibrous filling materials. In addition, he noted that the characteristics of different filling materials could possibly be analyzed theoretically rather than by performing extensive experimental measurements.

1.1.4 Augspurger's Circuit Model

Observing that objective information on transmission line loudspeakers is rare, Augspurger [10] in 2000 developed an electrical lumped-element model that could be used to simulate acoustical transmission line systems. His model was an altered version of Locanthi's

[11] analog transmission line model, which was developed to analyze acoustical horns. Augspurger added shunt resistors to account for sound attenuation by the fibrous filling and included a shunt stub to allow for the case where the loudspeaker is recessed into the tube.

Augspurger's model consisted of 32 sections containing resistors, inductors, and capacitors that model the acoustical parameters of the line. He varied the values of the components in each section to model different transmission line geometries such as flares and tapers and to account for changes in attenuation with frequency. A schematic of his analogous circuit model is shown in Figure 2. In this model, the parameters that model the loudspeaker mechanical system and the acoustical parameters of the transmission line and its filling are reflected into the electrical circuit of the loudspeaker. Therefore, the variables of the circuit are currents and voltages rather than the variables of mechanical or acoustical systems.

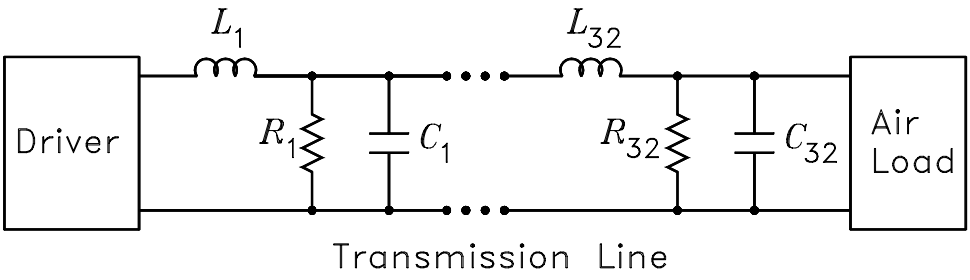

Figure 2. Augspurger's analogous circuit model of transmission line.

The inductors in the above figure model the compliance of the air in the tube and the capacitors model the mass of the air in the tube. To more accurately model the damping material, Augspurger made the resistor values vary with frequency. He never revealed the manner in which he determined the resistor values or their frequency dependence. However, he claimed to employ four empirical parameters, which he noted could be called "unscientific twiddle factors," to model the effects of the damping material. His model did not include the effects of fiber motion, but he stated that it is not certain that fiber motion

is important.

Using a circuit simulation program, Augspurger repeatedly ran simulations of his model while adjusting values of the loudspeaker and pipe parameters. By doing this, he obtained several designs that he referred to as optimized, meaning that they possessed second order low-frequency slopes and minimum pass-band ripple while obtaining efficiencies matching that of an equivalent closed-box system.

Augspurger demonstrated that it was possible to model damped acoustical transmission lines as electrical transmission lines, and he considered the effects on the system of varying the geometry of the transmission line from that of a simple straight pipe. Though he showed numerous simulated plots of transmission line systems having various geometries, he presented few experimental results. He simply stated that the simulated results exactly matched the measured results. To realize transmission line designs that were not explicitly simulated and presented by Augspurger, it would be necessary to go through a trial and error adjustment process using a circuit simulation tool.

1.2 Air Flow and Sound Propagation in Fibrous Materials

Flow resistance is a quantity that relates the acoustic pressure drop per unit length through an acoustical material to the mechanical velocity of the air particles flowing through the material. It is typically measured by directing a low-magnitude, constant-velocity air current through a sample of material and measuring the resulting pressure drop [12]. Symbolically, this measurement can be expressed as

$$p_s = R_f \ell_s u_a \tag{8}$$

where p_s is the pressure drop across the sample, R_f is the flow resistance, ℓ_s is the length of the sample, and u_a is the particle velocity. The units of flow resistance are $\mathrm{N\,s\,m^{-4}}$.

Numerous papers have discussed the calculation of flow resistance based on theoretical considerations or experimental measurements. In Tarnow [13], the flow resistance of randomly placed cylinders placed both parallel and perpendicular to the air flow is determined

by the use of Vornoi polygons. Bradbury [9] gives an equation for flow resistance that is determined from both theoretical considerations and experimental observations. Bies and Hanson [14] present a equation that gives the flow resistance based on the fiber diameter and bulk density. Similar equations are presented in Nichols [12] and in Beranek [15]. An empirical formula for the flow resistance in polyester materials is given by Garai and Pompoli [16].

Calculation of the flow resistance from the methods described in the papers referenced above requires a detailed knowledge of the physical characteristics of the fibers. In addition, these papers assume idealized fibers and fiber arrangements. The empirical formula of [16] requires knowledge of only the fiber packing density. This equation applies specifically for polyester fibers only. In the present work, an empirical formula for the flow resistance of fiberglass in an acoustic transmission line that is based on packing density is presented. This formula has a similar relationship to packing density as do the formulas given in [9], [16], and [14].

Sound propagation in fibrous materials is often based on the theory of porous materials [35]. In the papers referenced below, the pores in the material are assumed to be interconnected in a random, isotropic way. With two exceptions, the material is assumed to be rigid. Zwikker and Kosten [17] discuss the propagation of sound in a single, small, air-filled tube through a solid. Biot [18], [19], Tarnow [20], and Allard et al. [21] include the possibility that the porous structure is not stationary. Lambert [22] investigates sound propagation in porous foam. Lambert and Tesar [23] and Tarnow [24] investigate sound propagation in fibrous materials. These papers all require that the pore radius of the fibrous material be known or determined a priori. Attenborough [25] includes the additional properties of tortuosity, porosity, and pore shape factor in determining the sound propagation characteristics.

In this work, the particular case of fiberglass in a transmission line loudspeaker is considered. Although the properties of a sound wave in fiberglass can be theoretically modeled

by the methods presented in the above papers, a more practical approach is used here that suffices for the study of transmission line loudspeakers. The reason for this is that loudspeaker designers do not have the instrumentation required to determine the pore diameter or tortuosity of fiberglass. A loudspeaker designer requires a straightforward and practical means of determining how a given packing density of fiberglass will affect the performance of a transmission line loudspeaker.

When a transmission line is filled with lower packing densities of fiberglass, the fiberglass is highly nonuniform. There can be large air spaces between fiberglass layers. In addition, the fiberglass density can vary greatly from layer to layer. Neither of these possibilities is considered in the theoretical derivations presented here because the wavelength of sound in transmission line loudspeakers is large compared to the distances between non-uniform layers. It is believed that empirical equations for the fiberglass characteristics would give acceptable results. In this work, an electro-acoustical circuit model is developed for a fiber filled acoustical transmission line. It is demonstrated that the circuit parameters in the model can be easily determined from measured data.

1.3 Contributions of this Research

A new electro-acoustical analogous circuit model for a transmission line loudspeaker system is developed. The analogous circuit model includes the electrical and mechanical properties of the loudspeaker driver and the acoustical properties of a fiber-filled acoustical transmission line that is used to acoustically load the back side of the loudspeaker diaphragm. A mechano-acoustical analysis of a wave propagating in the fiber-filled transmission line is developed that includes the acoustical properties of the air in the tube and the mechanical properties of the fibers. It is shown that the line and fibers can be modeled by separate lumped parameter electrical transmission lines that are coupled through the flow resistance of the fibers. The transmission line model is used to derive two coupled second-order differential equations that govern the motion of the air particles and fibers in

the tube. The two equations are solved simultaneously to obtain fourth-order differential equations for the air particle motion and for the fiber motion. A mathematical solution to these equations is described that admits the possibility of four waves propagating in the air in the tube and four waves propagating in the fibers. The circuit models that are developed can be analyzed with very powerful electrical circuit analysis computer programs such as SPICE.

A simplification to the model is described that has been found to yield acceptable agreement with the measurements made with a loudspeaker driver mounted on a fiber-filled tube. It is shown that measurements of the electrical input impedance to the loudspeaker driver can be used to extract the acoustical parameters of the tube and the mechanical parameters of the fibers. The simplified model is compared to the two published transmission line loudspeaker models. It is shown that the model developed here predicts results that better agree with measured data than these two models do. The simplified model can be analyzed with circuit simulator computer programs such as SPICE.

A refinement of the lossy voice-coil inductance model developed in [26] is described that better models the effects of the magnetic flux outside of the lossy magnetic core in a loudspeaker driver. It is shown that the modification predicts the electrical impedance of the voice coil that agrees better with measured data at frequencies greater than the driver resonance frequency.

CHAPTER 2

MODELING OF ELECTROACOUSTIC SYSTEMS

2.1 Electrical, Mechanical, and Acoustical Analogous Circuits

The two variables in electrical circuits that are used to calculate the power delivered by a source to a load are voltage and current. Force and velocity are the variables in mechanical systems that are analogous to voltage and current in electrical circuits [27], [28]. Similarly, pressure and volume velocity are the variables in acoustical systems that are analogous to voltage and current in electrical circuits [27], [28]. In modeling mechanical and acoustical systems with electrical circuits, the analogs must be assigned so that they relate the variables in the mechanical and acoustical systems to those in electrical circuits in such a way that power relations are not changed.

There are two classes of analogs that are commonly used. These are impedance analogs and mobility analogs [27], [29]. In impedance analogous circuits, voltage is analogous to mechanical force and to acoustic pressure. Current is analogous to mechanical velocity and to acoustical volume velocity. In contrast, in mobility analogous circuits, voltage is analogous to mechanical velocity and to acoustical volume velocity. Current is analogous to mechanical force and to acoustic pressure. The two types of circuits are related by the principle of duality. The dual of a circuit is one which has an impedance equal to the reciprocal of the impedance of the original circuit. When the dual of a circuit containing series elements is made, the new circuit contains parallel elements. Similarly, when the dual of a circuit containing parallel elements is made, the new circuit contains series elements. In the following, both impedance and mobility analogous circuits are used to model mechanical systems. Only impedance analogous circuits are used to model acoustical systems.

The concept of electrical impedance can be used to relate the voltages and currents in an electrical circuit if the time variations are taken to be of the form $\exp(st)$, where s is the complex frequency. For sinusoidal steady-state time variations, the complex frequency is

taken to be $s = j\omega$, where $j = \sqrt{-1}$ and ω is the radian frequency with units $\mathrm{rad\,s^{-1}}$. In this case, the electrical impedance Z_E relates the phasor voltage e to the phasor current i. The relation is

$$e = Z_E i. \tag{9}$$

The units of Z_E are $\mathrm{V\,A^{-1}}$.

In mechanical analogous circuits, the analogous relation is

$$f = Z_M u \tag{10}$$

where f is the phasor force with units N, u is the phasor velocity with units $\mathrm{m\,s^{-1}}$, and Z_M is the mechanical impedance. The units of Z_M are $\mathrm{N\,s\,m^{-1}}$.

In acoustical analogous circuits, the analogous relation is

$$p = Z_A U \tag{11}$$

where p is the phasor pressure with units Pa, U is the phasor volume velocity with units $\mathrm{m^3\,s^{-1}}$, and Z_A is the acoustical impedance. The units of Z_A are $\mathrm{N\,s\,m^{-5}}$.

In mechanical analogous circuits, the force f is the force applied to a non-deformable mass and the velocity u is its velocity. In acoustical analogous circuits, the pressure p is the acoustic pressure at a surface and the volume velocity U is the time rate of change of the velocity of air flowing through the surface. If all air particles flow through the surface at the same velocity, the volume velocity is given by the area of the surface multiplied by the particle velocity. That is, $U = Su$, where S is the area and u is the particle velocity. In electrical circuits, power is calculated as the product of voltage and current. In mechanical analogous circuits, it is calculated as the product of force and velocity. In acoustical analogous circuits, it is calculated as the product of pressure and volume velocity.

2.2 Elements of Mechanical Circuits

This section presents an overview of the three lumped-parameter circuit elements of mechanical systems. These are mechanical mass M_M, compliance C_M, and resistance R_M.

The mechanical symbols for these are shown in Figure 3. It is noted that the mass can have only a single velocity. In contrast, the two ends of the compliance and resistance can move at different velocities. For this reason, the mechanical equations reviewed below involve the difference velocity $u = u_1 - u_2$ for these elements. The elements which are used to model these mechanical elements in electrical circuits are reviewed in this section.

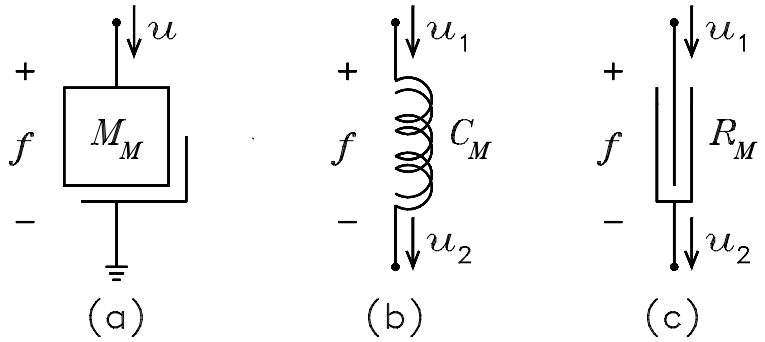

Figure 3. Mechanical element symbols. (a) Mass. (b) Compliance. (c) Resistance.

2.2.1 Mechanical Mass

If a force f is applied to a mechanical mass M_M, the force is related to the velocity u of the mass by Newton's second law given by

$$f = M_M \frac{du}{dt}. \tag{12}$$

For time variations of the form $\exp(j\omega t)$, this relation becomes

$$f = j\omega M_M u. \tag{13}$$

It follows that the mass M_M is analogous to an inductor of the same value in an impedance analogous circuit. The inductor has the impedance $j\omega M_M$. In a mobility analogous circuit, the mass is analogous to a capacitor of the same value. The capacitor has the impedance $(j\omega M_M)^{-1}$. The units of mechanical mass are kg.

2.2.2 Mechanical Compliance

If a force f is applied between the two ends of a spring, the force is related to the velocity difference u between the ends of the spring by the relation

$$f = \frac{1}{C_M} \int u dt \tag{14}$$

where C_M is the compliance of the spring. This relation assumes that the spring is linear and is operated in its linear region. The compliance is the reciprocal of the spring constant and has the units $\mathrm{m\,N^{-1}}$. For time variations of the form $\exp(j\omega t)$, the relation becomes

$$f = \frac{1}{j\omega C_M} u. \tag{15}$$

It follows that the compliance C_M is analogous to a capacitor of the same value in an impedance analogous circuit. The capacitor has the impedance $(j\omega C_M)^{-1}$. In a mobility analogous circuit, the capacitor is analogous to an inductor of the same value. The inductor has the impedance $j\omega C_M$. In the following, it is assumed that mechanical springs are linear and they are operated in their linear region. The units of mechanical compliance are $\mathrm{m\,N^{-1}}$.

2.2.3 Mechanical Resistance

Dissipative losses in mechanical systems that arise from linear mechanisms are modeled by a mechanical resistance. The relation between force f and velocity u for a linear dissipative loss is

$$f = R_M u \tag{16}$$

where R_M is the mechanical resistance. It follows that the resistance R_M is analogous to a resistor of the same value in an impedance analogous circuit. The resistor has the impedance R_M. In a mobility analogous circuit, the resistor is analogous to a resistor having a value equal to the reciprocal of the mechanical resistance. The resistor has the impedance R_M^{-1}. Although friction losses are dissipative, they are not linear. For this reason, friction cannot be modeled accurately by linear analogous circuits. In the following, it is assumed that mechanical losses are linear. The units of mechanical resistance are $\mathrm{N\,s\,m^{-1}}$.

2.3 Elements of Acoustical Circuits

An overview of the three lumped-parameter circuit elements of acoustical systems is presented in this section. These are acoustical mass M_A, acoustical compliance C_A, and acoustical resistance R_A. The circuit elements which are used to model these elements in electrical circuits are reviewed. Because only impedance analogous models are used in the following, the mobility circuit analogs are omitted.

2.3.1 Acoustical Mass

Voltage is analogous to pressure and current is analogous to volume velocity in impedance analogous circuits of acoustical systems. Let a pressure difference p be applied between two ends of a cylindrical tube of air having a cross section S and length ℓ, where ℓ is small compared to a wavelength. The applied force can be written $f = Sp$. If the air density in the tube is ρ_0, Newton's second law of motion for the mass of air in the tube is

$$Sp = \rho_0 S\ell \frac{du}{dt} \tag{17}$$

where $\rho_0 S\ell$ is the air mass and u is its velocity. When the tube of air moves, the volume velocity that flows through the surface area S is given by $U = Su$. It follows then that the pressure is related to the volume velocity by

$$p = \frac{\rho_0 \ell}{S} \frac{dU}{dt}. \tag{18}$$

For time variations of the form $\exp(j\omega t)$, this relation can be written

$$p = j\omega M_A U \tag{19}$$

where M_A is the acoustical mass given by

$$M_A = \frac{\rho_0 L_T}{S}. \tag{20}$$

It follows that the acoustical mass is analogous to an inductor of the same value in the electrical analogous circuit. The inductor has the acoustical impedance $j\omega M_A$. The units of acoustical mass are $\mathrm{kg\,m^{-4}}$.

2.3.2 Acoustical Compliance

Figure 4 illustrates a closed vessel containing a volume of air V that is compressed by the motion of a piston in one of its walls. When a force f is applied to the piston, it moves with a velocity u, causing a volume velocity U to be emitted into the vessel, thus compressing the air and generating an acoustic pressure p. The pressure generates a restoring force on the piston that opposes its motion. If it is assumed that the displacement of the piston is small so that the change in the center of gravity of the air in the vessel can be neglected, the restoring force can be modeled by a linear spring having the mechanical compliance $C_M = V/\rho_0 c^2 S^2$, where S is the area of the piston [27].

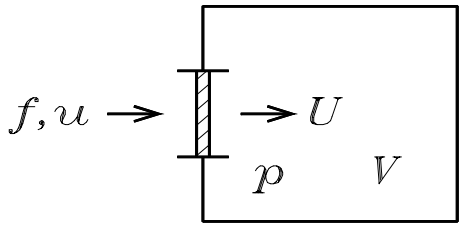

Figure 4. Closed volume of air with moveable piston.

Following Equation (15) for the mechanical spring having a compliance C_M, the relation between the restoring force f and the piston velocity u can be written

$$f = \frac{\rho_0 c^2 S^2}{j\omega V} u. \tag{21}$$

In this equation, the force can be written $f = pS$ and the velocity can be written $u = U/S$. When these substitutions are made, the equation can be written

$$p = \frac{1}{j\omega C_A} U \tag{22}$$

where C_A is the acoustical compliance of the air in the vessel given by

$$C_A = \frac{V}{\rho_0 c^2}. \tag{23}$$

In an impedance analogous circuit, this compliance is modeled as a capacitor having the impedance $(j\omega C_A)^{-1}$. The units of acoustical compliance are $\mathrm{m}^4\,\mathrm{s}^2\,\mathrm{kg}^{-1}$.

2.3.3 Acoustical Resistance

When a volume velocity U flows through a fibrous material, a pressure drop is generated that is proportional to the volume velocity. This can be expressed mathematically by the equation

$$p = R_A U \tag{24}$$

where R_A is the acoustical resistance of the material. Any stationary structure which exhibits an acoustical resistance exerts an aerodynamic drag force on the flow of air that opposes the air flow.

Examples of acoustical resistances are mesh screens, perforated sheets, and fibrous materials, such as fiberglass and spun polyester fibers. Figure 5 illustrates these simple structures. The fibrous material forces the air to flow through narrow openings and past narrow solid structures, just as the screens do. However, its structure is much less ordered. Unlike screens, the fibers of the fibrous materials are not rigidly fixed and are able to be moved by the air flow. Because they are able to move, they can introduce mechanical mass and compliance effects into the system. The units of acoustical resistance are $\mathrm{N\,s\,m^{-5}}$.

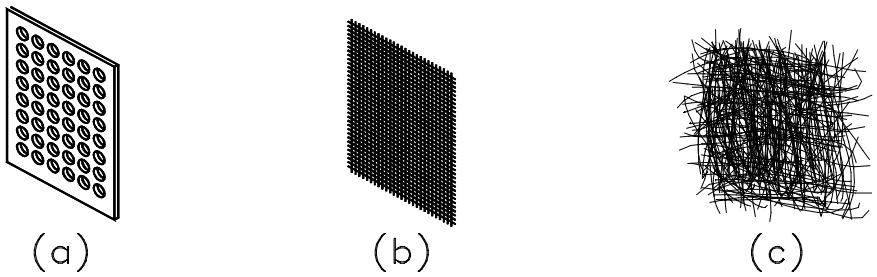

Figure 5. Illustrations of (a) a perforated sheet, (b) a mesh screen, and (c) a fibrous material.

The magnitude of the drag force resulting from a resistive structure, and consequently the magnitude of the acoustical resistance, is proportional to the velocity of the air and is dependent on the physical properties of the structure. A discussion of this is given in [13]. In general, smaller spaces between the fibers of a mesh result in a larger resistance. Similarly, smaller diameter holes in a perforated screen result in a larger resistance. For

fibrous materials, a larger ratio of fibers to air, that is a higher packing density, results in a larger resistance. For a given packing density, smaller diameter fibers result in a larger resistance than do larger diameter fibers.

The arrangement of the fibers also affects the resulting acoustical resistance. The fibers can be oriented either perpendicular or parallel to the air flow, or arranged randomly in a tangled manner. Parallel fibers tend to produce less resistance than do perpendicular fibers, because the cross-sectional area perpendicular to the air flow is smaller. Thus there is much less interaction between the air and the fibers.

To some extent, the papers discussed in Chapter 1 all concern the absorptive effects of damping materials on sound waves. Although the materials seem to have a frequency-dependent behavior, the effects appear to be primarily related to the flow resistance of the material.

Flow resistance is a quantity that relates the pressure drop per unit length through an acoustical material to the mechanical velocity of the air particles flowing through the material. It is typically measured by directing a low-magnitude constant-velocity air current through a sample of material and measuring the resulting pressure drop [12]. Symbolically, this measurement can be expressed as

$$p_s = R_f \ell_s u_a \tag{25}$$

where p_s is the pressure drop across the sample, R_f is the flow resistance, ℓ_s is the length of the sample, and u_a is the particle velocity. The units of flow resistance are $\mathrm{N\,s\,m^{-4}}$.

The flow resistance and its relationship to packing density for a given damping material are important considerations in the practical construction of transmission line loudspeakers. To create a transmission line system that agrees with a modeled response, it is necessary to know the amount of a given material that must be packed into the transmission line to achieve a required flow resistance.

Several quantitative relationships between packing density and flow resistance have been presented in the literature. An equation for fibrous materials, that is given in [9]

which is based on both experimental observations and theoretical considerations [30], is given by

$$R_f = \frac{27}{16}\frac{4\mu}{a_f^2}d^{1.4} \tag{26}$$

where μ is the coefficient of viscosity of air, a_f is the radius of the fibers that make up the material, and d is the volume concentration. The latter is the ratio of the fiber volume to the total volume in the tube given by $d = P_D/\rho_f$, where P_D is the packing density and ρ_f is the bulk density of the fibrous material.

Another expression for the flow resistance that is given in [13] is

$$R_f = \frac{4\mu}{a_f^2}\frac{d}{0.640\ln(1/d) - 0.737 + d}. \tag{27}$$

Both Equations (26) and (27) have been altered here from the original forms to allow them to be compared more easily. Although the equations are very different, it was found in this research that adjustment of the parameters in them cause the two equations to predict approximately the same values for R_f over a limited range of values for the volume concentration d.

Acoustical resistance is closely related to flow resistance. Flow resistance relates pressure to particle velocity according to Equation (25). This equation defines the flow resistance in terms of both a mechanical variable (particle velocity u) and an acoustical variable (pressure p). To obtain the acoustical resistance R_A that results from the flow resistance R_f, Equation (25) must be written in terms of volume velocity. The expression $u = U/S$ can be used in Equation (25) to obtain

$$p = \frac{R_f \ell_s}{S}U. \tag{28}$$

When this expression is compared with Equation (24), it can be seen that the acoustical resistance resulting from an acoustical resistive structure having length ℓ_s, area S, and flow resistance R_f is given by

$$R_A = \frac{R_f \ell_s}{S}. \tag{29}$$

2.4 Analogous Circuits of a Loudspeaker Driver

The cross-section diagram of a typical loudspeaker driver is shown in Figure 6. The loudspeaker is an electromechanical device that converts an applied electrical current into a mechanical motion. That motion creates an acoustic pressure wave that is radiated from the diaphragm. The current is applied to the voice coil, which is a coil of wire suspended in a magnetic field. This coil exhibits both a resistance and an inductance. The current in the voice coil interacts with the magnetic field to generate a force which is coupled to the diaphragm. The diaphragm has a mass. Its inner and outer suspensions exhibit a spring constant or compliance. In addition, the suspensions exhibit mechanical damping losses. When the diaphragm moves, it radiates an acoustical wave into the air load on each side. In addition, its motion generates a back electromotive force (emf) in the voice coil which opposes the flow of current. The analogous circuits for the loudspeaker model the elements in the electrical, mechanical, and acoustical systems. The coupling between the three systems is modeled by controlled voltage and current sources.

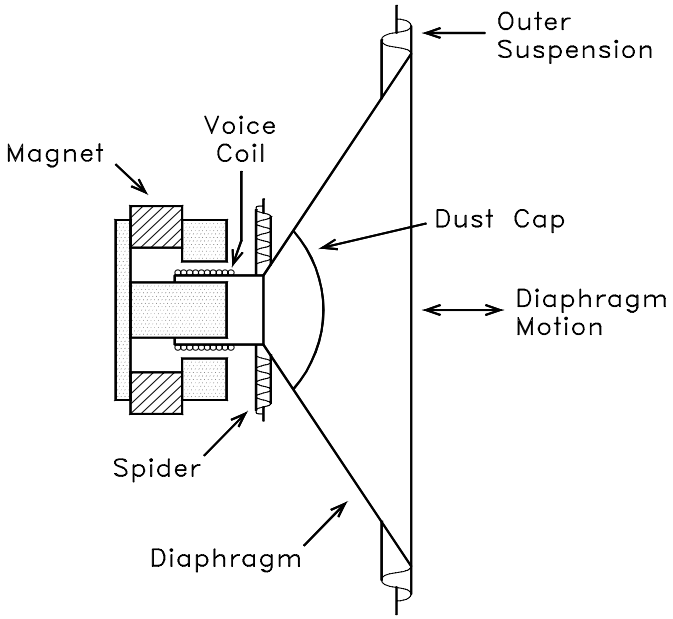

Figure 6. Diagram of loudspeaker driver.

2.4.1 The Electrical Circuit

The electrical input terminals to a loudspeaker connect to what is called the voice coil. This is a coil of wire which is wound on a cylindrical former. It exhibits both an inductance and a resistance. It is immersed in a magnetic field such that the direction of the field is perpendicular to the direction of current flow in the coil. The current flow exerts a force on the coil which causes it to move. Its motion generates a voltage that is called the back emf. This voltage opposes the flow of current and is given by

$$e_c = B\ell u_D \tag{30}$$

where B is the magnetic field density (T), ℓ is the effective length of wire (m) that cuts that field, and u_D is the mechanical velocity of the voice coil ($\mathrm{m\,s^{-1}}$). Because the voice coil is mechanically coupled to the diaphragm, this velocity is also the mechanical velocity of the diaphragm.

The analogous circuit that models the electrical part of the loudspeaker is shown in Figure 7 [27], [26]. In the figure, e_g is the electrical input voltage from the amplifier that is connected across the voice-coil terminals, and i_c is the voice-coil current. The resistor R_E models the electrical resistance of the voice coil. The elements $L_{E1}(\omega)$ and L_{E2} model the lossy voice-coil inductance. The controlled source e_c models the back emf in the voice coil resulting from its motion.

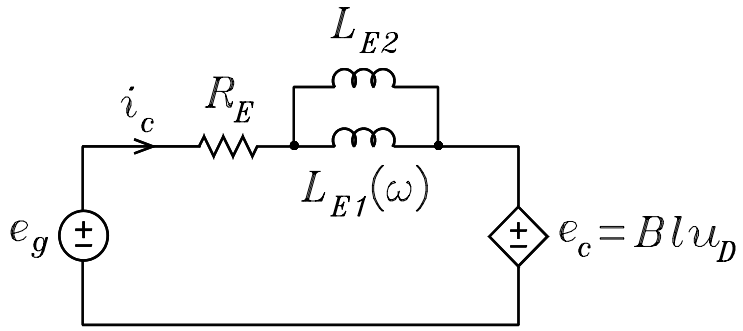

Figure 7. Impedance analogous circuit of the electrical part of a loudspeaker driver.

The inductor model consists of two inductors in parallel. The inductor L_{E2} is a lossless inductor. The inductor $L_{E1}(\omega)$ is a lossy inductor which has a frequency dependent impedance. To a good approximation [26], the impedance of $L_{E1}(\omega)$ can be written

$$Z_{E1}(\omega) = (j\omega)^{n_e} L_e \tag{31}$$

where n_e and L_e are parameters that must be determined from measurements. The units of L_e are $\Omega\,\mathrm{s}^{n_e}$. It can be shown [26] that the equivalent circuit having the impedance $Z_{E1}(\omega)$ is a parallel RL circuit where the elements are frequency dependent and are given by

$$R_1 = \frac{L_e \omega^{n_e}}{\cos(n_e \pi/2)} \tag{32}$$

$$L_1 = \frac{L_e \omega^{n_e - 1}}{\sin(n_e \pi/2)}. \tag{33}$$

For $n_e = 0$, it follows that $R_1 = L_e$ and $L_1 = \infty$. In this case, $L_{E1}(\omega)$ is a pure resistor. For $n_e = 1$, it follows that $R_1 = \infty$ and $L_1 = L_e$. In this case $L_{E1}(\omega)$ is a lossless inductor. Typically, the value of n_e is in the range from 0.6 to 0.7 for most loudspeaker drivers. The loudspeaker driver used in the experimental measurements of this research had an unusually low value of $n_e = 0.447$.

2.4.2 The Mechanical Circuit

The loudspeaker diaphragm and voice coil exhibit a mechanical mass. The suspension exhibits a mechanical compliance and mechanical damping resistance R_{MS}. Figure 3 shows the mechanical diagrams for these elements. The relationships between the phasor force f and phasor velocity u for the mass, the compliance, and the resistance, respectively, are

$$f = j\omega M_M u \tag{34}$$

$$f = \frac{1}{j\omega C_M} u \tag{35}$$

$$f = R_M u \tag{36}$$

where f and u are phasor functions of frequency. For the compliance and the resistance, the velocity u is the difference velocity between each end, that is $u = u_1 - u_2$. Because the mass is assumed to be non deformable, it has only one velocity.

The mechanical portion of the loudspeaker consists of the piston and its suspension. There are two suspensions, an inner suspension, which is called the spider, and the outer suspension, which is called the surround. These two elements center the voice coil in the magnetic field of the magnet and provide a mechanical restoring force that restores the piston to its rest position in the absence of an applied current. The two suspensions exhibit mechanical losses which damp the motion of the system. A schematic diagram that represents the mechanical system is shown in Figure 8. In this circuit, the mass M_{MD} models the total moving mass. The compliance C_{MS} represents the suspensions. The resistance R_{MS} between the mass and the zero-velocity ground reference models the damping losses in the suspension.

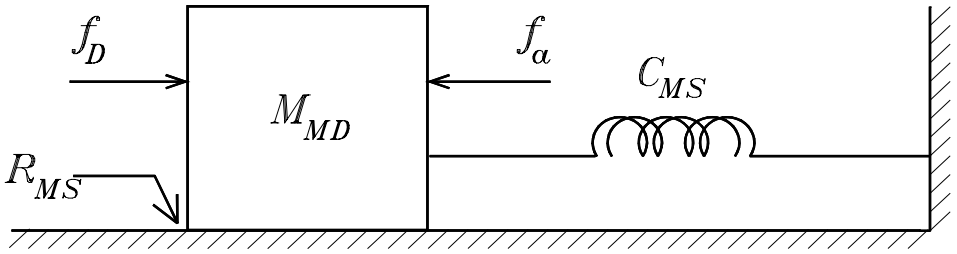

Figure 8. Mechanical system of loudspeaker driver.

The force f_D is the force generated by the flow of the current in the voice coil. It is given by

$$f_D = B\ell i_c. \tag{37}$$

The force f_a represents the opposing force caused by the air load on the diaphragm when it moves. This force always opposes the motion of the diaphragm. It is proportional to the pressure difference between the front and back sides of the loudspeaker diaphragm and is

given by

$$f_a = p_D S_D \tag{38}$$

where p_D is the pressure difference from the front to the back of the diaphragm and S_D is the area of the diaphragm.

The force f_D applied to the diaphragm by the voice coil must equal the sum of the forces opposing its motion. This can be written in phasor form

$$f_D = j\omega M_{MD} u_D + \frac{1}{j\omega C_M} u_D + R_M u_D + f_a. \tag{39}$$

It follows from this equation that the electrical impedance analogous circuit which models the mechanical part of the loudspeaker driver is that shown in Figure 9.

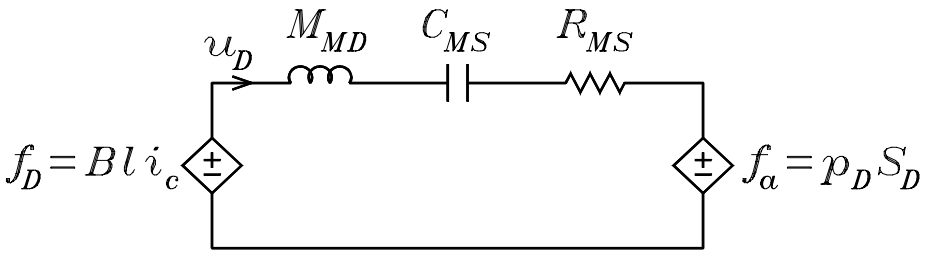

Figure 9. Impedance analogous circuit of the mechanical part of a loudspeaker driver.

2.4.3 The Acoustical Circuit

When the loudspeaker diaphragm moves, it emits a volume velocity given by $U_D = u_D S_D$. This volume velocity flows through the acoustical impedances that model the air loads on both sides of the diaphragm to create the pressure difference p_D. Thus the acoustical part of the loudspeaker driver can be modeled by the circuit shown in Figure 10. In the figure, Z_{AF} and Z_{AB} are the acoustical impedances seen by the front and back, respectively, of the diaphragm. In the following, each of these impedances are approximated by that for a circular piston in an infinite baffle.

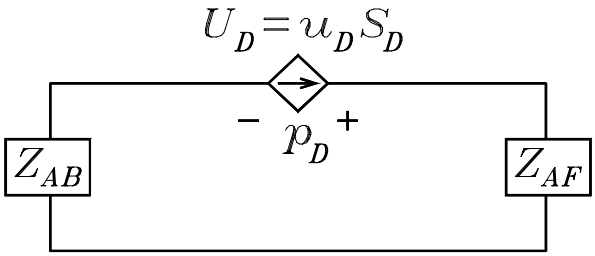

Figure 10. Impedance analogous circuit of the acoustical part of a loudspeaker driver.

2.4.4 The Combination Circuit

If the loudspeaker electrical, mechanical, and acoustical parameters modeled by the elements in Figures 7, 9, and 10 are known, the circuits can be used to calculate such quantities as the velocity of the diaphragm, the volume velocity that it emits, and the electrical input impedance of the voice coil. It follows from the electrical analogous circuit that the voice-coil current i_c is given by

$$i_c = \frac{e_g - B\ell u_D}{Z_{ET}} \tag{40}$$

where Z_{ET} is the electrical impedance

$$Z_{ET} = R_E + \left[(j\omega)^{n_e} L_e\right] \| \, (j\omega L_{E2}) \tag{41}$$

where the symbol $\|$ denotes a parallel combination of impedances, i.e. the product divided by the sum. The mechanical velocity u_D is given by

$$u_D = \frac{B\ell i_c - p_D S_D}{Z_{MD}} \tag{42}$$

where Z_{MD} is the mechanical impedance

$$Z_{MD} = j\omega M_{MD} + \frac{1}{j\omega C_{MS}} + R_{MS}. \tag{43}$$

The pressure difference p_D across the diaphragm is given by

$$p_D = u_D S_D (Z_{AF} + Z_{AB}). \tag{44}$$

For a non-zero R_g, the value of R_E in Equation (41) can be increased to account for it. The output resistance of most contemporary audio amplifiers is negligible.

If Equations (40) and (44) are used to eliminate i_c and p_D from Equation (42), the following expression is obtained:

$$\frac{B\ell e_g}{Z_{ET}} = u_D \left[Z_{MD} + \frac{(B\ell)^2}{Z_{ET}} + S_D^2 (Z_{AF} + Z_{AB}) \right]. \tag{45}$$

The quantity $B\ell e_g / Z_{ET}$ on the left side of this equation has units of force (N). In a mechanical impedance analogous circuit, the velocity u_D on the right side of the equation is modeled by a current. It follows that the analogous circuit for the equation is the that given in Figure 11. The series elements in this circuit model mechanical impedances. The units of mechanical impedance are $\mathrm{N\,s\,m^{-1}}$.

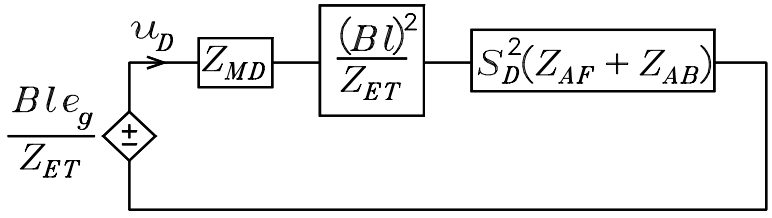

Figure 11. Mechanical combination circuit of a loudspeaker driver.

With $U_D = u_D S_D$, an alternate form of Equation (45) is

$$\frac{B\ell e_g}{Z_{ET} S_D} = U_D \left[\frac{(B\ell)^2}{Z_{ET} S_D^2} + \frac{Z_{MD}}{S_D^2} + (Z_{AF} + Z_{AB}) \right]. \tag{46}$$

In this equation, the quantity on the left side has the units of pressure (Pa). In an acoustical analogous circuit, the volume velocity U_D on the right side is modeled as a current. It follows that an analogous circuit for this equation is the circuit shown in Figure 12, where the impedance Z_{AD} is the acoustical impedance given by

$$\begin{aligned} Z_{AD} &= \frac{Z_{MD}}{S_D^2} \\ &= j\omega \frac{M_{MD}}{S_D^2} + \frac{R_{MS}}{S_D^2} + \frac{1}{j\omega S_D^2 C_{MS}}. \end{aligned} \tag{47}$$

In the circuit, the series elements model acoustical impedances. The units of acoustical impedance are acoustical ohms ($\mathrm{N\,s\,m^{-5}}$).

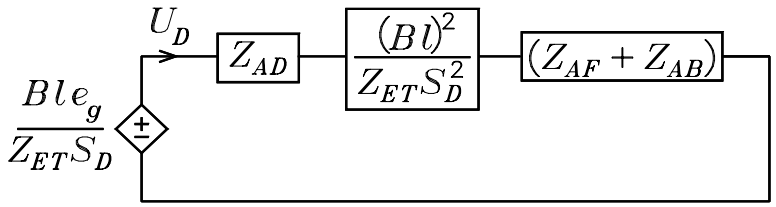

Figure 12. Acoustical combination circuit of a loudspeaker driver.

2.5 Impedance Relationships

In the development of Figure 11, the electrical and acoustical circuits are "reflected" into the mechanical circuit to obtain a single analogous circuit that explicitly shows the effects of the impedances of the three separate but linked circuits on the mechanical velocity u_D. By examining the terms of Equation (45), the relationships between the reflected impedances can be found. The last term on the right side of the equation gives the general relationship between reflected mechanical and acoustical impedances.

To obtain the mechanical impedance that results from an acoustical impedance in a system linked by a mechano-acoustical transducer, the acoustical impedance is multiplied by the piston area squared, that is

$$Z_M = S_D^2 Z_A \tag{48}$$

where Z_M is a mechanical impedance having the units of mechanical ohms ($\mathrm{N\,s\,m^{-1}}$) and Z_A is the acoustical impedance having the units of acoustical ohms ($\mathrm{N\,s\,m^{-5}}$). When the expressions for the impedances of the circuit elements are substituted for Z_M and Z_A, the following equations that relate mechanical mass M_M, compliance C_M, and resistance R_M to acoustical mass M_A, compliance C_A, and resistance R_A are

$$M_A = \frac{M_M}{S_D^2} \tag{49}$$

$$C_A = C_M S_D^2 \tag{50}$$

$$R_A = \frac{R_M}{S_D^2}. \tag{51}$$

The second term of Equation (45) illustrates the general relationship between reflected electrical and mechanical impedances in a system linked by a electromagnetic mechanical transducer. The relation is

$$Z_M = \frac{(B\ell)^2}{Z_E}. \tag{52}$$

The impedance $(Z_E)^{-1}$ is known of as the dual of the impedance Z_E. In this case, it is scaled by the factor $(B\ell)^2$ to convert to a mechanical impedance. This can be converted into an acoustical impedance by dividing by S_D^2 to obtain

$$Z_A = \frac{(B\ell)^2}{S_D^2 Z_E}. \tag{53}$$

These transformations appear in Figures 11 and 12.

Some rules for reflecting the circuit elements of Figures 7, 9, and 10 from one circuit into another can be determined by examining how the equations in Section 2.4.4 are obtained. In the reflected circuits, the controlled sources are replaced by lumped-element equivalent circuits. Although it is not explicitly shown in Figures 7, 9, and 10, the controlled voltage sources representing e_c and f_a are controlled by the currents through the the sources. For example, when Equation (44) is used to replace p_D in the equation for $f_a = p_D S_D$, it can be seen that f_a becomes a function of u_D.

When a controlled voltage source is controlled by the current through the source, it can be replaced by a passive impedance given by the ratio of the voltage to the current. In the case of the source f_a in Figure 9, this impedance is $S_D^2 (Z_{AF} + Z_{AB})$. This is the same as what is obtained from Equation (48) that reflect an acoustical impedance into a mechanical impedance.

The controlled source f_D in Figure 9 is controlled not only by the current u_D through it but also by the independent source e_g in Figure 7. This can be seen when Equation (40) is used in the expression $f_D = B\ell i_c$. Thus the controlled force source f_D can be replaced by a reflected electrical impedance given by Equation (52) in series with the reflected force source $B\ell e_g / Z_{ET}$ that results from the independent voltage source e_g.

2.6 Air-Load Impedances

Figure 10 shows the two acoustical impedances Z_{AF} and Z_{AB} which model the external air load on the loudspeaker diaphragm. These impedances represent the ratio of the phasor pressure at the center of the diaphragm to the phasor volume velocity emitted by the diaphragm. There are two well-known analogous circuits for this air load impedance that are based on the analysis of a plane circular piston vibrating in an infinite baffle and in the end of a long tube. Although these circuits are derived for a flat piston, they can be used to accurately model the loudspeaker diaphragm at low frequencies where the wavelength is large compared to the diameter of the diaphragm [27].

Figure 13 illustrates a loudspeaker mounted in an infinite baffle and on a long tube. In the figure, Z_{AL} denotes the acoustical impedance seen by the free-air side of the diaphragm. Because of the symmetry of the infinite-baffle mounting, the same impedance is seen by both the front and the back sides of the loudspeaker diaphragm. The acoustical impedance for either of these configurations can be modeled by the circuit shown in Figure 14 [27].

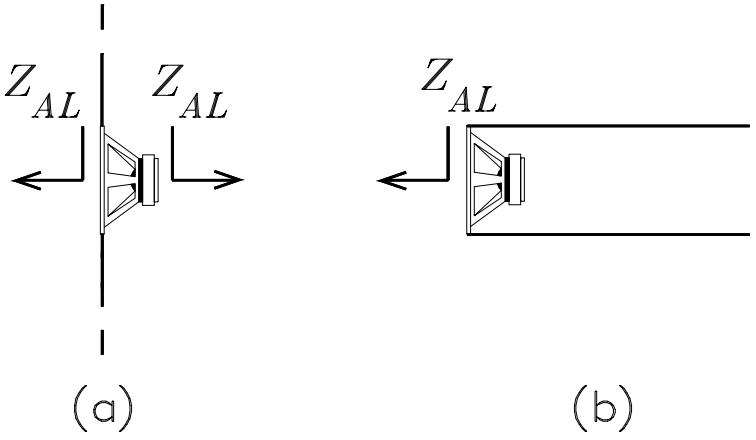

Figure 13. A driver mounted on (a) an infinite baffle and on (b) a tube.

For the piston mounted in an infinite baffle, the circuit element values are given by

$$M_{A1} = \frac{8\rho_0}{3\pi^2 a_D} \tag{54}$$

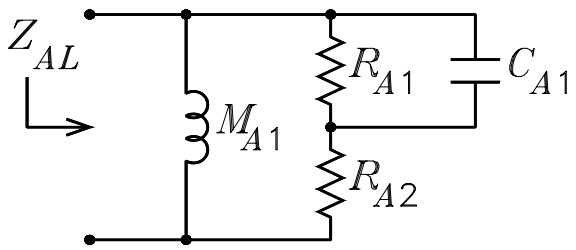

Figure 14. Circuit model of the impedance seen by an oscillating piston on either an infinite baffle or a tube.

$$R_{A1} = \frac{0.4410\rho_0 c}{\pi a_D^2} \tag{55}$$

$$R_{A2} = \frac{\rho_0 c}{\pi a_D^2} \tag{56}$$

$$C_{A1} = \frac{5.94 a_D^3}{\rho_0 c^2} \tag{57}$$

where a_D is the diaphragm radius. For the piston mounted at the end of a long tube, the element values are given by

$$M_{A1} = \frac{0.6133\rho_0}{\pi a_D} \tag{58}$$

$$R_{A1} = \frac{0.5045\rho_0 c}{\pi a_D^2} \tag{59}$$

$$R_{A2} = \frac{\rho_0 c}{\pi a_D^2} \tag{60}$$

$$C_{A1} = \frac{0.55\pi^2 a_D^3}{\rho_0 c^2}. \tag{61}$$

For calculations at low frequencies, the acoustical mass M_{A1} in each of these circuits exhibits an impedance that is small compared to that of the other elements that are in parallel with it. Because the smaller impedance in a parallel circuit dominates, the impedance of the circuit can be approximated by that of the mass alone [27]. This approximation is used in the following.

2.7 The Voice-Coil Electrical Impedance

The voice-coil impedance of the loudspeaker is its electrical impedance. If the diaphragm is blocked so that it cannot move, this impedance would be combined impedance of the

resistance and inductance of the coil of wire. If the diaphragm is not blocked, a back emf is generated in the voice coil when it moves that is proportional to the velocity of the coil. This voltage is modeled by the voltage-controlled voltage source e_c in Figure 7. This source can be replaced with a passive lumped-parameter impedance that is called the motional impedance of the voice coil. This impedance is derived in this section.

At very low frequencies, the voice-coil impedance is approximately equal to its resistance R_E shown in Figure 7. As frequency is increased, the series mass M_{MD} and compliance C_{MS} in the mechanical circuit of Figure 9 exhibit a series resonance which causes the mechanical velocity u_D in that figure to exhibit a maximum. The series resonance of the mechanical circuit causes the voltage-controlled voltage source e_c in Figure 7 to exhibit a maximum, thus causing the current i_c to exhibit a minimum. It follows that the voice-coil electrical impedance exhibits a maximum at this resonance frequency. As frequency is increased further, the mechanical velocity u_D decreases, causing the electrical impedance Z_E to decrease to a value approaching the voice-coil resistance R_E. The impedance then increases as frequency is increased. This increase is caused by the lossy voice-coil inductance. In the high frequency range where the inductive impedance dominates, the magnitude of the impedance increases at a rate of n_e decades per decade, where n_e is the exponent in the lossy inductance impedance equation given by Equation (31).

When Equation (44) is used to eliminate the acoustic pressure difference p_D from Equation (42), it follows that the diaphragm mechanical velocity u_D is given by

$$u_D = \frac{B\ell i_c}{Z_{MD} + S_D^2 \left(Z_{AF} + Z_{AB}\right)}. \tag{62}$$

This equation can be used to eliminate u_D from Equation (40) to obtain an equation involving only e_g and i_c. This equation is

$$e_g = i_c \left[Z_{ET} + \frac{(B\ell)^2}{S_D^2} \frac{1}{Z_{AD} + Z_{AF} + Z_{AB}} \right] \tag{63}$$

where Z_{AD} is the acoustical impedance associated with the mechanical impedance Z_{MD}.

It is given by

$$Z_{AD} = \frac{Z_{MD}}{S_D^2}. \tag{64}$$

The electrical input impedance Z_{VC} is the ratio e_g to i_c. It is given by

$$Z_{VC} = Z_{ET} + \frac{(B\ell)^2}{S_D^2} \frac{1}{Z_{AD} + Z_{AF} + Z_{AB}}. \tag{65}$$

The second term in this equation is the motional impedance. The acoustical impedance term $(Z_{AD} + Z_{AF} + Z_{AB})^{-1}$ in this equation in interpreted as the impedance of the dual circuit of three series acoustical impedances. This dual impedance is scaled by the factor $(B\ell)^2 / S_D^2$ to convert it into an electrical impedance. This is consistent with the observations in Section 2.5. Because taking the dual of a circuit with series elements converts the circuit into elements in parallel, the motional impedance consists of parallel elements in the electrical analogous circuit of the voice coil.

If the loudspeaker is mounted in an infinite baffle, at low frequencies Z_{AF} and Z_{AB} can be modeled by acoustical masses having a value M_{A1} given by Equation (54). For this case, Z_{AF} and Z_{AB} can be combined with M_{AD} to give the total acoustical mass of the diaphragm. This is denoted by M_{AS} and is given by

$$M_{AS} = M_{AD} + 2M_{A1}. \tag{66}$$

With this definition, the electrical impedance of the voice coil given by Equation (65) for the loudspeaker in an infinite baffle can be written

$$\begin{aligned} Z_{VC} &= R_E + \left[(j\omega)^{n_e} L_e\right] \| (j\omega L_{E2}) \\ &\quad + \frac{1}{j\omega C_{MES} + (R_{ES})^{-1} + (j\omega L_{CES})^{-1}} \end{aligned} \tag{67}$$

where C_{MES}, R_{ES}, and L_{CES} are given by

$$L_{CES} = \frac{(B\ell)^2 C_{AS}}{S_D^2} \tag{68}$$

$$C_{MES} = \frac{S_D^2 M_{AS}}{(B\ell)^2} \tag{69}$$

$$R_{ES} = \frac{(B\ell)^2}{S_D^2 R_{AS}}. \tag{70}$$

Equation (67) makes it possible to draw an equivalent circuit that models the electrical impedance of the loudspeaker. The first two terms represent the electrical impedance of the blocked voice coil. The third term models the motional impedance that results from the mechanical suspension of the loudspeaker driver and its acoustical air load. It is the reciprocal of the sum of three admittances. It follows that the motional impedance is the parallel combination of three elements, a capacitor C_{MES}, an inductor L_{CES}, and a resistor R_{ES}. the equivalent circuit is shown in Figure 15.

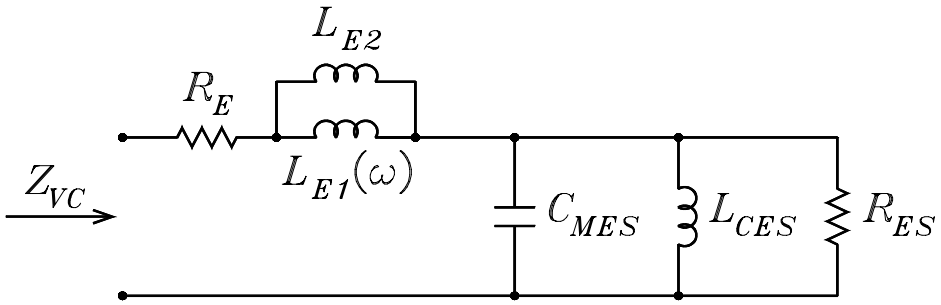

Figure 15. Equivalent circuit model of the driver voice-coil impedance.

A plot of the measured magnitude of the input impedance of one of the test loudspeakers used in this work is shown in Figure 16. Also shown in the figure are plots of the magnitudes of the impedance of the individual terms in Equation (67) that were calculated from the loudspeaker parameters that were estimated from the measurements. The figure illustrates how the individual terms combine to form the total impedance.

2.8 Measuring the Voice-Coil Impedance

Measured voice-coil impedance data can be used to determine the significant parameters of a loudspeaker. Basic techniques for making these measurements and calculating the parameters are described in [3]. For this research, an automated data acquisition system was used to measure the data. The system consisted of a computer controlled Audio Precision System Two analyzer that is manufactured by Audio Precision, Inc. This device is

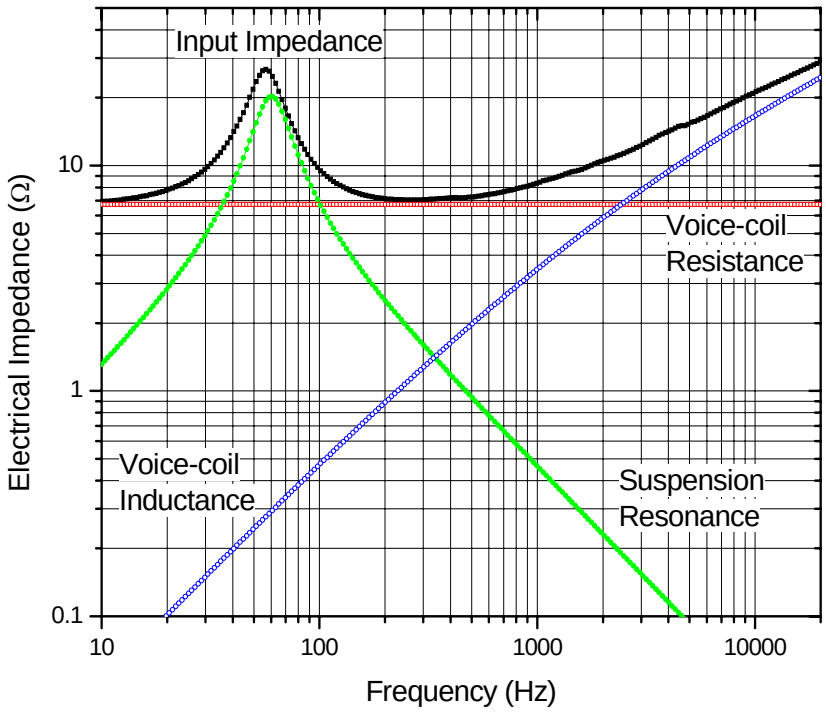

Figure 16. Driver input impedance and impedance components.

capable of automatically making automated audio-related measurements at frequencies in the audio band. Example measurements are gain, phase, and distortion versus frequency. The analyzer is capable of generating both analog and digital test signals. It is connected to a personal computer and controlled through a software package that is called APWIN [31]. Test procedures are written in a modified version of Visual Basic called AP Basic that controls the analyzer.

A technical note [32] is provided by Audio Precision, Inc. that gives a procedure for making impedance measurements. However, it was determined that the procedure given in the technical note is incorrect, so a new procedure was developed for this work. A schematic diagram showing the analyzer test setup for impedance measurement is shown in Figure 17. The AP analyzer was programmed to place a specified value resistor R_g in series with its output voltage e_g. By measuring the amplitude and phase of the voltage on both sides of the resistor, the impedance can be calculated. Knowing the value of R_g, the

electrical input impedance can be calculated from the relation

$$Z_{VC} = \frac{e_1}{i_1} = R_g \frac{e_1}{e_g - e_1}. \tag{71}$$

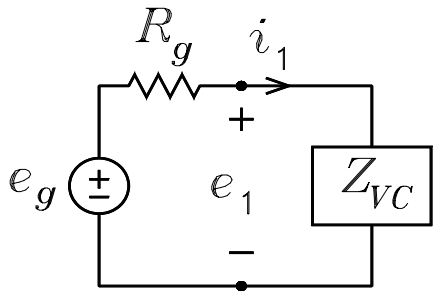

Figure 17. Experimental setup for measuring the voice-coil impedance.

If e_g is considered to have a phase reference of zero and e_1 is complex and of the form $E_m \exp(j\theta)$, it can be shown that the magnitude and phase of the voice-coil impedance Z_{VC} are given by

$$|Z_{VC}| = \frac{R_g}{\sqrt{\left(\frac{e_g}{E_m}\right)^2 - 2\frac{e_g}{E_m}\cos\theta + 1}} \tag{72}$$

$$\arg(Z_{VC}) = \tan^{-1}\left(\frac{\frac{e_g}{E_m}\sin\theta}{\frac{e_g}{E_m}\cos\theta - 1}\right). \tag{73}$$

To obtain the voice-coil impedance data versus frequency with the AP analyzer, a test procedure that implements Equations (72) and (73) was written. This procedure is given in Appendix A. The procedure sweeps the frequency of e_g while making measurements of the magnitude and phase of e_g and e_1 versus frequency. From the data obtained, the magnitude and phase of the voice-coil impedance are calculated. The frequency, magnitude, and phase data are exported to a file, and graphs of the magnitude and phase of the measured impedance versus frequency are generated.

2.9 The Loudspeaker Driver Parameters

The parameters R_E, L_e, n_e, L_{E2}, M_{AS}, C_{AS}, R_{AS}, S_D, and $B\ell$ determine the circuit elements in the loudspeaker model of Figures 7, 9, and 10. These parameters are functions

of the loudspeaker construction and the materials that it is fabricated from. Because the parameters determine the impedance of the equivalent circuit in Figure 15, it follows that numerical values of the parameters for a given loudspeaker can be found from measured data of the loudspeaker electrical impedance as a function of frequency.

As can be seen from the impedance plots in Figure 16, the magnitude of the impedance caused by the fundamental velocity resonance dominates over the voice-coil inductance term at lower frequencies. The opposite is true at higher frequencies. The resistance term R_E is constant with frequency, and it dominates where both the resonance term and the voice-coil inductance term are small. This occurs at zero frequency and in the transition region between the velocity resonance peak and the voice-coil inductance dominance.

Although M_{AS}, C_{AS}, R_{AS}, R_E, and $B\ell$ fully specify the low-frequency behavior of a loudspeaker, drivers are often characterized by an equivalent set of parameters known as the small-signal parameters. These five parameters are related to the circuit-element parameters by the following equations:

$$f_s = \frac{1}{2\pi\sqrt{M_{AS}C_{AS}}} \tag{74}$$

$$Q_{MS} = \frac{1}{R_{AS}}\sqrt{\frac{M_{AS}}{C_{AS}}} \tag{75}$$

$$Q_{ES} = \frac{1}{R_{AE}}\sqrt{\frac{M_{AS}}{C_{AS}}} \tag{76}$$

$$Q_{TS} = \frac{Q_{MS}Q_{ES}}{Q_{MS}+Q_{ES}} \tag{77}$$

$$V_{AS} = \rho_0 c^2 C_{AS}. \tag{78}$$

In these equations, f_s is the velocity resonance frequency, Q_{MS} is the mechanical quality factor, Q_{ES} is the electrical quality factor, Q_{TS} is the total quality factor, and V_{AS} is the volume compliance. The volume compliance V_{AS} is the equivalent closed volume of air that, when compressed by a piston having the same area as the loudspeaker diaphragm, exhibits a compliance equal to the loudspeaker suspension compliance C_{AS}.

The electrical impedance of the voice coil given in Equation (67) can be expressed by an equivalent expression involving these small-signal parameters. This equation expresses the velocity resonance term in the form of a second-order, band-pass transfer function given by

$$\begin{aligned} Z_{VC} &= R_E + \left[(j\omega)^{n_e} L_e\right] \| (j\omega L_{E2}) \\ &\quad + R_{ES} \frac{(1/Q_{MS})(j\omega/\omega_s)}{(j\omega/\omega_s)^2 + (1/Q_{MS})(j\omega/\omega_s) + 1}. \end{aligned} \tag{79}$$

where $\omega_s = 2\pi\, f_s$. The resistance R_{ES} in this equation is defined in Equation (70). It can be shown that this equation reduces to

$$R_{ES} = \frac{Q_{MS}}{Q_{ES}} R_E. \tag{80}$$

2.9.1 Determination of the Low-Frequency Circuit Elements

To determine the values of M_{AS}, C_{AS}, R_{AS}, and $B\ell$ for a given loudspeaker, the measurements are made at frequencies low enough to consider the voice-coil inductance to have a negligible impedance. This is because it usually has little effect at the lower frequencies where the velocity resonance parameters dominate the impedance. The equation for the input impedance given by Equation (67) with $L_{E1}(\omega) = 0$ and $L_{E2} = 0$ can be fit to the low-frequency portion of the measured impedance versus frequency graph to obtain values for L_{CES}, C_{MES}, and R_{ES}. Data analysis software that implements the Levenberg-Marquardt fitting routine [33], [34] was used to simplify this task in this research.

The value of R_E can be easily measured with a dc ohmmeter and used in the curve fitting routines. To determine values for M_{AS}, C_{AS}, R_{AS}, and $B\ell$ from values of L_{CES}, C_{MES}, and R_{ES}, more information is needed because four parameters are to be determined. A fourth equation must be known.

To obtain a fourth equation, the impedance versus frequency can again be measured after the loudspeaker system is altered in a known way. One way to do this is to add a known additional mass to the loudspeaker diaphragm. This can be done by placing small

magnets or a magnet and an iron material on both sides of the diaphragm so that their attraction clamps them to the diaphragm. It is probably best to place at least two pairs of these weights, one on each side of the diaphragm center along a diameter so that the diaphragm remains mechanically balanced.

A second method of adding additional mass is to press pieces of plumber's putty on the diaphragm. The putty adheres to the diaphragm and can later be removed. When calculating the loudspeaker parameters for a system with added mass, the diaphragm area must be known. In addition, an accurate scale must be available to measure the weights. The magnets can be measured once and marked with their weights, but the putty would most probably have to be measured each time.

Another way of altering the system is to place a known acoustical compliance C_T on one side of the diaphragm. The compliance C_T can be created by placing the loudspeaker on a test box. Let this be a closed box of air having a volume V_T. To reduce losses added to the system, the box must not be lined or filled with any fibrous materials. At frequencies where the box dimensions are much less than a wavelength, the impedance of the box can be modeled as an acoustical compliance. This compliance is given by

$$C_T = \frac{V_T}{\rho_0 c^2}. \tag{81}$$

In the analogous circuit, C_T combines in series with C_{AS}. When Equation (67) is fit to the impedance curve with the added compliance, the new value of L_{CES} obtained is given by

$$L_{CES}^{new} = \frac{(B\ell)^2}{S_D^2} \frac{C_{AS} C_T}{C_{AS} + C_T}. \tag{82}$$

This equation and Equations (68) through (70) can be used to solve for the parameter values from the measured impedance data by the curve fitting routines.

Equation (67), in which all of the parameters are contained, can be simultaneously fitted to the voice-coil impedance curves obtained with and without the loudspeaker mounted on the test box. When fitting the off-box impedance curve to the measured data, L_{CES} given

by Equation (68) is used in Equation (67). When fitting the on-box impedance curve, L_{CES}^{new} is used. The parameters $B\ell$ and R_E are shared between the two equations, that is they are unchanged by the addition of the test compliance box.

The acoustical resistance R_{AS} that models the mechanical losses in the system does not change significantly with the addition of the test box if it is assumed that the box introduces negligible losses. This loss can be determined experimentally by comparing the amplitudes of the measured impedance peaks at the resonance frequencies with and without the box. A lossless box results in no height change, while box losses cause a reduction of this amplitude. Addition of the box causes the acoustical mass load on one side of the loudspeaker diaphragm to change compared to its value in free air. This change is small and is commonly neglected in modeling the box [3], [4].

To apply the curve fitting routines to the measured data, initial estimates of the parameters to be estimated must be known. To determine these, a method described in [3] was used. This method involves calculating the parameters from measurements of the voice-coil impedance at three test frequencies. The dc voice-coil resistance R_E is found by measuring the resistance of the voice coil with an ohmmeter. Figure 18 shows the plot of the measured voice-coil impedance versus frequency in the band around the fundamental resonance frequency for the loudspeaker used used for Figure 16. The resonance frequency f_s is the frequency at which the impedance exhibits a peak and can be read directly from the impedance data. It follows from Equation (79) that the magnitude of the input impedance curve at $f = f_s$ rises to $R_E + R_{ES}$ if the frequency is low enough so that the impedance rise due to the voice-coil inductance can be neglected.

Figure 18 shows a horizontal dashed line intersecting the vertical axis at the level $|Z_{VC}| = R_1$. Let the frequencies at which this line crosses the impedance curve on each side of the resonance peak be denoted by f_1 and f_2. With these definitions, it follows that

$$|Z_{VC}(2\pi f_1)| + |Z_{VC}(2\pi f_2)| = 2R_1. \tag{83}$$

It can be shown [3] that Equations (79) and (83) can be solved simultaneously for Q_{MS} to

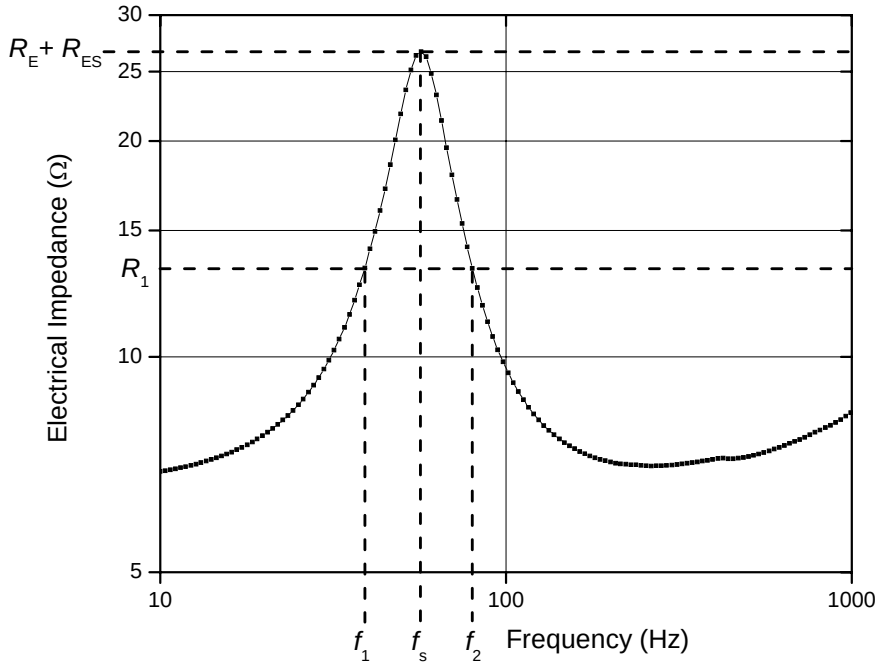

Figure 18. Driver input impedance curve used to determine the small-signal parameters.

obtain

$$Q_{MS} = \frac{f_s}{f_2 - f_1}\sqrt{\frac{(R_E + R_{ES})^2 - R_1^2}{R_1^2 - R_E^2}}. \tag{84}$$

If R_1 is chosen to be the geometric mean of R_E and $(R_E + R_{ES})$ given by

$$R_1 = \sqrt{R_E\,(R_E + R_{ES})} \tag{85}$$

it is straightforward to show that Q_{MS} can be calculated from the following simplified equation

$$Q_{MS} = \frac{f_s}{f_2 - f_1}\sqrt{\frac{R_E + R_{ES}}{R_E}}. \tag{86}$$

Equations (75) and (76) can be combined to obtain the relationship between Q_{MS} and Q_{ES} in terms of the measured values for R_E and R_{ES}. It is given by

$$\begin{aligned} Q_{ES} &= Q_{MS}\frac{R_{AE}}{R_{AS}} \\ &= Q_{MS}\frac{R_E}{R_{ES}}. \end{aligned} \tag{87}$$

With Q_{MS} found from Equation (84), Q_{ES} and Q_{TS} can be solved for with Equations (87) and (77).

To measure the volume compliance V_{AS} of the loudspeaker, the driver is mounted on the closed test box of volume V_T and the voice-coil impedance is measured. Let the on-box parameters be denoted as f_{CT}, Q_{MCT}, Q_{ECT}, and Q_{TCT}. The resonance frequency f_{CT} and mechanical quality factor Q_{MCT} for the on-box impedance curve can be determined by the procedure described above for the off-box data. In this case, the resonance frequency and electrical quality factor, respectively, on the test box are given by

$$f_{CT} = \frac{1}{2\pi\sqrt{M_{ACT}C_{AT}}} \tag{88}$$

$$Q_{ECT} = \frac{S_D^2 R_E}{(B\ell)^2}\sqrt{\frac{M_{ACT}}{C_{AT}}} \tag{89}$$

where C_{AT} is the combined acoustical compliance of the suspension and the test box given by

$$C_{AT} = \frac{C_{AS}C_T}{C_{AS}+C_T}. \tag{90}$$

Equations (78) and (81) can be used to rewrite Equation (90) as

$$C_{AT} = \frac{1}{\rho_0 c^2}\frac{V_{AS}V_T}{V_{AS}+V_T}. \tag{91}$$

To eliminate the unknown quantity M_{ACT}, the product of Equations (88) and (89) is taken to obtain

$$f_{CT}\,Q_{ECT} = \frac{1}{2\pi\,R_{AE}C_{AT}}. \tag{92}$$

Similarly, for the off-box case the following equation is obtained

$$f_s\,Q_{ES} = \frac{1}{2\pi\,R_{AE}C_{AS}}. \tag{93}$$

When the ratio of the two above equations is taken, it is found that

$$\begin{aligned}\frac{f_{CT}\,Q_{ECT}}{f_s\,Q_{ES}} &= \frac{C_{AS}}{C_{AT}} \\ &= 1+\frac{V_{AS}}{V_T}.\end{aligned} \tag{94}$$

This equation can be solved for V_{AS} to obtain

$$V_{AS} = V_T\left(\frac{f_{CT}\,Q_{ECT}}{f_s\,Q_{ES}}-1\right). \tag{95}$$

This equation can be used to calculate the volume compliance V_{AS} of the loudspeaker from the measured off-box and on-box impedance data.

2.9.2 Determination of the Voice-coil Inductance Parameters

In [26], the contribution of the voice-coil inductance to the voice-coil input impedance is modeled as a lossy inductor having an impedance of the form $(j\omega)^{n_e}L_e$. When the magnitude of this impedance is plotted versus frequency, it exhibits a constant slope of n_e decades per decade when plotted on log-log scales. The phase exhibits the value $n_e \times 90^\circ$. The value of n_e can range from 0 to 1. For $n_e = 0$, the impedance is that of a pure resistance, and for $n_e = 1$ it is that of a pure inductance. From Figure 16, it can be seen that the voice-coil impedance shown for the driver used in this research does approach a constant slope at high frequencies, making the lossy inductor a good model at high frequencies.

In the course of this work, it was found that the lossy voice-coil inductor model can be improved by including a lossless inductor in parallel with the lossy inductor. The lossless inductor models the inductance that results from that part of the magnetic field generated by current in the voice coil that does not flux through the magnet structure of the loudspeaker. The addition of this inductor better models the effects of the voice-coil inductance on the loudspeaker input impedance in the mid-frequency region above the fundamental resonance frequency. In the measurement of several drivers, it was found that for loudspeakers having values of n_e greater than approximately $n_e = 0.7$, the addition of the lossless inductor has little effect on the accuracy of the voice-coil impedance model.

It follows from Equation (67) that the measured voice-coil impedance is modeled as the sum of three terms. Once M_{AS}, C_{AS}, R_{AS}, $B\ell$, and R_E are determined from measured impedance data, the motional impedance term, along with the dc voice-coil resistance R_E, can be subtracted from the measured voice-coil impedance to obtain the contribution to the impedance of the voice-coil inductance. When this is done, the magnitude and phase plots of the impedance that results from the voice-coil inductance alone can be obtained. Figure 19 shows this data for the test loudspeaker used for Figure 16.

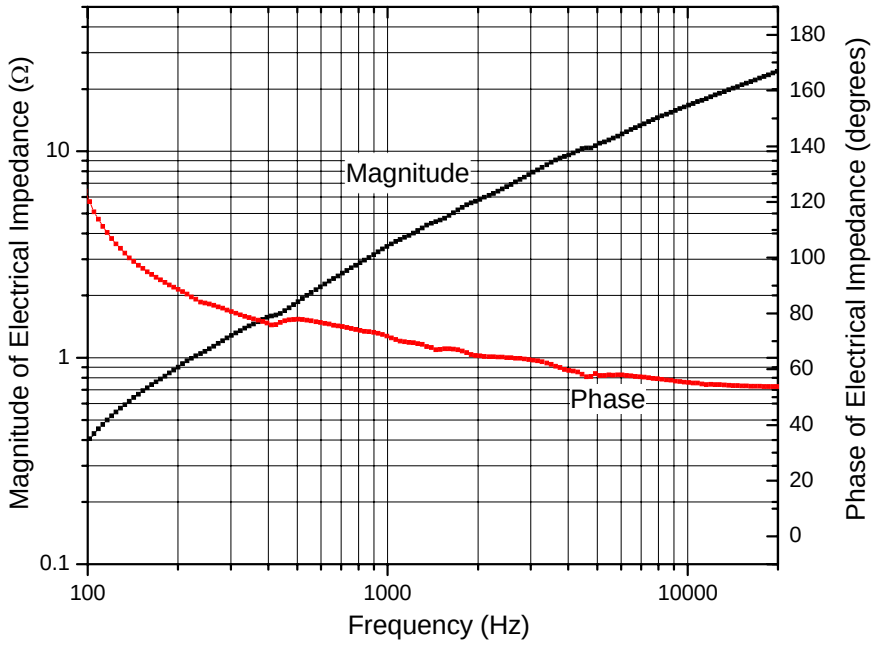

Figure 19. Measured magnitude and phase of the voice-coil inductance term.

Figure 19 shows that the slope of the magnitude plot is approximately unity (one decade per decade) at the lower frequencies, which is the characteristic of the impedance of a lossless inductor. As frequency is increased, the slope approaches a constant less than unity, which is the characteristic of the lossy inductor model. This slope at higher frequencies approaches a value equal to the exponent n_e in Equation (31). Thus the measured data indicate that the lossless inductor L_{E2} in parallel with the lossy inductor $L_{E1}(\omega)$ is required to accurately model the voice-coil impedance data in the figure. "Glitches" in the impedance data that are the result of mechanical resonances in the diaphragm are not accounted for in the model.

The impedance of the lossless inductor L_{E2} becomes large at higher frequencies, so the impedance of the parallel combination of the two inductors given by $\left[(j\omega)^{n_e} L_e\right] \parallel (j\omega L_{E2})$ at high frequencies mostly results from the lossy inductor contribution. Thus at high frequencies, L_{E2} can be neglected and the curve-fitting method described in [26] can be used to estimate L_e and n_e.

A simpler method than that described in [26] was used to estimate values for L_e and

n_e from the measured data for this work. It uses the measured magnitude and phase of the impedance at a single high frequency well above the fundamental resonance frequency. This frequency must be high enough so that the impedance of the lossless inductor L_{E2} can be considered to be large compared to the impedance of the lossy inductor $L_{E1}(\omega)$. In this case, the impedance of the lossy inductor can be written

$$\begin{aligned} Z_{E1} &= (j\omega)^{n_e} L_e \\ &= e^{jn_e\pi/2} (\omega)^{n_e} L_e. \end{aligned} \tag{96}$$

When the impedance is written in this form, it can be seen that the magnitude of the impedance is given by

$$|Z_{E1}| = (\omega)^{n_e} L_e \tag{97}$$

and the phase in radians is a constant given by

$$\arg(Z_{E1}) = \frac{n_e\pi}{2}. \tag{98}$$

The magnitude and phase of the voice-coil inductance contribution at a single high frequency can be obtained from the data for Figure 19 and used in Equations (97) and (98) to solve for values of L_e and n_e. The frequency at which the magnitude and phase are obtained might be chosen to be 20 kHz. This frequency corresponds to what is commonly taken to be the high-frequency limit of the audio band.

If the impedance is measured at frequencies above 20 kHz, better results for L_e and n_e might possibly be obtained because the effect of L_{E2} is further diminished as the frequency is increased. However, at too high a frequency, electrical resonances that result from the capacitance of the voice-coil winding can affect the impedance. Figure 20 is a plot of the magnitude of the voice-coil impedance from 10 Hz to 200 kHz for the test loudspeaker. It can be seen that the slope of the curve becomes steeper at approximately 50 kHz, indicating that the impedance model of the voice-coil inductance changes at higher frequencies.

Once L_e and n_e are obtained, L_{E2} can be experimentally adjusted to obtain the best curve fit between the measured and modeled voice-coil impedance data. It was found that

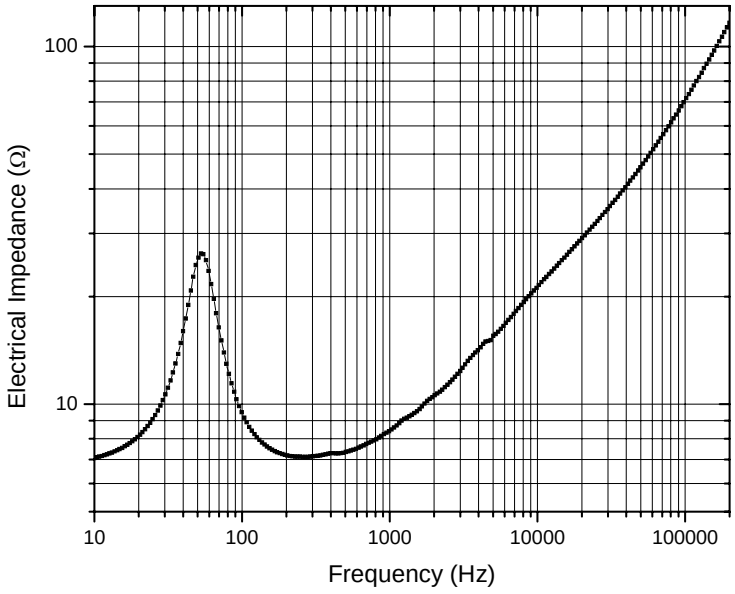

Figure 20. Measured driver input impedance from 10Hz to 200kHz.

Table 1. Parameter values for six inch driver.

M_{AD}	R_{AS}	C_{AS}	$B\ell$	a_D	R_E	L_e	n_e	L_{E2}
54.4	7799.85	1.2856×10^{-7}	4.50	0.06	6.7	0.1554	0.4465	0.00085

this can be quickly done by trial and error. Alternately, a curve-fitting routine can be used. In the process, some adjustments to the values obtained for L_e and n_e can be made to obtain the best curve fit. For the test loudspeaker impedance data shown in Figure 16, the parameters found by curve-fitting are given in Table 1.

Figure 21 shows plots of the high-frequency voice-coil impedance of the test loudspeaker along with plots of the impedance of the lossless inductor L_{E2}, the lossy inductor $L_{E1}(\omega)$, and the parallel combination of the two latter impedances. It can be seen that the parallel combination exhibits excellent agreement with the measured impedance. The figure illustrates that the corner frequency in the transition from the lossless inductor region to the lossy inductor region for the test loudspeaker is approximately 2 kHz.

Figure 22 shows a plot of the measured and modeled voice-coil impedance data for the test loudspeaker. There are two modeled curves, one in which the voice-coil impedance

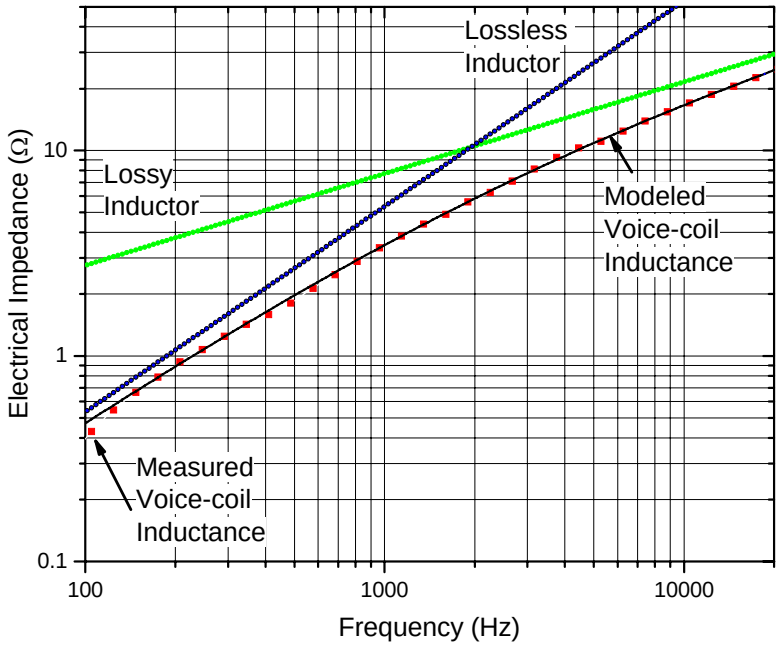

Figure 21. Measured and modeled voice-coil inductance impedances.

is modeled as only a lossy inductor and one in which it is modeled as parallel lossless and lossy inductors. When only the lossy inductor is used in the model, the impedance magnitude is too large in the mid-frequency region. The addition of the lossless inductor L_{E2} decreases the modeled impedance and eliminates this problem.

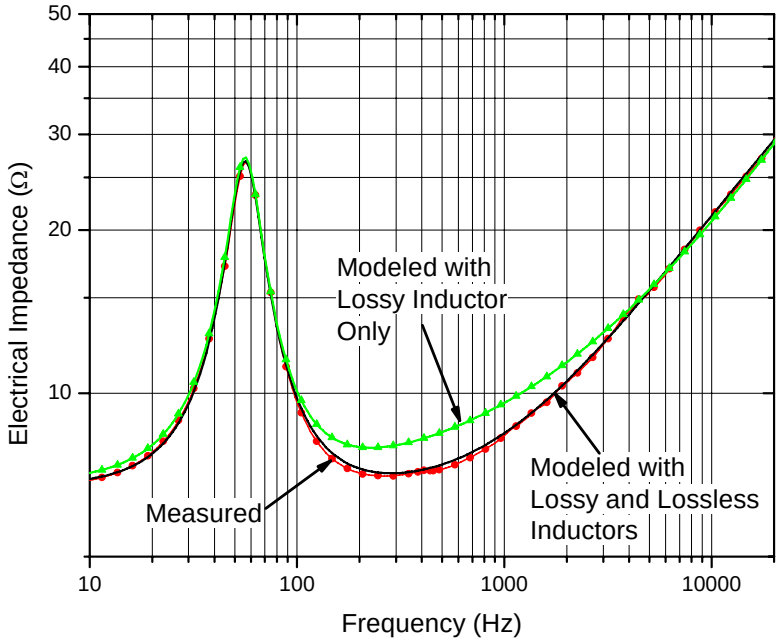

Figure 22. Comparison of measured and modeled driver input impedances.

CHAPTER 3

THE TRANSMISSION LINE MODEL

This chapter presents the development of the electro-acoustical analogous circuit model of an acoustical transmission line that is filled with a fibrous filling. First, the homogeneous acoustical wave equations for the acoustic pressure and particle velocity are reviewed. These equations model the wave propagation in a source free region. The analogous circuit model is then developed for an unfilled line. Finally, modifications are made to the model for the unfilled line to account for the addition of filling into the line.

3.1 The Acoustical Wave Equations

The homogeneous acoustical wave equations for the acoustic pressure p an the particle velocity $\overrightarrow{u}$ in an acoustical wave propagating in free air are [27]

$$\nabla^2 p - \frac{1}{c^2}\frac{\partial^2 p}{\partial t^2} = 0 \tag{99}$$

$$\overrightarrow{\nabla}^2 \overrightarrow{u} - \frac{1}{c^2}\frac{\partial^2 \overrightarrow{u}}{\partial t^2} = 0 \tag{100}$$

where $\nabla^2 p$ is the scalar Laplacian of p and $\overrightarrow{\nabla}^2 \overrightarrow{u}$ is the vector Laplacian of $\overrightarrow{u}$. In rectangular coordinates, these are given by

$$\nabla^2 p = \frac{\partial^2 p}{\partial x^2} + \frac{\partial^2 p}{\partial y^2} + \frac{\partial^2 p}{\partial z^2} \tag{101}$$

$$\overrightarrow{\nabla}^2 \overrightarrow{u} = \frac{\partial u_x}{\partial x}\widehat{x} + \frac{\partial u_y}{\partial y}\widehat{y} + \frac{\partial u_z}{\partial z}\widehat{z}$$

where $\widehat{x}$, $\widehat{y}$, $\widehat{z}$ are the unit vectors in the x, y, and z directions, respectively. The parameter c in the wave equations is the velocity of sound given by

$$c = \sqrt{\frac{\gamma_a P_0}{\rho_0}} \tag{102}$$

where γ_a is the ratio of the specific heat of air at constant pressure to the specific heat at constant volume, P_0 is the ambient air pressure, and ρ_0 is the density of air.

The propagating sound wave is fully described by its pressure p and particle velocity $\overrightarrow{u}$ as a function of position and time. If the source is assumed to vibrate sinusoidally, the time and position dependence of p and $\overrightarrow{u}$ can be isolated and expressions for the two quantities written as

$$p\left(\overrightarrow{r},t\right)=\mathrm{Re}\left[p\left(\overrightarrow{r}\right)e^{j\omega t}\right] \tag{103}$$

$$\overrightarrow{u}\left(\overrightarrow{r},t\right)=\mathrm{Re}\left[\overrightarrow{u}\left(\overrightarrow{r}\right)e^{j\omega t}\right]. \tag{104}$$

In these equation, $p\left(\overrightarrow{r}\right)$ is the phasor pressure and $\overrightarrow{u}\left(\overrightarrow{r}\right)$ is the phasor particle velocity, both as functions of the position vector $\overrightarrow{r}$.

When these expressions are substituted into Equations (99) and (100), the following equations are obtained

$$\mathrm{Re}\left\{\left[\nabla^2 p\left(\overrightarrow{r}\right)+\frac{\omega^2}{c^2}p\left(\overrightarrow{r}\right)\right]e^{j\omega t}\right\}=0 \tag{105}$$

$$\mathrm{Re}\left\{\left[\nabla^2\overrightarrow{u}\left(\overrightarrow{r}\right)+\frac{\omega^2}{c^2}\overrightarrow{u}\left(\overrightarrow{r}\right)\right]e^{j\omega t}\right\}=0. \tag{106}$$

In order for these equations to be equal to zero for all time t, it follows that the terms in the square brackets must be identically zero. Thus the phasor forms of the homogeneous wave equations can be written

$$\nabla^2 p+k^2 p=0 \tag{107}$$

$$\nabla^2\overrightarrow{u}+k^2\overrightarrow{u}=0 \tag{108}$$

where the parameter k is called the wavenumber. It is given by

$$k=\frac{\omega}{c}. \tag{109}$$

Although not explicitly shown, p and $\overrightarrow{u}$ are phasor functions of the position vector $\overrightarrow{r}$.

Equations (107) and (108) are known as the reduced wave equations or Helmholtz equations. These equations can be used to solve for the phasor pressure and particle velocity in free air. To recover the time dependence of these two quantities, the phasor solutions are

multiplied by $\exp(j\omega t)$ and the real part of the resulting expression is found. The phasor solutions for p and $\vec{u}$ are related by [27]

$$\vec{\nabla} p = -j\omega\rho_0 \vec{u}\,. \tag{110}$$

3.2 The Unfilled Transmission Line

Before the development of the general electro-acoustical analogous circuit model for a filled transmission line, the simplest implementation of an unfilled line is first considered. The geometry is a straight, rigid tube having a circular cross-section area. Such a geometry is also referred to as a plane wave tube. It is assumed that the tube is sinusoidally driven by a vibrating piston at one end of the tube having the same diameter as the tube.

Figure 23 illustrates the system. The vibrating piston at the left end of the tube generates a plane wave in the tube. In this case, the equations that describe acoustical wave propagation in the tube are one dimensional. Because the piston is assumed to be rigid, a one-dimensional plane wave mode can be assumed to be generated in the tube. The assumption that the piston vibrates sinusoidally in time allows the time dependence to be removed from the analysis so that the phasor form of the acoustical equations developed in Section 3.1 can be used.

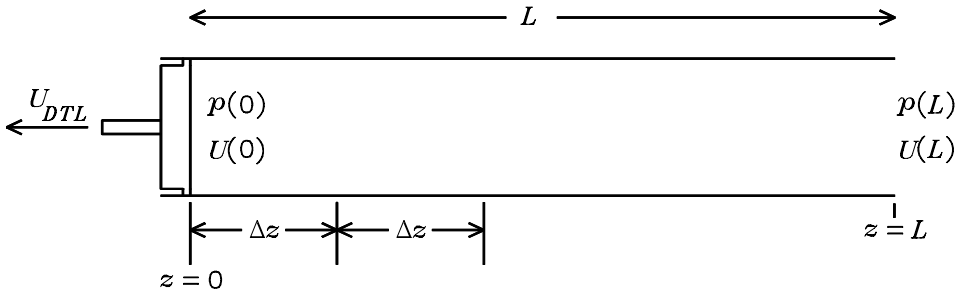

Figure 23. Diagram of transmission line.

The acoustical impedance presented by the line to the piston source in Figure 23 is the ratio of the pressure $p(0)$ at the piston to the volume velocity $U(0)$ that it emits into the line. In the following section, this impedance is solved for by solving the equations

reviewed in Section 3.1 for the acoustical wave in the line. In Section 3.2.2, the electro-acoustical analogous circuit model of the system is developed.

3.2.1 An Acoustical Solution

The pressure and particle velocity inside the tube must satisfy the homogeneous wave equations given in Equations (99) and (100). Because the wave in the tube is assumed to be a plane wave, its amplitude and phase vary only with the distance z along the length of the tube. This allows Equation (107) to be simplified to

$$\frac{d^2 p(z)}{dz^2} + k^2 p(z) = 0. \tag{111}$$

The general solution to this second-order differential equation gives the pressure in the tube as a function of the distance z from the piston. The solution is given by

$$p(z) = p_{0+} e^{-jkz} + p_{0-} e^{+jkz} \tag{112}$$

where p_{0+} is the amplitude of a wave travelling in the $+z$ direction and p_{0-} is the amplitude of a wave travelling in the $-z$ direction. The two waves combine to give the total pressure. When Equation (110) is applied to Equation (112), an expression for the particle velocity is obtained. It is

$$u(z) = \frac{1}{\rho_0 c} \left(p_{0+} e^{-jkz} - p_{0-} e^{+jkz} \right). \tag{113}$$

The acoustical input impedance to the unfilled line is the ratio of the pressure $p(0)$ to the volume velocity $U(0)$ at the source end of the line. It is given by

$$\begin{aligned} Z_{AT} &= \frac{p(0)}{U(0)} \\ &= \frac{p(0)}{S_T u(0)} \\ &= \frac{\rho_0 c}{S_T} \frac{p_{0+} + p_{0-}}{p_{0+} - p_{0-}} \end{aligned} \tag{114}$$

where S_T is the cross-sectional area of the transmission line.

If the tube is infinitely long, there is no wave travelling in the $-z$ direction that occurs from reflections. In this case, the reverse propagating wave is absent and $p_{0-} = 0$. In

this case, the input impedance to the line is called the characteristic impedance Z_C. From Equation (114) with $p_{0-} = 0$, it follows that Z_C is given by

$$Z_C = \frac{\rho_0 c}{S_T}.$$

At the load end of the line, the ratio of $p(L_T)$ to $U(L_T)$ is equal to the acoustical impedance Z_{AL} of the load impedance. It follows that this is given by

$$\begin{aligned} Z_{AL} &= \frac{p(L_T)}{U(L_T)} \\ &= \frac{\rho_0 c}{S_T} \frac{p_{0+} e^{-jkL_T} + p_{0-} e^{+jkL_T}}{p_{0+} e^{-jkL_T} - p_{0-} e^{+jkL_T}}. \end{aligned} \tag{115}$$

This equation can be manipulated to obtain a following relationship between p_{0+} and p_{0-}. It is

$$p_{0+} = \frac{\frac{\rho_0 c}{S_T} p_{0-} e^{+jkL_T} + Z_{AL} p_{0-} e^{+jkL_T}}{Z_{AL} e^{-jkL_T} - \frac{\rho_0 c}{S_T} e^{-jkL_T}}. \tag{116}$$

When Equation (116) is substituted into Equation (114), p_{0+} and p_{0-} can be eliminated, to solve for the acoustical input impedance to the unfilled tube. It is given by

$$Z_{AT} = \frac{\rho_0 c}{S_T} \frac{Z_{AL} + j \frac{\rho_0 c}{S_T} \tan(kL_T)}{\frac{\rho_0 c}{S_T} + j Z_{AL} \tan(kL_T)} \tag{117}$$

$$= Z_C \frac{Z_{AL} + j Z_C \tan(kL_T)}{Z_C + j Z_{AL} \tan(kL_T)} \tag{118}$$

where the identities

$$\cos(\theta) = \frac{1}{2}\left(e^{j\theta} + e^{-j\theta}\right) \tag{119}$$

$$\sin(\theta) = \frac{1}{j2}\left(e^{j\theta} - e^{-j\theta}\right) \tag{120}$$

have been used to simplify the equation.

3.2.2 The Electroacoustic Analogous Circuit of the Line

Let the transmission line be modeled as a series of segments of length Δz as shown in Figure 23, where Δz is the length of the line divided by the number of segments. The air in each segment possesses both an acoustical mass and an acoustical compliance. Because

the line is assumed to be lossless, no acoustical resistance is present. Each segment can be modeled by the electrical analogous circuit shown in Figure 24, where m_{a1} is the acoustical mass of the air in each volume segment and c_{a1} is the acoustical compliance of the air in the segment. $U(z)$ is the volume velocity of the air in the tube at position z and $p(z)$ is the pressure at position z.

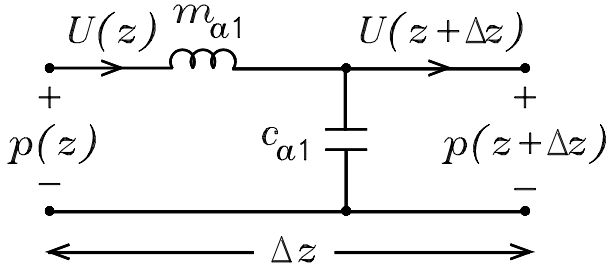

Figure 24. Electroacoustic model for a section of transmission line.

Let m_{aa} be the acoustical mass per unit length and c_{aa} be the acoustical compliance per unit length on the line. These are given by

$$m_{aa} = \frac{\rho_0}{S_T} \tag{121}$$

$$c_{aa} = \frac{S_T}{\rho_0 c^2}. \tag{122}$$

It follows that the values of m_{a1} and c_{a1} in Figure 24 can be written

$$m_{a1} = m_{aa}\Delta z \tag{123}$$

$$c_{a1} = c_{aa}\Delta z. \tag{124}$$

If Δz is made small enough so that the transmission line model is composed of a large number of segments, the line can be modeled as a lumped element model, as is done in obtaining the model of [10]. However, an exact solution can be obtained in the limit as Δz goes to zero. The exact solution makes it unnecessary to use a circuit simulator or write circuit equations to find the pressure and volume velocity at a point in the transmission line.

A pressure wave in any acoustical system results from the mechanical movement of air. The acoustical variables are mechanical variables that are scaled by the area over which the mechanical force acts. This scaling is the link between the mechanical system and the acoustical system. Analogous circuits can be used to model a mechanical system, just as they can model an acoustical system. Because of the close link between the systems, an acoustical system can be represented as a mechanical system, and vice-versa. However, unlike a mechanical mass, air can be compressed and rarefied. This requires the introduction of additional acoustical impedances that are not required if the air is modeled as a non-deformable mechanical mass.

From Section 2.3, it is clear that the acoustical variables of pressure p and volume velocity U are closely related to the mechanical variables of force f and velocity u. Because the acoustical equations are derived from the equations of mechanics, the acoustical system is fundamentally a mechanical system.

The electro-acoustical model of Figure 24 is equivalent to a mechanical diagram of the transmission line as a linked mass-spring system as shown in Figure 25. Each mechanical mass in this figure is related to the corresponding acoustical mass in Figure 24 by $m_{m1} = m_{a1}S^2$, where S is the area of the tube. The mechanical compliance of each spring is related to the corresponding acoustical compliance in Figure 24 by $c_{m1} = c_{a1}/S^2$.

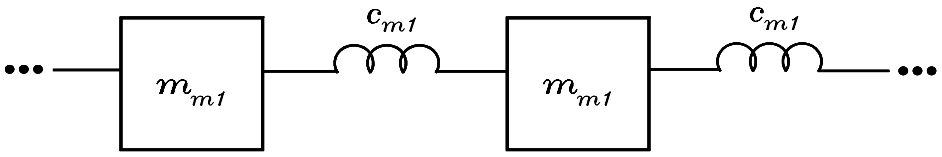

Figure 25. Mechanical system representation of unfilled transmission line.

3.2.2.1 The Wave Equations and their Solutions

With reference to Figure 24, the following equations can be written

$$p\,(z + \Delta z) = p\,(z) - U\,(z)\; j\omega m_{aa}\,\Delta z \tag{125}$$

$$U(z+\Delta z) = U(z) - j\omega c_{aa} p(z+\Delta z)\,\Delta z. \tag{126}$$

These can be rearranged to obtain

$$\frac{p(z+\Delta z) - p(z)}{\Delta z} = -U(z)\, j\omega m_{aa} \tag{127}$$

$$\frac{U(z+\Delta z) - U(z)}{\Delta z} = -j\omega c_{aa} p(z+\Delta z). \tag{128}$$

In the limit as $\Delta z \to 0$, the following first-order differential equations are obtained

$$\frac{dp(z)}{dz} = -j\omega m_{aa} U(z) \tag{129}$$

$$\frac{dU(z)}{dz} = -j\omega c_{aa} p(z). \tag{130}$$

When the derivative of Equation (129) is taken with respect to z and Equation (130) is used to eliminate $dU(z)/dz$, the following equation for $p(z)$ results

$$\frac{d^2 p(z)}{dz^2} + \omega^2 c_{aa} m_{aa} p(z) = 0. \tag{131}$$

Similarly, an equation for $U(z)$ is found to be

$$\frac{d^2 U(z)}{dz^2} + \omega^2 c_{aa} m_{aa} U(z) = 0. \tag{132}$$

The solutions to these differential equations represent plane waves traveling in the tube and are given by

$$p(z) = p_{0+} e^{-\gamma z} + p_{0-} e^{+\gamma z} \tag{133}$$

$$U(z) = U_{0+} e^{-\gamma z} + U_{0-} e^{+\gamma z} \tag{134}$$

where γ is the propagation constant given by

$$\gamma = j\omega\sqrt{c_{aa} m_{aa}}. \tag{135}$$

The phase velocity of the propagating wave is

$$\begin{aligned} c &= \frac{\mathrm{Im}(\gamma)}{\omega} \\ &= \frac{1}{\sqrt{c_{aa} m_{aa}}}. \end{aligned} \tag{136}$$

In Equations (133) and (134), p_{0+} and U_{0+} are the amplitudes of the waves traveling in the $+z$ direction, and p_{0-} and U_{0-} are the amplitudes of the waves traveling in the $-z$ direction. These amplitudes are related to each other by the characteristic impedance of the line Z_C as follows:

$$U_{0+} = \frac{p_{0+}}{Z_C} \tag{137}$$

$$U_{0-} = \frac{-p_{0-}}{Z_C} \tag{138}$$

where

$$Z_C = \sqrt{\frac{m_{aa}}{c_{aa}}}. \tag{139}$$

3.2.2.2 The Line Input Impedance

Figure 26 illustrates the block diagram of an acoustical transmission line having a length L_T and a cross-sectional area S_T. The impedance Z_{AL} is the acoustical impedance presented by the terminating air load on the line. This impedance is discussed in Section 2.6, where the values are those for a piston in the end of a long tube.

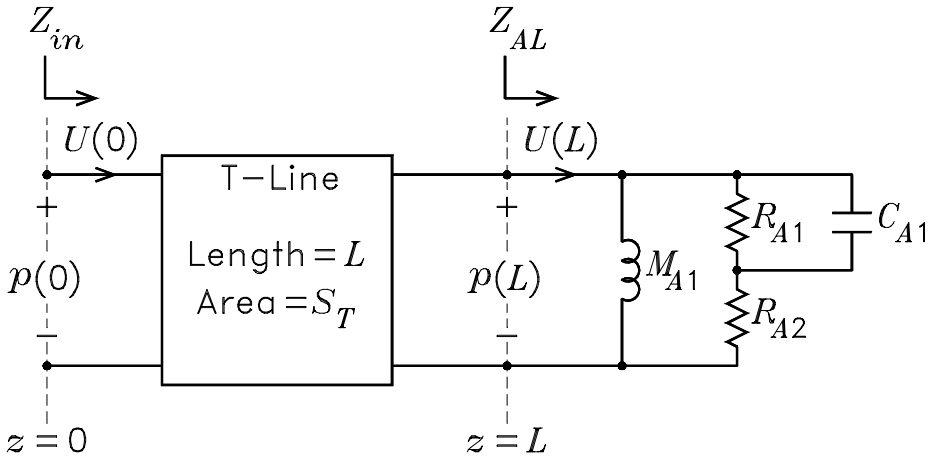

Figure 26. Block diagram of transmission line.

At any point in the line, the acoustical impedance is equal to the ratio of the acoustic pressure to the volume velocity. It follows from Equations (133), (134), (137), and (138)

that the acoustical impedance at $z = L_T$ can be written

$$\begin{aligned} Z_{AL} &= \frac{p\,(L_T)}{U\,(L_T)} \\ &= \frac{p_{0+}e^{-\gamma L_T} + p_{0-}e^{+\gamma L_T}}{\frac{p_{0+}}{Z_C}e^{-\gamma L_T} + \frac{p_{0-}}{Z_C}e^{+\gamma L_T}}. \end{aligned} \tag{140}$$

When this equation is solved for p_{0-} as a function of p_{0+}, the following equation is obtained

$$p_{0-} = p_{0+}\frac{Z_{AL} - Z_C}{Z_{AL} + Z_C}e^{-2\gamma L_T}. \tag{141}$$

The input impedance to the line is the ratio of the pressure at the source to the volume velocity emitted by the source, i.e., the acoustical impedance at $z = 0$. It is given by

$$\begin{aligned} Z_{AT} &= \frac{p\,(0)}{U\,(0)} \\ &= Z_C\frac{p_{0+} + p_{0-}}{p_{0+} - p_{0-}}. \end{aligned} \tag{142}$$

When the expression for p_{0-} given in Equation (141) is substituted into Equation (142), it follows that the expression for the acoustical input impedance to the transmission line is given by

$$Z_{AT} = Z_C\frac{Z_{AL} + Z_C\tanh(\gamma L_T)}{Z_C + Z_{AL}\tanh(\gamma L_T)}. \tag{143}$$

If the expressions for γ and Z_C given by Equations (135) and (139) are substituted into Equation (143), the expression becomes

$$Z_{AT} = \sqrt{\frac{m_{aa}}{c_{aa}}}\,\frac{Z_{AL} + \sqrt{\frac{m_{aa}}{c_{aa}}}\tanh\left(j\omega\sqrt{m_{aa}c_{aa}}L_T\right)}{\sqrt{\frac{m_{aa}}{c_{aa}}} + Z_{AL}\tanh\left(j\omega\sqrt{m_{aa}c_{aa}}L_T\right)}. \tag{144}$$

With the aid of Equations (121), (122), and (136), and the identity $\tanh(jx) = j\tan(x)$, this equation becomes

$$Z_{AT} = \frac{\rho_0 c}{S_T}\frac{Z_{AL} + j\frac{\rho_0 c}{S_T}\tan(kL_T)}{\frac{\rho_0 c}{S_T} + jZ_{AL}\tan(kL_T)} \tag{145}$$

which is identical to Equation (117). Thus the expression for the input impedance that is obtained from an electrical analogous circuit model of the line is identical to the impedance obtained by the acoustical solution of Section 3.2.1.

3.3 The Filled Transmission Line

When the transmission line is filled with a fibrous filling material, the characteristics of the line are altered. The flow resistance of the material introduces an acoustical resistance to the system. In addition, because the fibers can be moved by the air flow in the line, mechanical compliance and mass effects are introduced.

The electro-acoustical lumped element model developed by Augspurger assumes that the fibers do not move and only contribute a frequency-dependent acoustical resistance. The model developed by Bradbury treats the fibers as though they do not have a mechanical compliance, making them unrestrained and completely free to move. In addition, he assumed that the fibers contributed both mass and resistance to the system. It has been found in this work that neither the model of Augspurger or the model of Bradbury accurately model all of the features found in measured input impedance data. When a wave propagates down the tube, the fibers move. However, they are constrained by both the walls of the tube and by each other. These constraints limit the fiber motion and make the fiber compliance a significant parameter in the system.

In the following, a new electro-acoustical model is presented that models the filled line in such a way that it is consistent with the data measured for this work. The model considers the filled line as two linked transmission lines. One is an acoustical transmission line that models the acoustical wave that propagates down the tube. The other is a mechanical transmission line that models the mechanical wave that propagates down the filling fibers in accompaniment with the acoustical wave. The two transmission lines are linked by the flow resistance of the fibers. If the flow resistance is zero, the coupling between the lines disappears.

3.3.1 Fibrous Material Characteristics

The fibrous materials that are commonly used as a filling material in acoustical transmission lines can be divided into two classes. The first is that of a tangle, where long fibers are intertwined in no discernible pattern. An example of this type of material is polyester fiber

in which there is no organized structure among the fibers. The density of the material can vary locally, but the material as a whole can be considered to have an average packing density, and thus have an average acoustical resistance. The air in the line can flow around any of the locally dense areas through a surrounding less dense area. The acoustical resistance of the material can be thought of as being formed by many acoustical resistors connected in parallel, with the total resistance of the material equal to the parallel combination of the resistors. If the wavelength of the acoustical wave is large compared to the average distance between the local variations in density, the density variations have little effect on the total acoustical resistance.

The other form of fibrous materials is that found in fiberglass. Fiberglass is composed of easily seen layers, where each layer shares some of the fibers of the adjacent layers. The fibers that cross between layers hold the structure together and mechanically couple the layers to each other. Each layer consists of fibers oriented roughly parallel to the layer. In some layers, the fibers are loosely packed. In others, the fibers are more densely packed. When the layers are oriented perpendicular to the direction of airflow, the fibers impede the airflow across the entire cross section of the layer. Thus in layered materials, dense layers can contribute a large acoustical resistance to the system. Because the layers are coupled, not only is it possible for the individual fibers of a layer to move, but the entire layer can also move roughly as a single object.

The acoustical resistance of materials of this type can be modeled by series acoustical resistances, where each resistance models the resistance of an individual layer. The total acoustical resistance of each layer can be thought of as composed of resistors in parallel. Depending on the variation in packing density, the resistance variation from one layer to another can be large, whereas in the randomly tangled materials, there are no abrupt changes in resistance with changes in position along the length of the line. A photograph of a sample of fiberglass showing its layered structure is shown in Figure 27.

Figure 27. Photograph that illustrates the layered structure of fiberglass.

3.3.2 The Mechanical Model of the Filling Material

To obtain a mechanical model of filling in an acoustical transmission line, the physical characteristics of the filling and the constraints on the motion of its fibers must be considered. Each length Δz of the material possesses mass. If the packing density is considered to be uniform, the mass per unit length can be calculated as the product of the packing density and the area given by

$$m_{mf} = P_D S_T \tag{146}$$

where P_D is the packing density in $\mathrm{kg\,m^{-3}}$ and S_T is the cross-sectional area of the line.

The fibers in each length also exhibit a mechanical compliance. When a force is applied to the fibers, they can stretch or compress but will return to their starting position when the force is removed. This assumes that the force is not so large to compress the layers. The kinked fibers act as springs that are attached to both adjacent fiber layers and constrained at the tube walls. Friction between the fibers and the tube walls holds the material in place. If the fibers are free-floating in the tube, there is no restoring force resulting from the constraint at the tube wall. In this case, the material exhibits only a compliance between

adjacent layers.

As the fibers in the material move, frictional losses can occur as the fibers rub against each other. The fibers are not free to move along with the flow of air in the tube because they are limited in their range of motion by other fibers. Because the density of the fibrous material cannot be completely uniform, each fiber does not move in the same way as other fibers.

Despite the complex physical structure of the fibrous material, it has been found in this work that its bulk characteristics per unit length of the line can be modeled by the mechanical system of Figure 28. In this system, any non-linear characteristics of the fibers, such as a limited range of motion, are assumed to be negligible. The model also assumes that the material is uniform. This is valid if the wavelength of the acoustical wave is large compared to the distance between local variations in density.

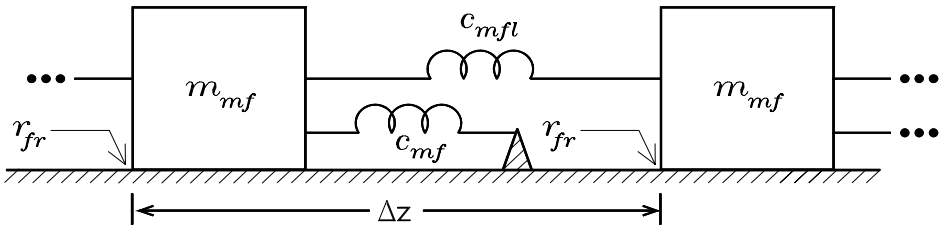

Figure 28. Mechanical system representation of the fibrous material.

The mechanical mass m_{mf} models the total mass of the fibers in the length Δz. The mechanical compliance $c_{mf\ell}$ models the total mechanical coupling compliance among fibers in the length Δz. The mechanical compliance c_{mf} models the total compliance between the fibers and the tube walls in the length Δz. The mechanical resistance r_{fr} models the total mechanical losses in the length Δz. The total values are obtained by multiplying the per unit values by the length Δz. In principal, the parameters in the model could be determined if sufficient information about the physical properties of the material is known. In practice, however, it is more convenient to estimate the values from experimental measurements. Although not indicated on the figure, all mechanical parameters in the model are dependent

on the packing density P_D.

3.3.3 The Coupled Transmission Line System

As indicated by Equation (3), the fiber system of Figure 28 is linked to the air system of Figure 25 through the flow resistance. When these two systems are combined, the complete mechanical transmission line system shown in Figure 29 is obtained. The resistance $S_T R_f$ between the air and fiber masses models the mechanical flow resistance. A vibrating loudspeaker piston moving with velocity u_D and placed on one end of the line causes the nearby air to move with the same velocity. The resulting frictional force between the moving air and the fibers causes the fibers to move in response to the moving air.

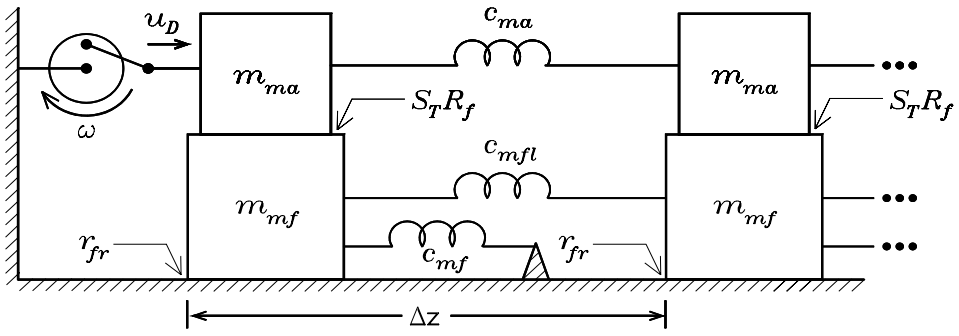

Figure 29. Mechanical system representation of the filled transmission line.

The value of the flow resistance determines the degree of interaction between the acoustical and the mechanical systems. If the flow resistance is zero, the air does not "see" the fibers at all. In this case, the line behaves like the unfilled line modeled by the system of Figure 25. If the flow resistance is infinite, the air and fibers are completely linked and move together.

The net volume of air in the transmission line is reduced by the volume occupied by the fibers. To account for this, the expressions for m_{ma} and c_{ma} must be altered from the unfilled line expressions given by $m_{ma} = \rho_0 S_T$ and $c_{ma} = 1/\rho_0 c^2 S_T$. The modified expressions are

$$m_{ma} = \rho_0 S_T \left(1 - \frac{P_D}{\rho_f}\right) \tag{147}$$

$$c_{ma} = \frac{\left(1 - \frac{P_D}{\rho_f}\right)}{\rho_0 c^2 S_T} \tag{148}$$

where $\left(1 - P_D/\rho_f\right)$ is the fraction of the line volume occupied by air.

For the typical packing densities that are used in transmission line loudspeaker systems, the filling material occupies a small portion of the tube volume. In this case, the values for m_{ma} and c_{ma} given by the above expressions differ little from the values given by the expressions for the unfilled line.

3.3.4 The Circuit Model

A mobility analogous circuit that models the mechanical system of Figure 29 is shown in Figure 30. The node voltages, which represent either fiber or air velocities, are labeled at positions z and $z + \Delta z$ along the line. In the acoustical part of the line, the node voltages are analogous to particle velocity and the branch currents are analogous to an acoustical force given by the acoustic pressure multiplied by the area of the tube. In the mechanical part of the line, the node voltages are analogous to mechanical velocity and the branch currents are analogous to mechanical force. The two models are coupled by resistors which are inversely proportional to the flow resistance R_f. If the flow resistance is zero, these resistors become open circuits. If the flow resistance is infinite, these resistors become short circuits.

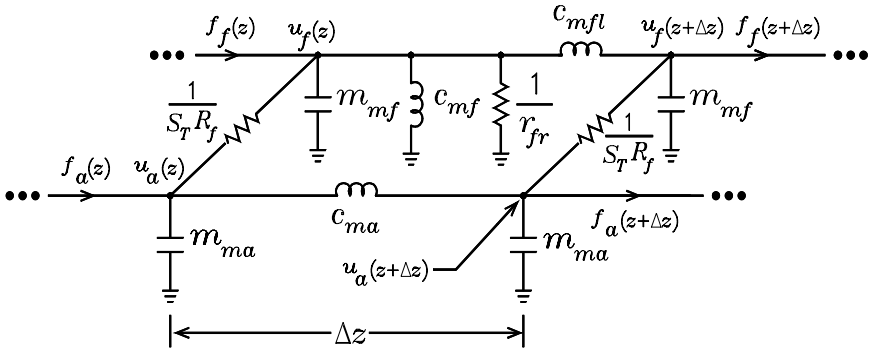

Figure 30. Mobility circuit model of a filled transmission line.

The acoustical and mechanical portions of the transmission line in Figure 30 can be

separated by modeling the node voltages on each side of the resistors labeled $1/S_T R_f$ with voltage controlled voltage sources. The circuit can then be separated into two circuits, an acoustical circuit that models the airflow and a mechanical circuit that models the fiber movement. The two circuits together form a coupled mechano-acoustical model of the filled transmission line. The separated analogous circuit is shown in Figure 31.

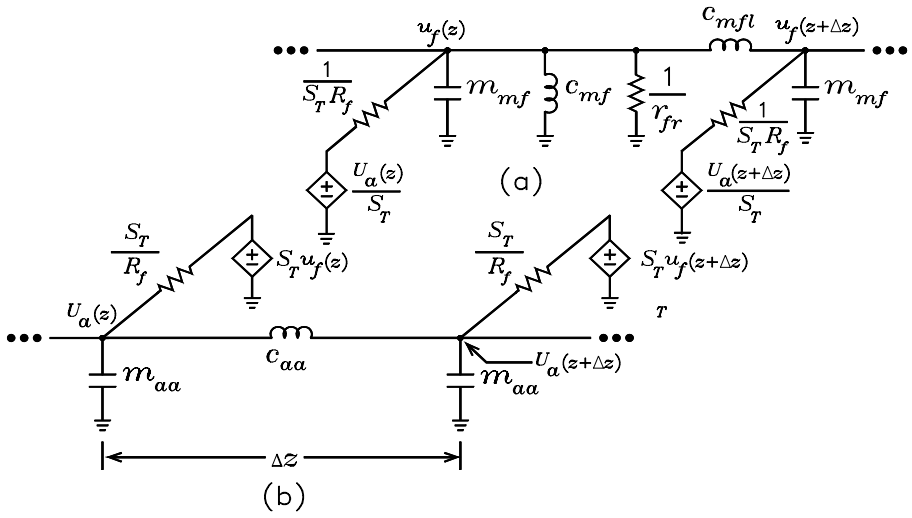

Figure 31. Separate mobility analogous circuits of the filled transmission line. (a) Mechanical analogous circuit. (b) Acoustical analogous circuit.

In obtaining the acoustical part of the circuit of Figure 31(b) from the circuit in Figure 30, the relationships given in Section 2.5 have been used to change the variables so that node voltages are analogous to volume velocity and branch currents are analogous to acoustic pressure. In the circuit of Figure 31(b), $U_a = u_a S_T$ is the volume velocity of the air, $U_D = u_D S_T$ is the volume velocity emitted by the piston source, $m_{aa} = m_{ma}/S_T^2$ is the acoustical mass of air per unit length, and $c_{aa} = c_{ma} S_T^2$ is the acoustical compliance of air per unit length.

The mobility analogous circuits in Figure 31 can be converted into impedance analogous circuits by taking the electrical duals of the mobility circuits. These dual circuits are shown in Figure 32. The circuits model a segment of transmission line having a length Δz. The per unit length parameters are shown multiplied by the length Δz of the segment. In

the mechanical part of the circuit, voltage is analogous to force and current is analogous to velocity. In the acoustical part, voltage is analogous to pressure and current is analogous to volume velocity.

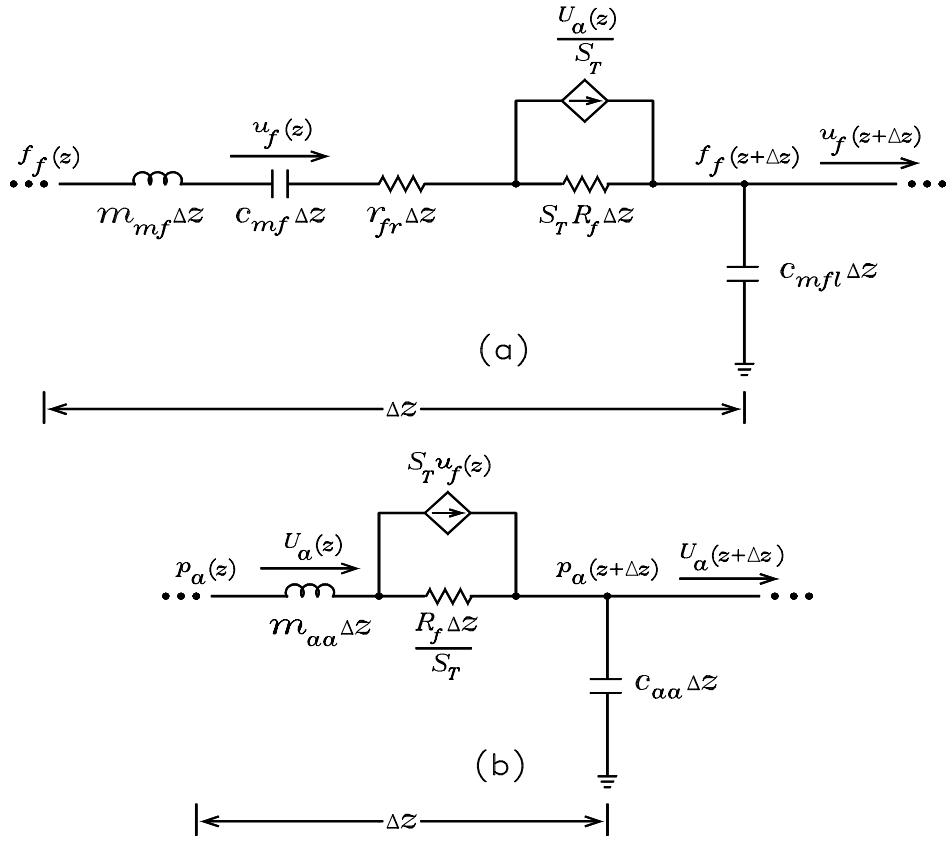

Figure 32. Impedance analogous circuit model of a filled transmission line. (a) Mechanical model of the fibers. (b) Acoustical model of the air.

The interaction between the mechanical and acoustical parts of the circuits in Figure 32 is modeled by current controlled current sources. Both Augspurger's [10] and Bradbury's [9] models can be shown to be special cases of this more general model.

In arriving at his model, Augspurger assumed that the fibrous material is stationary in the tube. The case of stationary fibers can be modeled by letting $c_{mf} = 0$ in Figure 32. Physically, this would be equivalent to making the fibers rigid and attaching them to the walls of the tube. Under these conditions, the fiber velocity $u_f(z)$ is zero and the mechano-acoustical model of Figure 32 reduces to an acoustical line alone that has the

same form as the acoustical equivalent of Augspurger's model shown in Figure 2.

Bradbury modeled the fibrous material as being moveable and having mass, but he neglected the constraint of the tube wall. He also did not include the compliant link among fibers. To impose Bradbury's assumptions on the model, c_{mf} is replaced with a short circuit, r_{fr} is replaced with a short circuit, and $c_{mf\ell}$ is replaced with a short circuit. For these conditions, the model of Figure 32(a) reduces to Bradbury's model shown in Figure 33. Note that replacement of $c_{mf\ell}$ with a short circuit is equivalent to the assumption that adjacent fibers do not mechanically couple. That is, one fiber does not exert a mechanical force on an adjacent fiber.

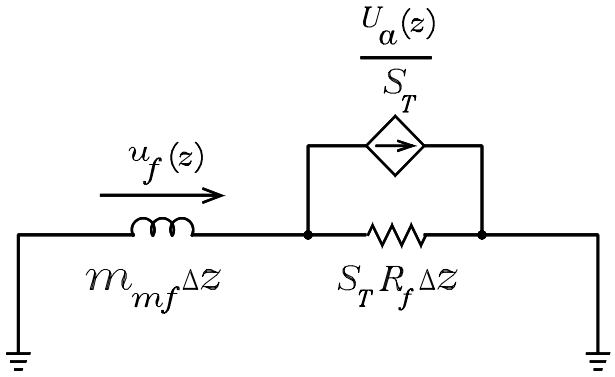

Figure 33. Mechanical model of a length of fibers assuming no wall constraints or compliant links.

In Figure 33, the fiber velocity $u_f(z)$ can be calculated by current division of $U_a(z)/S_T$ between the circuit elements $m_{mf}\Delta z$ and $S_T R_f \Delta z$. It is given by

$$u_f(z) = \frac{U_a(z)}{S_T} \frac{S_T R_f \Delta z}{S_T R_f \Delta z + j\omega m_{mf} \Delta z}. \tag{149}$$

This equation can be rewritten in terms of acoustical impedances as

$$S_T u_f(z) = U_a(z) \frac{R_f \Delta z / S_T}{R_f \Delta z / S_T + j\omega m_{af} \Delta z} \tag{150}$$

where $m_{af} = m_{mf}/S_T^2$ is the acoustical mass that results from the mechanical mass m_{mf} given by

$$m_{af} = \frac{m_{mf}}{S_T^2}. \tag{151}$$

Consider the circuit shown in Figure 34. It follows by current division that the current $S_D u_f(z)$ is the same as that given by Equation (150) which was obtained from the circuit in Figure 33. It follows that the controlled source $S_T u_f(z)$ in Figure 32(b) can be replaced with the acoustical mass $m_{af}\Delta z$ shown in Figure 34. This analogous circuit is equivalent to Bradbury's model. The propagation constant for a wave on this acoustical transmission line has the same form as the propagation constant given in Equation (5) that was derived by Bradbury.

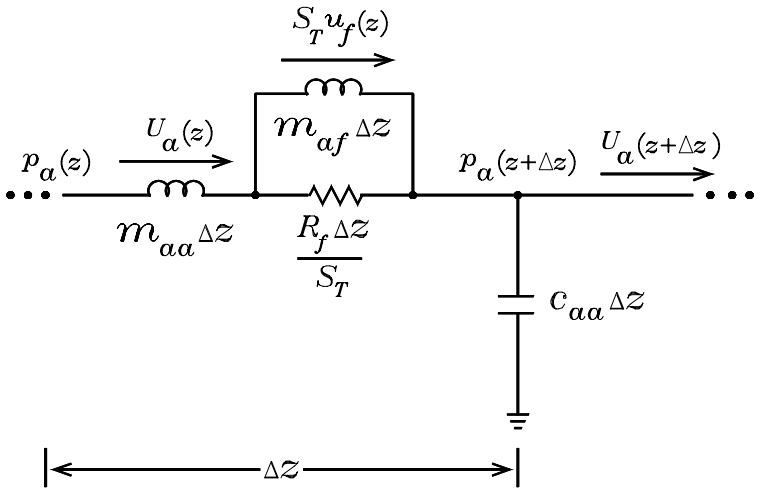

Figure 34. Acoustical model of transmission line airflow assuming no wall constraints and no compliant coupling among fibers.

A more general case of special interest is when the fibers are constrained by the walls of the tube but are not compliantly linked to each other. That is, it is assumed that adjacent fibers do not mechanically couple. In this case, $c_{mf\ell}$ is replaced with a short circuit in Figure 32(a). In this case, it follows that the acoustical part of Figure 32(b) simplifies to the analogous circuit shown in Figure 35, where m_{af} is given by Equation 151 and

$$c_{af} = S_T^2 c_{mf} \tag{152}$$

$$r_{afr} = \frac{r_{fr}}{S_T^2}. \tag{153}$$

Some observations can be made from this circuit. If m_{af} is infinite, r_{afr} is infinite, or c_{af} is zero, then the current $S_T u_f(z)$ is zero. In this case, the fibers are stationary and do

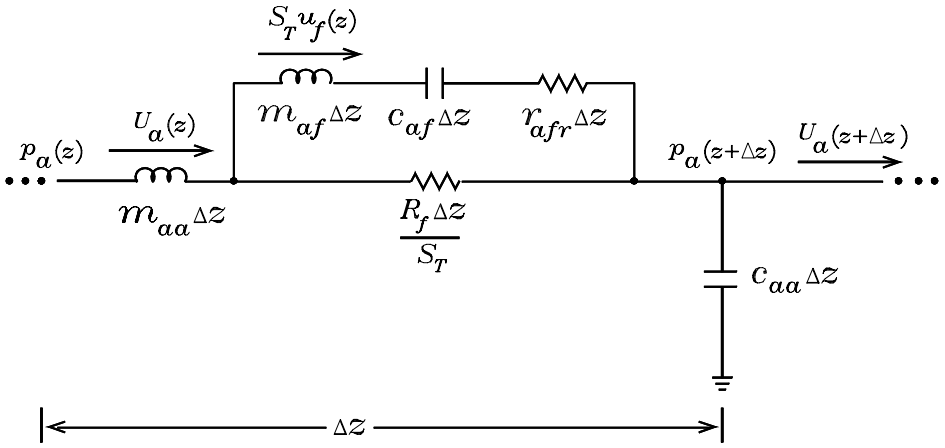

Figure 35. Simplified acoustical model of airflow in the transmission line assuming the fibers are not coupled.

not move. If Bradbury's conclusion that the fibers are moved by the airflow is incorrect, this would probably result from a large value of r_{afr}. If the fibers are completely free to move, as Bradbury assumed, then they would have mass ($m_{af} \neq 0$), be infinitely compliant ($c_{af} = \infty$), and not rub against each other ($r_{fr} = 0$). Unlike Bradbury's model, the analogous circuit of Figure 35 predicts that the pressure drop across the circuit that results from a dc volume velocity is entirely due to the flow resistance R_f, as it should be by the definition of flow resistance. If the fibers can move freely, the circuit reduces to that shown in Figure 34. If the fibers are stationary, the circuit becomes the acoustical impedance analog of Augspurger's model.

3.4 Solutions to the Filled-Line Model

To solve for expressions for the acoustic pressure $p_a(z)$, the air volume velocity $U_a(z)$, the mechanical force on the fibers $f_f(z)$, and the mechanical fiber velocity $u_f(z)$ in the model of Figure 32, a method similar to that used in Section 3.2.2 for the unfilled line can be employed. The compliant link among fibers that is modeled by $c_{mf\ell}\Delta z$ makes it possible for a mechanical wave to travel through the fibrous structure. Because of this, the filled model results in a fourth order differential equation that must be solved, whereas the

unfilled model resulted in a second order differential equation.

3.4.1 Derivation of the Wave Equations

For the circuits in Figure 32, the following equations can be written:

$$p_a(z+\Delta z) = p_a(z) - U_a(z)\left(z_a + \frac{R_f}{S_T}\right)\Delta z + U_f(z)\frac{R_f}{S_T}\Delta z \tag{154}$$

$$U_a(z+\Delta z) = U_a(z) - j\omega c_{aa}\Delta z p_a(z+\Delta z) \tag{155}$$

$$f_f(z+\Delta z) = f_f(z) - u_f(z)\left(z_m + S_T R_f\right)\Delta z + u_a(z) R_f S_T \Delta z \tag{156}$$

$$u_f(z+\Delta z) = u_f(z) - j\omega c_{mf\ell}\Delta z f_f(z+\Delta z)$$

where z_m is the series mechanical impedance per unit length given by

$$z_m = j\omega m_{mf} + r_{fr} + \frac{1}{j\omega c_{mf}} \tag{157}$$

and z_a is the series acoustical impedance per unit length given by

$$z_a = j\omega m_{aa}. \tag{158}$$

In the limit as $\Delta z \to 0$, the following differential equations are obtained

$$\frac{dp_a(z)}{dz} = -U_a(z)\left(z_a + \frac{R_f}{S_T}\right) + u_f(z) R_f \tag{159}$$

$$\frac{dU_a(z)}{dz} = -j\omega c_{aa} p_a(z) \tag{160}$$

$$\frac{df_f(z)}{dz} = -u_f(z)(z_m + S_T R_f) + U_a(z) R_f \tag{161}$$

$$\frac{du_f(z)}{dz} = -j\omega c_{mf\ell} f_f(z). \tag{162}$$

These equations can be combined to obtain second-order equations for the analogous currents $U_a(z)$ and $u_f(z)$. To obtain the equation for $U_a(z)$, the derivative with respect to z of Equation (160) is taken, and the resulting equation is solved for $dp_a(z)/dz$ to obtain

$$\frac{dp_a(z)}{dz} = -\frac{1}{j\omega c_{aa}}\frac{d^2U_a(z)}{dz^2}. \tag{163}$$

When this expression is used to eliminate $dp_a(z)/dz$ in Equation (159), the following equation results:

$$-\frac{1}{j\omega c_{aa}}\frac{d^2U_a(z)}{dz^2} = -U_a(z)\left(z_a + \frac{R_f}{S_T}\right) + u_f(z)\,R_f. \tag{164}$$

Similarly, Equations (162) and (161) can be combined to obtain

$$-\frac{1}{j\omega c_{mf\ell}}\frac{d^2u_f(z)}{dz^2} = -u_f(z)\,(z_m + S_T R_f) + U_a(z)\,R_f. \tag{165}$$

Equation (164) is a wave equation in $U_a(z)$, and Equation (165) is a wave equation in $u_f(z)$. The two equations are coupled through the flow resistance R_f. The last term in each equation results from this coupling between the acoustical and mechanical transmission lines. If the flow resistance R_f is zero, the lines are uncoupled and Equation (164) for $U_a(z)$ reduces to Equation (132) for the unfilled line.

The above equations can be combined further to obtain an equation involving $U_a(z)$ alone and an equation involving $u_f(z)$ alone. Equation (165) can be solved for $U_a(z)$ to obtain

$$U_a(z) = -\frac{1}{j\omega c_{mf\ell}R_f}\frac{d^2u_f(z)}{dz^2} + \frac{u_f(z)}{R_f}(z_m + S_T R_f). \tag{166}$$

If the second derivative of Equation (166) is taken, the resulting equation gives the following expression relating $d^2U_a(z)/dz^2$ and $u_f(z)$:

$$\frac{d^2U_a(z)}{dz^2} = -\frac{1}{j\omega c_{mf\ell}R_f}\frac{d^4u_f(z)}{dz^4} + (z_m + S_T R_f)\frac{1}{R_f}\frac{d^2u_f(z)}{dz^2}. \tag{167}$$

Equations (166) and (167) can be used to eliminate the $U_a(z)$ terms in Equation (164). The result is a fourth-order differential equation that describes the mechanical fiber velocity $u_f(z)$. It is

$$\frac{-1}{\omega^2 c_{aa}c_{mf\ell}}\frac{d^4u_f(z)}{dz^4} - A_2\frac{d^2u_f(z)}{dz^2} + \left[(z_m + r_m)(z_a + r_a) - R_f^2\right]u_f(z) = 0 \tag{168}$$

where

$$r_a = \frac{R_f}{S_T} \tag{169}$$

is the acoustical resistance per unit length that results from the flow resistance, and

$$r_m = S_T R_f \tag{170}$$

is the mechanical resistance per unit length that results from the flow resistance, and A_2 is given by

$$A_2 = \frac{z_m + r_m}{j\omega c_{aa}} + \frac{z_a + r_a}{j\omega c_{mf\ell}}. \tag{171}$$

In a similar manner, a fourth-order equation in $U_a(z)$ can be found. It is given by

$$\frac{-1}{\omega^2 c_{aa} c_{mf\ell}} \frac{d^4 U_a(z)}{dz^4} - A_2 \frac{d^2 U_a(z)}{dz^2} + \left[(z_m + r_m)(z_a + r_a) - R_f^2 \right] U_a(z) = 0. \tag{172}$$

The differential equations for $u_f(z)$ and $U_a(z)$ given in Equations (168) and (172) have the same form. The solutions to these equations represent waves traveling in the transmission line, either in air or in the mechanical structure of the fibrous material. The identical form of the two equations implies that the U_a and u_f waves are governed by the same propagation constant γ. Because the equations are of fourth order, there are four possible wave solutions to each, two propagating in the $+z$ direction and two propagating in the $-z$ direction.

3.4.2 Solutions to the Wave Equations

To solve for the propagation constant γ, it is assumed that the solutions to Equations (168) and (172) are of the form $A\exp(-\gamma z)$, where A is the amplitude of the wave and γ is the complex propagation constant which has the form

$$\gamma = \alpha + j\beta. \tag{173}$$

In this equation, α is the attenuation constant and β is the phase constant.

When $A\exp(-\gamma z)$ is substituted for $u_f(z)$ in Equation (168), the following equation is obtained:

$$\frac{-1}{\omega^2 c_{aa} c_{mf\ell}} \gamma^4 + A_2 \gamma^2 + \left[(z_m + r_m)(z_a + r_a) - R_f^2 \right] = 0. \tag{174}$$

This equation is a second-order equation in γ^2 that has solutions given by

$$\gamma = \pm \left\{ \frac{A_2 \pm \sqrt{A_2^2 + \frac{4}{\omega^2 c_{aa} c_{mf\ell}} \left[(z_m + r_m)(z_a + r_a) - R_f^2 \right]}}{2 \frac{-1}{\omega^2 c_{aa} c_{mf\ell}}} \right\}^{1/2} . \tag{175}$$

This equation represents four solutions, depending on the assignment of plus and minus signs. Two values of γ are the negative of other values. The same solutions can be obtained from Equation (172).

The four possible solutions for γ given by Equation (175) represent four propagating waves in the filled transmission line. Two of the waves are the forward and reverse propagating waves that travel primarily in the mechanical structure of the fibrous material. Two are the forward and reverse propagating waves that travel primarily in the air. Because of the coupling between the waves, the acoustical parameters affect the propagation constant of the mechanical wave, and vice-versa.

The four solutions for γ can be written in the forms

$$\gamma_1 = \sqrt{\frac{Z_A + Z_B}{2}} \tag{176}$$

$$\gamma_2 = \sqrt{\frac{Z_A - Z_B}{2}} \tag{177}$$

$$\gamma_3 = -\sqrt{\frac{Z_A + Z_B}{2}} \tag{178}$$

$$\gamma_4 = -\sqrt{\frac{Z_A - Z_B}{2}} \tag{179}$$

where

$$Z_A = \frac{r_a + z_a}{z_{caa}} + \frac{r_m + z_m}{z_{cmf\ell}} \tag{180}$$

$$\begin{aligned} Z_B \;=\; & \frac{1}{z_{caa} z_{cmf\ell}} \left\{ -4 z_{caa} z_{cmf\ell} \left[R_f^2 + (r_a + z_a)(r_m + z_m) \right] \right. \\ & \left. + \left[(r_a + z_a) z_{cmf\ell} + (r_m + z_m) z_{caa} \right]^2 \right\}^{1/2} \end{aligned} \tag{181}$$

and z_{caa} and $z_{cmf\ell}$ are the impedances given by

$$z_{caa} = \frac{1}{j\omega c_{aa}} \tag{182}$$

$$z_{cmf\ell} = \frac{1}{j\omega c_{mf\ell}}. \tag{183}$$

Because $\gamma_3 = -\gamma_1$ and $\gamma_4 = -\gamma_2$, it follows that the total solutions for the volume velocity $U_a(z)$ and $u_f(z)$ can be written

$$U_a(z) = U_{01}e^{-\gamma_1 z} + U_{02}e^{-\gamma_2 z} + U_{03}e^{\gamma_1 z} + U_{04}e^{\gamma_2 z} \tag{184}$$

$$u_f(z) = u_{01}e^{-\gamma_1 z} + u_{02}e^{-\gamma_2 z} + u_{03}e^{\gamma_1 z} + u_{04}e^{\gamma_2 z}. \tag{185}$$

where U_{01}, U_{02}, u_{01}, and u_{02} are the amplitudes of the waves propagating in the $+z$ direction and where U_{03}, U_{04}, u_{03}, and u_{04} are the amplitudes of the waves propagating in the $-z$ direction. When Equations (160) and (162) are applied to Equations (184) and (185), expressions for the acoustic pressure and mechanical force are obtained. They are

$$p_a(z) = -z_{caa}\left(-U_{01}\gamma_1 e^{-\gamma_1 z} + -U_{02}\gamma_2 e^{-\gamma_2 z} + U_{03}\gamma_1 e^{\gamma_1 z} + U_{04}\gamma_2 e^{\gamma_2 z}\right) \tag{186}$$

$$f_f(z) = -z_{cmf\ell}\left(-u_{01}\gamma_1 e^{-\gamma_1 z} + -u_{02}\gamma_2 e^{-\gamma_2 z} + u_{03}\gamma_1 e^{\gamma_1 z} + u_{04}\gamma_2 e^{\gamma_2 z}\right). \tag{187}$$

3.4.3 Determination of the Wave Amplitudes

To determine the wave amplitudes in Equations (184) through (187), the boundary conditions at each end of transmission line system are employed. With reference to Figure 23, the volume velocity at the source end of the line is equal to the volume velocity U_T emitted by the loudspeaker diaphragm into the tube. To obtain a solution, it is assumed that the frequency is low enough so that the acoustic pressure at the open end of the tube is zero. This is equivalent to the assumption that $Z_{AL} = 0$ in Figure 26.

To simplify the expressions, let the origin in Figure 23 be shifted so that the piston source is located at position $z = -L_T$ and the open end of the tube is located at $z = 0$. The boundary conditions can be written

$$U_a(-L_T) = U_T \tag{188}$$

$$p_a(0) = 0. \tag{189}$$

Because the fibers at the source end of the line are unrestrained, the force satisfies the boundary condition

$$f_f(-L_T) = 0. \tag{190}$$

This can also be seen from the mechanical part of the analogous circuit in Figure 30. The current, which is analogous to the mechanical force $f_f(-L_T)$, must be zero at the source end of the line. At the load end of the mechanical part, the current, which is analogous to the mechanical force $f_f(0)$, must also be zero. That is, the fibers are unrestrained. Thus the force satisfies the boundary condition

$$f_f(0) = 0. \tag{191}$$

These boundary conditions are consistent with those used in [20].

For the boundary conditions of Equations (189) and (190), Equations (186) and (187) become

$$\gamma_1 (U_{01} - U_{03}) + \gamma_2 (U_{02} - U_{04}) = 0 \tag{192}$$

$$\gamma_1 (u_{01} - u_{03}) + \gamma_2 (u_{02} - u_{04}) = 0. \tag{193}$$

These equations are satisfied if

$$U_{03} = U_{01} \tag{194}$$

$$U_{04} = U_{02} \tag{195}$$

$$u_{01} = u_{03} \tag{196}$$

$$u_{02} = u_{04}. \tag{197}$$

When the above relations are used in Equations (184), (185), (186), and (187), it follows that the solutions in the line are given by

$$U_a(z) = 2U_{01}\cosh(\gamma_1 z) + 2U_{02}\cosh(\gamma_2 z) \tag{198}$$

$$u_f(z) = 2u_{01}\cosh(\gamma_1 z) + 2u_{02}\cosh(\gamma_2 z) \tag{199}$$

$$p_a(z) = -z_{caa}\left[2\gamma_1 U_{01}\sinh\left(\gamma_1 z\right) + 2\gamma_2 U_{02}\sinh\left(\gamma_2 z\right)\right] \tag{200}$$

$$f_f(z) = -z_{cmf\ell}\left[2\gamma_1 u_{01}\sinh\left(\gamma_1 z\right) + 2\gamma_2 u_{02}\sinh\left(\gamma_2 z\right)\right]. \tag{201}$$

Equations (164) and (165) can be used to relate the wave amplitudes of the acoustical volume velocity and the fiber mechanical velocity. to obtain

$$U_{01,02} = \frac{R_f}{z_a + r_a - z_{caa}\gamma_{1,2}^2} u_{01,02}. \tag{202}$$

Similarly, Equation (165) and (164) can be used to obtain the relation

$$u_{01,02} = \frac{R_f}{z_m + r_m - z_{cmf\ell}\gamma_{1,2}^2} U_{01,02}. \tag{203}$$

Although it is not obvious, these equations are equivalent. That is, one equation can be changed into the other by using the relationships between the parameters. However, only one of the two equations is required to obtain expressions for the wave amplitudes.

For the boundary conditions at the source end of the line given by Equations (188) and (191), Equations (198) and (201) can be written as

$$2U_{01}\cosh(-\gamma_1 L_T) + 2U_{02}\cosh(-\gamma_2 L_T) = U_T \tag{204}$$

$$2\gamma_1 u_{01}\sinh(-\gamma_1 L_T) + 2\gamma_2 u_{02}\sinh(-\gamma_2 L_T) = 0. \tag{205}$$

When Equations (202), (204), and (205) are solved for the wave amplitudes, the following equations are obtained

$$U_{01} = \frac{1}{2}\frac{U_T\gamma_2 M_2}{\gamma_2 M_2\cosh\left(\gamma_1 L_T\right) - \gamma_1 M_1\coth\left(\gamma_2 L_T\right)\sinh\left(\gamma_1 L_T\right)} \tag{206}$$

$$U_{02} = \frac{1}{2}\frac{U_T\gamma_1 M_1}{\gamma_1 M_1\cosh\left(\gamma_2 L_T\right) - \gamma_2 M_2\coth\left(\gamma_1 L_T\right)\sinh\left(\gamma_2 L_T\right)} \tag{207}$$

$$u_{01} = \frac{1}{2R_f}\frac{U_T\gamma_2 M_1}{\gamma_2\cosh\left(\gamma_1 L_T\right) - \gamma_1\frac{M_1}{M_2}\coth\left(\gamma_2 L_T\right)\sinh\left(\gamma_1 L_T\right)} \tag{208}$$

$$u_{02} = \frac{1}{2R_f}\frac{U_T\gamma_1 M_2}{\gamma_1\cosh\left(\gamma_2 L_T\right) - \gamma_2\frac{M_2}{M_1}\coth\left(\gamma_1 L_T\right)\sinh\left(\gamma_2 L_T\right)} \tag{209}$$

where M_1 and M_2 are defined by

$$M_{1,2} = z_a + r_a - z_{caa}\gamma_{1,2}^2. \tag{210}$$

These expressions can be substituted into Equations (198) through (201) to obtain equations for $U_a(z)$, $u_f(z)$, $p_a(z)$, and $f_f(z)$ in terms of the parameters of the transmission line and the fibers.

The input impedance to the transmission line, Z_{AT} is the ratio of pressure to volume velocity at $z = -L_T$. It follows that this is given by

$$Z_{AT} = \frac{z_{caa}^2 \gamma_1 \gamma_2 (\gamma_1 - \gamma_2)(\gamma_1 + \gamma_2)}{\gamma_2 M_2 \coth(\gamma_1 L_T) - \gamma_1 M_1 \coth(\gamma_2 L_T)}. \tag{211}$$

3.4.4 Simplified Expressions

The above analysis applies to the most general case of fibrous filling materials, where the fibers are coupled to each other and to the tube walls. An acoustical analysis of fibrous materials in [20] accounted for the coupling among fibers in calculating the attenuation of sound in fiberglass slabs of large area. However, measured data for several transmission line configurations during the course of this work indicate that the acoustical input impedance to the line can be well described by the circuit of Figure 35 in which the coupling among adjacent fibers is neglected. This is possibly because the area of the fibers used in this investigation was smaller than the area used in [20]. The smaller area makes the coupling between the fibers and the tube wall dominate over the coupling among adjacent fibers. The large slab area used in [20] permitted the fibers to move a significant distance, especially near the center of the slab, before the movement was restrained by the wall at the load end where the boundary condition was the mechanical velocity of the fibers is zero.

For the case of no coupling among fibers as modeled by the circuit of Figure 35, the input impedance has the same form as Equation (143):

$$Z_{AT} = Z_C \frac{Z_{AL} + Z_C \tanh(\gamma L_T)}{Z_C + Z_{AL} \tanh(\gamma L_T)} \tag{212}$$

where Z_C and γ are given by

$$Z_C = \sqrt{\left[j\omega m_{aa} + \left(j\omega m_{af} + r_{afr} + \frac{1}{j\omega c_{af}} \right) \| R_f \right] z_{caa}} \tag{213}$$

$$\gamma = \sqrt{\frac{j\omega m_{aa} + \left(j\omega m_{af} + r_{afr} + \frac{1}{j\omega c_{af}} \right) \| R_f}{z_{caa}}}. \tag{214}$$

If the pressure at the open end of the line is assumed to be zero as is done in the derivation of Equation (211), the input impedance for the case of no coupling among fibers becomes

$$Z_{AT} = Z_C \tanh(\gamma L_T). \tag{215}$$

The circuit model of the unfilled line shown in Figure 24 has the same form as the circuit model of the filled line with uncoupled fibers shown in Figure 35 as well as the models of Figures 2 and 34. Each of these models is composed of a series impedance and a shunt compliance. Thus the expressions for the pressure and volume velocity as functions of position for any of these models have the same form as those for the unfilled line.

The expressions for the simplified model with uncoupled fibers can be obtained by replacing the impedance $j\omega m_{aa}$ in the unfilled-line expressions of Section 3.2.2 by the acoustical impedance given by

$$j\omega m_{aa} + \left(j\omega m_{af} + r_{afr} + \frac{1}{j\omega c_{af}} \right) \| R_f .$$

The expressions for the acoustic pressure and volume velocity on the line are

$$p(z) = p_{0+} e^{-\gamma z} + p_{0-} e^{+\gamma z} \tag{216}$$

$$U(z) = U_{0+} e^{-\gamma z} + U_{0-} e^{+\gamma z} \tag{217}$$

where γ is given by Equation (214). As with the unfilled line, the coefficients U_{0+} and U_{0-} are related to the pressure coefficients by

$$U_{0+} = \frac{p_{0+}}{Z_C} \tag{218}$$

$$U_{0-} = \frac{-p_{0-}}{Z_C}. \tag{219}$$

To solve for the coefficients in the pressure and volume velocity expressions, the system boundary conditions must be imposed. Because the fibers are uncoupled, the system can support only an acoustical wave, so only the two acoustical conditions given by Equations (188) and (189) are necessary. These two conditions and Equations (216) and (217) can be solved to obtain expressions for the coefficients. The coefficients are given by

$$p_{0+} = \frac{U_T Z_C}{2\cosh(\gamma L_T)} \tag{220}$$

$$p_{0-} = \frac{-U_T Z_C}{2\cosh(\gamma L_T)} \tag{221}$$

$$U_{0+} = \frac{U_T}{2\cosh(\gamma L_T)} \tag{222}$$

$$U_{0-} = \frac{-U_T}{2\cosh(\gamma L_T)}. \tag{223}$$

where U_T is the acoustical volume velocity emitted by the piston source into the tube.

When these expressions are used in the expressions for $p(z)$ and $U(z)$ given by Equations (216) and (217), the following simplified expressions are obtained

$$p(z) = -Z_C U_T \frac{\sinh(\gamma z)}{\cosh(\gamma L_T)} \tag{224}$$

$$U(z) = U_T \frac{\cosh(\gamma z)}{\cosh(\gamma L_T)}. \tag{225}$$

Because of the identical forms of the equivalent circuit models, these expressions apply to both the unfilled line and the filled line for the case of uncoupled fibers. Expressions for γ and Z_C given by Equations (135) and (139) are used for the case of the unfilled line and those given by Equations (214) and (213) are used for the case of the filled line with uncoupled fibers. The ratio of Equation (224) to Equation (225) for $z = -L_T$ gives Equation (215) for the acoustical input impedance Z_{AT} to the line.

CHAPTER 4

EVALUATION OF THE MODEL

To test the validity of the electro-acoustical models for the filled transmission line derived in Chapter 3, the modeled acoustical input impedance given by Equation (212) is compared in this chapter to the measured acoustical input impedance of several filled lines. A brief description of the experimental setup for taking the data is first given.

4.1 Experimental Setup

Figure 36 shows an illustration of the test setup used to acquire the transmission line data. The loudspeaker is mounted on one end of an acoustical transmission line of length L_T and cross-sectional area S_T. The other end of the line is open. The loudspeaker voice-coil terminals are connected to the output of the Audio Precision System Two analyzer described in Section 2.8. The tube is filled with fiberglass with different packing densities.

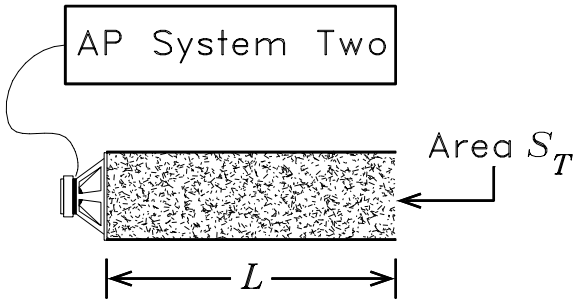

Figure 36. Illustration of test setup.

For this research, the transmission lines were rigid PVC tubes having diameters of 7.5 cm and 10 cm. Two different lengths were investigated. These were 925 mm and 1540 mm. The loudspeaker was held to the tube by elastic cords that attached to mounting brackets connected to the tube. Duct tape was wrapped around the joint between the tube and the loudspeaker flange to additionally secure the loudspeaker and to ensure an airtight seal. A photograph of the setup is shown in Figure 37.

Figure 37. Photograph of test setup.

The loudspeaker used had a six-inch frame diameter with the measured parameters given in Table 1 in Section 2.9.2. A plot of this loudspeaker input impedance and its modeled impedance is shown in Figure 22.

Cylindrical samples cut from sheets of fiberglass 9 cm thick were used to fill the tube. Each sample had a diameter slightly larger than the tube. For the samples of radius 7.5 cm, each sample weighed approximately 23.1 g. For the samples of radius 10 cm, each sample weighed approximately 41.2 g. The surface density ρ_{sf} was calculated to be $\rho_{sf} = 1.31\,\mathrm{kg\,m^{-2}}$. A photograph of fiberglass samples is shown in Figure 38. The fiberglass was R-13 utility fiberglass insulation manufactured by Owens Corning. Its initial packing density before being compressed or expanded to fill the transmission line was found to be $14.7\,\mathrm{kg\,m^{-3}}$.

To fill the line with fiberglass of a known packing density, an appropriate number of samples were aligned on a piece of scrim cloth and then stretched or compressed until the fiberglass was approximately uniformly distributed over a length equal to the tube length. The cloth was then wrapped around the samples to form a cylinder as shown in Figure 39. The wrapped cylinder was then pulled into the tube before the loudspeaker was attached.

Figure 38. Fiberglass samples used to fill the transmission line.

The wrapped cylinder, because it is slightly compressed when in the tube, was held in the tube by friction.

The packing density in $\mathrm{kg\,m^{-3}}$ of the fibers in the tube is given by

$$P_D = \frac{nm_s}{S_T L_T} \tag{226}$$

where n is the number of samples and m_s is the mechanical mass per sample. Because $\rho_{sf} = m_s/S_T$, where ρ_{sf} is the surface density, an alternative expression in terms of the surface density is given by

$$P_D = \frac{n\rho_{sf}}{L_T}. \tag{227}$$

4.2 Effect of the Transmission Line on the Voice-Coil Impedance

A plot of the input impedance versus frequency of a loudspeaker in free space has a single fundamental resonance peak that is the result of the mass and suspension compliance of the loudspeaker diaphragm. When the loudspeaker is placed on a transmission line, the transmission line resonances introduce additional variations into the voice-coil impedance plot. These variations are dependant on both the physical dimensions of the tube and the

Figure 39. Wrapped cylinder of fiberglass before it is inserted into the transmission line.

characteristics of the filling material.

4.2.1 The Unfilled Line

Figure 40 shows a graph of the magnitude of the measured loudspeaker voice-coil impedance both on and off of the unfilled tube of length $L_T = 925\,\text{mm}$ and radius $a_T = 7.5\,\text{cm}$. It can be seen that the tube introduces several additional peaks in the impedance curve. The fundamental resonance peak is moved to a lower frequency and its width is narrowed. Because the tube is unfilled, the variations in the input impedance are entirely the result of the tube and its interactions with the suspension resonance. The tube is a resonant load, whereas the air load on the loudspeaker when it is off the tube can be modeled as a simple acoustical mass.

The maxima in Figure 40 are well-defined, but the maxima frequencies are highly dependent on the mechanical suspension of the loudspeaker driver. However, the frequencies of the minima depend primarily on the tube dimensions and can be readily estimated.

The minima in the on-tube impedance curve occur approximately at frequencies where the tube length is an odd number of quarter wavelengths. At these frequencies, the pressure

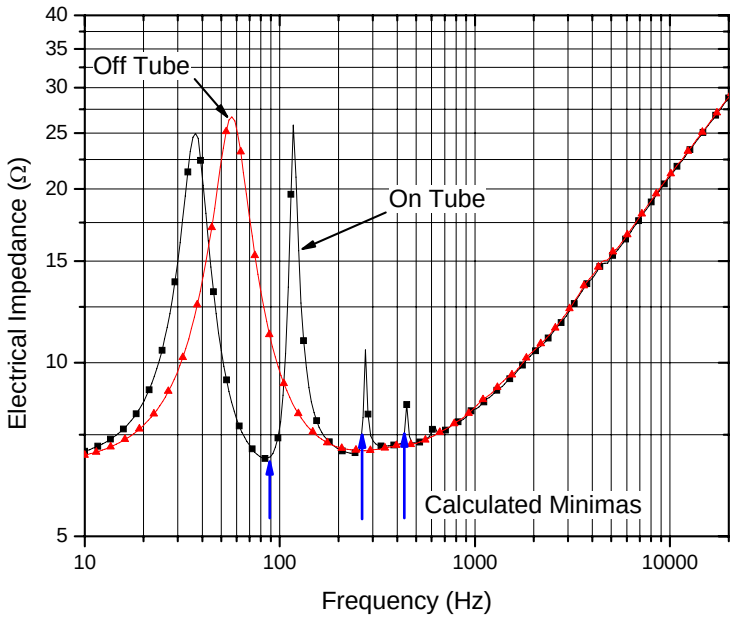

Figure 40. Plots of measured driver input impedance off and on an empty transmission line.

wave reflected from the open end of the tube combines with the source wave to create a high pressure at the source end of the tube. This high pressure causes the mechanical velocity of the diaphragm to exhibit a minimum, causing the motional impedance term in the voice-coil impedance to exhibit a minimum. The frequencies at which the voice-coil impedance exhibits a minimum are given by

$$f_n = \frac{nc}{4L_T} \tag{228}$$

where n is an odd integer, and c is the velocity of sound.

The frequencies calculated from Equation (228) are based on the assumption that the pressure at the end of the transmission line is zero. This is the equivalent to a short circuit load on an electrical transmission line. In practice, the air load external to the tube effectively increases the length of the tube so that the measured minima occur at frequencies slightly less than those predicted by Equation 228. To correct for this, an end correction L_{uf} [27] given by

$$L_{uf} = 0.6133a_T \tag{229}$$

where a_T is the tube radius can be added to the physical length L_T of the tube. The length L_{uf} is the length of a cylinder of air of density ρ_0 having the area of S_T that has a mass equal to the acoustical mass M_{A1} defined in Figure 14 for the air load external to the tube.

For $L_T = 925\,\text{mm}$, Equations (228) and (229) give the first three minima frequencies as 88.8 Hz, 266.5 Hz, and 444.1 Hz. These frequencies are indicated on Figure 40 and can be seen to correspond closely to the minima of the on-tube plot. However, these frequencies are only approximate. This is because only the tube characteristics have been used to calculate the minima frequencies. Although the tube primarily determines the minima frequencies, the parameters which determine the fundamental resonance frequency of the loudspeaker perturb them. If the length of the tube is such that the quarter-wavelength resonance frequency is greater than the suspension resonance frequency, the measured data indicate that the effect of the suspension is to slightly increase the minima frequencies from those calculated from Equations (228) and (229).

In Figure 40, it can be seen that this particular tube length results in a quarter-wavelength tube resonance near the loudspeaker suspension resonance frequency. This causes the suspension resonance peak to appear as though it is split into two separate peaks. If only the two lowest frequency peaks in the on-tube plot of Figure 40 are considered, the impedance curve of the loudspeaker on the tube is very similar to that of a loudspeaker on a vented box, where the minimum between the two peaks is a result of the Helmholtz resonance of the port air mass and the box air compliance. The vented box has only this single resonance, whereas the tube has multiple resonances that result in multiple minima and maxima in the curve. At higher frequencies, the voice-coil inductance dominates the input impedance and obscures any peaks that can be present.

In Section 2.7, the input impedance of a loudspeaker mounted on an infinite baffle given by Equation (67) was derived. If the loudspeaker is instead mounted such that its front side radiates from a tube but its back side radiates into a transmission line having an acoustical

input impedance Z_{AT}, it can be shown that the loudspeaker input impedance is given by

$$\begin{aligned} Z_{VC} &= R_E + \left[(j\omega)^{n_e} L_e\right] \| (j\omega L_{E2}) \\ &\quad + \frac{(B\ell)^2}{S_D^2} \frac{1}{j\omega M_{AD} + R_{AS} + (j\omega C_{AS})^{-1} + Z_{AL} + Z_{AT}}. \end{aligned} \tag{230}$$

where Z_{AL} is defined in Figure 14. Figure 41 is a plot of the measured on-tube input impedance and the input impedance modeled by Equation (230). The modeled impedance agrees well with the measured impedance.

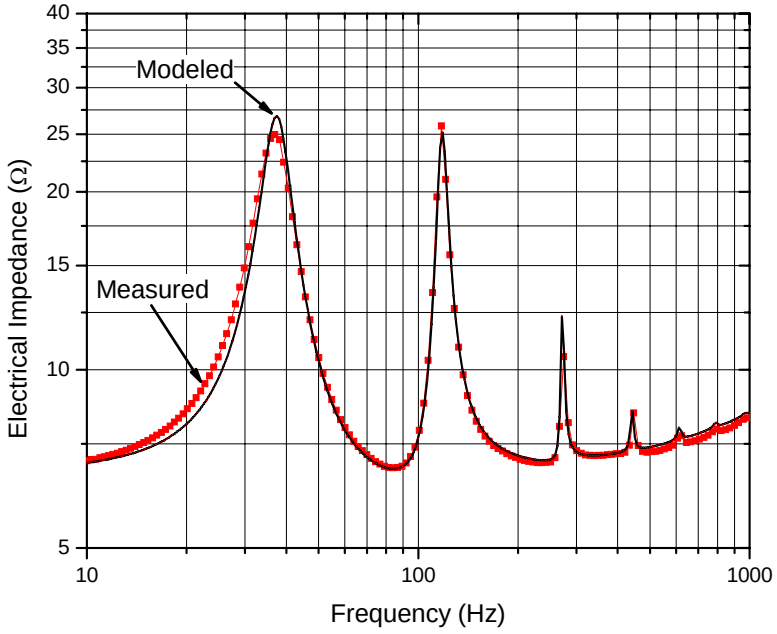

Figure 41. Measured and modeled input impedance of the driver on an empty transmission line.

The input impedance to the line Z_{AT} that is used in Equation (230) is given by Equation (212), where the flow resistance R_f is set to zero because the tube is unfilled. The values chosen for the other model parameters, m_{af}, c_{af}, and r_{af} are unimportant, because the fiber impedance that they determine is in parallel with $R_f = 0$.

The values for m_{aa} and c_{aa} in Equation (212) are given by

$$m_{aa} = \frac{\rho_0}{S_T} \tag{231}$$

$$c_{aa} = \frac{S_T}{\rho_0 c^2}. \tag{232}$$

For $\rho_0 = 1.18\,\mathrm{kg\,m^{-3}}$, $c = 345\,\mathrm{m\,s^{-1}}$, and $S_T = 176.71\,\mathrm{cm^2}$, the values of m_{aa} and c_{aa} are $66.77\,\mathrm{N\,s^2\,m^{-6}}$ and $1.26 \times 10^{-7}\,\mathrm{m^4\,N^{-1}}$, respectively.

Figure 42 illustrates how varying the length of the line affects the input impedance plot. The curves are modeled by Equation (230) with line lengths of 0.5, 1, and 1.5 m. The other parameters remain the same.

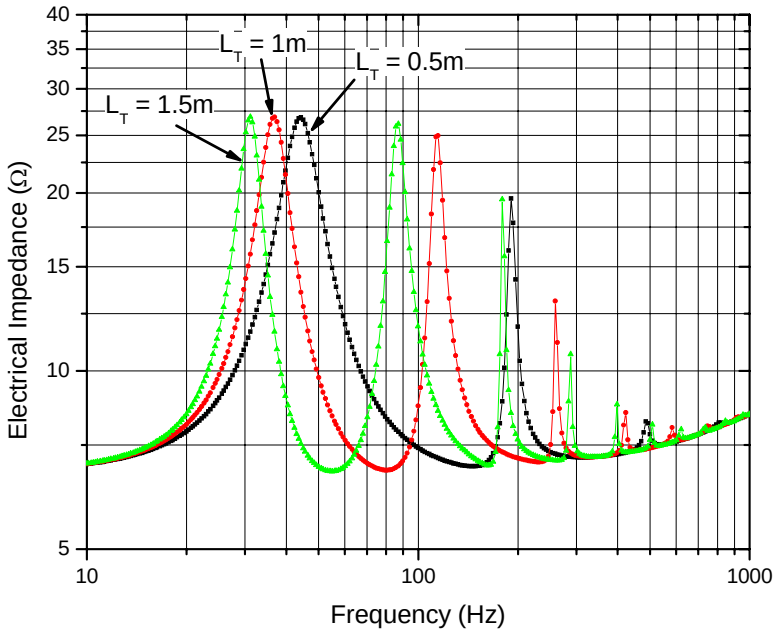

Figure 42. Plots of modeled input impedance of the driver on transmission lines of various lengths.

The impedance peaks of a longer transmission line are shifted to lower frequencies, and the height and number of peaks at higher frequencies are increased. Conversely, the impedance peaks of a shorter line are shifted to higher frequencies, and the height and number of peaks at higher frequencies are decreased.

As expected, if the line is made short enough so that the transmission line resonances can be neglected, the line acts as a pure mass load on the loudspeaker. As the line length approaches zero, Equation (230) gives approximately the free-space impedance of the loudspeaker. There is some variation, because the air load on the loudspeaker in free space is not the same as the loads on the ends of the transmission line that are modeled by the circuit of Figure 14. The modeled input impedance for $L_T = 0$ is that of the loudspeaker having

both front and back loads modeled as shown in Figure 14.

Figure 43 illustrates the modeled loudspeaker input impedance for short line lengths of 0.2, 0.1, and 0 m. Again, only the length of the line is varied. It can be seen that as the line length approaches zero, the peaks that result from line resonances disappear and the modeled impedance approaches that of the loudspeaker in free space.

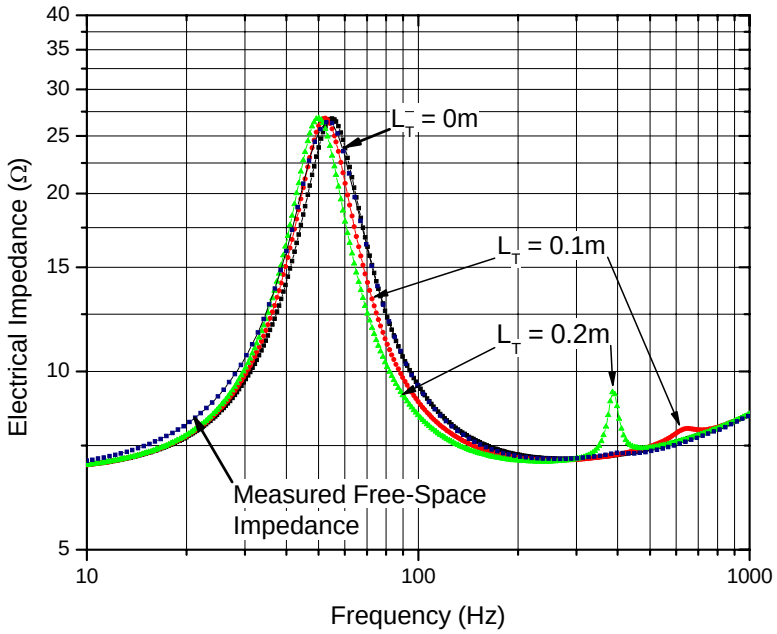

Figure 43. Modeled input impedance of driver on short transmission lines.

4.2.2 The Filled Line

When the line is filled with fiberglass, the characteristics of the loudspeaker input impedance result from not only the physical dimensions of the tube and the mechanical and electrical characteristics of the loudspeaker, but also from the characteristics of the fiberglass. Because the fiberglass can move, it can introduce resonances, just as the tube can. The fiberglass also introduces additional acoustical mass and resistance, because it restricts the flow of air into small openings. As the packing density of the fiberglass is increased, the tube resonances become less pronounced, because the reflected waves in the tube are attenuated by the filling.

Figures 44 and 45 show plots of measured input impedance for the loudspeaker on the unfilled 925 mm line and on the line filled with fiberglass to various packing densities. These densities correspond to the line filled with two, four, six, eight, and ten cylindrical fiberglass samples.

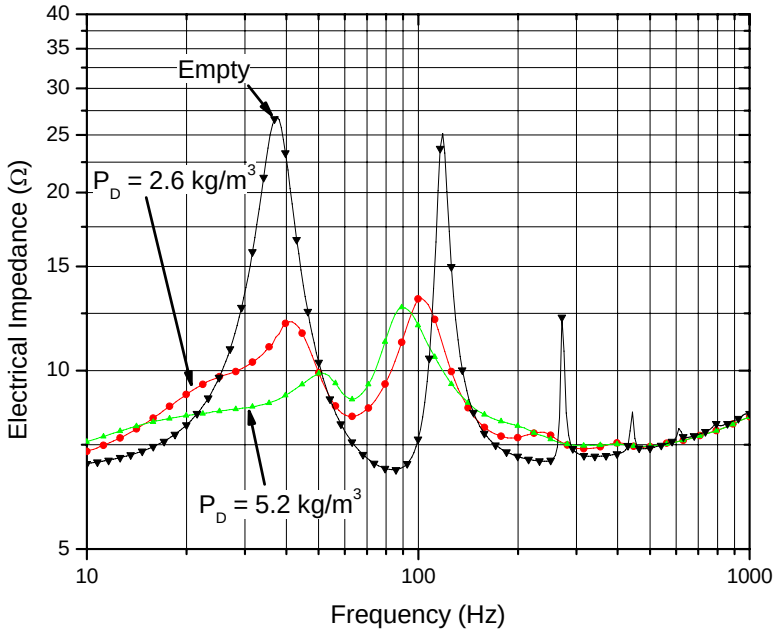

Figure 44. Measured input impedance of driver on line filled with fiberglass of various packing densities.

In Figures 44 and 45, it can be seen that the impedance of the loudspeaker on the filled line has two dominant peaks just as it does on the unfilled line, however both peaks are attenuated from the unfilled-line peaks. As the packing density is increased, the lower frequency peak progressively moves upward in frequency so that it is on the high-frequency side of the original upper peak for the two highest packing densities. The location of the original high-frequency peak does not exhibit as much variation with packing density. It remains between approximately 90 and 100 Hz.

The small variation in frequency of the higher frequency peak is because it results from a tube resonance, just as it does for the unfilled line. This resonance is determined by the physical length of the line, which is held constant. The lower frequency peak on the

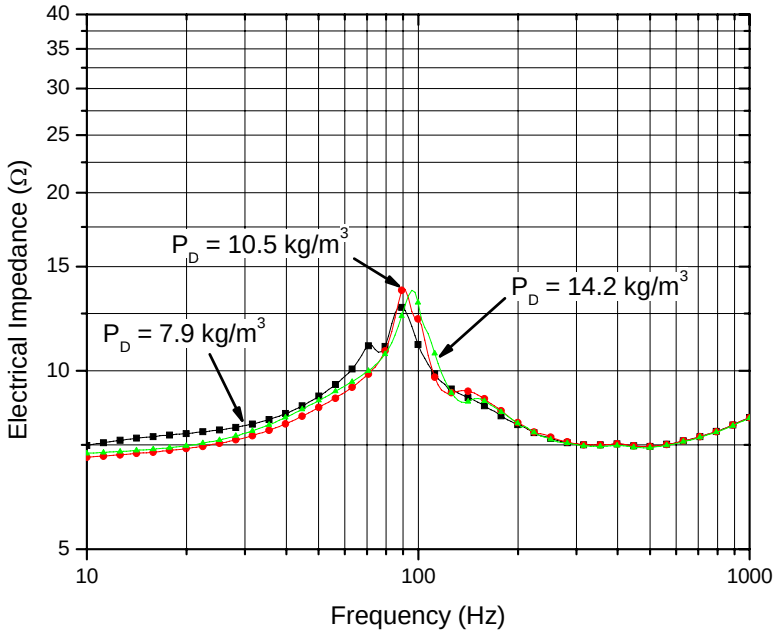

Figure 45. Measured input impedance of driver on line filled with fiberglass of various packing densities.

filled-line plots results from the fiber resonance modeled by m_{af}, r_{afr}, and c_{af} in Figure 35, whereas the lower-frequency peak of the unfilled-line plot results from a resonance between the tube mass and the suspension compliance. To see this, the acoustical input impedance of the line must be examined.

4.3 Acoustical Impedance of the Unfilled Line

Although it is possible to measure directly the acoustical input impedance, for this investigation it is instead obtained from the measured loudspeaker input impedance.

Equation (230) can be solved for Z_{AT} to obtain

$$Z_{AT} = \frac{(B\ell)^2}{S_D^2}\frac{1}{Z_{VC} - R_E - \left[(j\omega)^{n_e} L_e\right] \| (j\omega L_{E2})} - (j\omega M_{AD} + R_{AS} + \frac{1}{j\omega C_{AS}} + Z_{AL}). \quad (233)$$

If the loudspeaker parameters are accurately known, then the acoustical input impedance of the transmission line can be obtained by applying Equation (67) to measured loudspeaker input impedance data.

Because the loudspeaker driver is used as both the source and the receiver in the test setup illustrated in Figure 36, measurements become less accurate at frequencies far from the driver resonance frequency. This can be seen by examining Equation (230). At frequencies far from the driver resonance, the term $j\omega M_{AD} + R_{AS} + (j\omega C_{AS})^{-1}$ becomes much larger than the acoustical input impedance of the line Z_{AT}. Because of this, Z_{AT} cannot be accurately recovered from the measured driver input impedance data at these frequencies.

Figure 46 shows plots of the measured and modeled acoustical input impedance Z_{AT} for the unfilled line. As expected because of the good agreement of the curves of Figure 41, these two curves match closely. The modeled curve is calculated from Equation (212) with the assumptions that $R_f = 0$, $c = 345\ \mathrm{m\,s^{-1}}$ and $\rho_0 = 1.18\,\mathrm{kg\,m^{-3}}$. The approximate values of c and ρ_0 can result in the slight deviation of the measured and modeled responses. Also, the modeled air load on the loudspeaker and on the open end of the line may not be exact. By slightly increasing the length of the line in the model, the curves can be made to agree more closely.

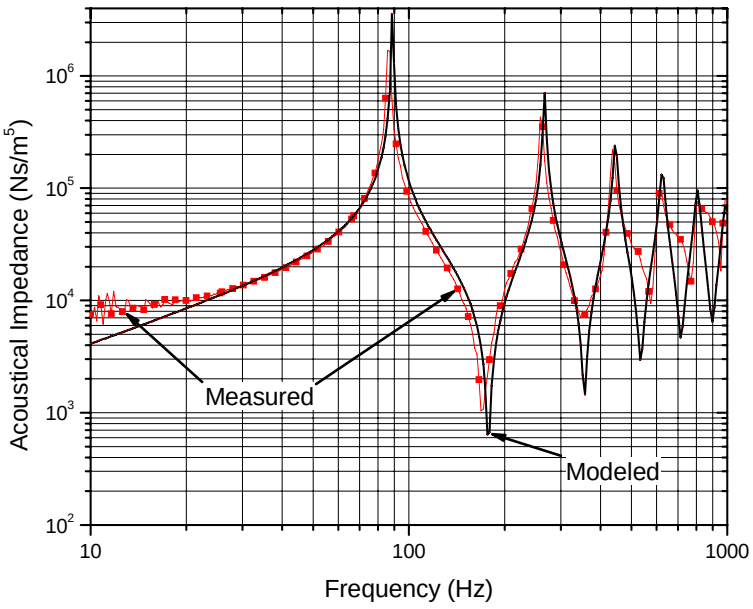

Figure 46. Measured and modeled plots of the acoustical input impedance to the transmission line.

It can be seen that at higher frequencies, the peaks of the measured and modeled acoustical input impedances are almost the same, but the nulls in the responses do not match as well. This is a result of the measurement technique. At the higher frequencies, the suspension impedance becomes much larger than the input impedance, so that it is difficult to recover the input impedance information from the sum of the two impedances. At the lowest frequencies, the measured response appears more resistive, while the modeled response appears more like the expected mass load. This deviation is again the result of the measurement technique.

To see more clearly how the input impedance of the line combines with the loudspeaker characteristics to form the loudspeaker input impedance curve, the last term of Equation (230) is examined. This term models the effects of the loudspeaker suspension and load. It can be thought of as the inverse of the sum of two electrical admittances Y_{E1} and Y_{E2} given by

$$Y_{E1} = \frac{S_D^2}{(B\ell)^2}\left(j\omega M_{AD} + R_{AS} + \frac{1}{j\omega C_{AS}} + Z_{AL}\right)$$

$$Y_{E2} = \frac{S_D^2}{(B\ell)^2} Z_{AT}.$$

Alternatively, the last term of Equation (230) can be thought of as the parallel combination of two electrical impedances given by the reciprocals of the above expressions:

$$Z_{E1} = \frac{(B\ell)^2}{S_D^2}\frac{1}{j\omega M_{AD} + R_{AS} + (j\omega C_{AS})^{-1} + Z_{AL}} \tag{234}$$

$$Z_{E2} = \frac{(B\ell)^2}{S_D^2}\frac{1}{Z_{AT}}. \tag{235}$$

The electrical impedance Z_{E1} results from the loudspeaker suspension and front air load and Z_{E2} results from the acoustical input impedance of the tube.

For the unfilled line, Equation (235) can be written

$$Z_{E2} = \frac{(B\ell)^2}{S_D^2}\frac{\frac{\rho_0 c}{S_T} + j\,Z_{AL}\tan(kL_T)}{\frac{\rho_0 c}{S_T}\left[Z_{AL} + j\frac{\rho_0 c}{S_T}\tan(kL_T)\right]} \tag{236}$$

where the expression for Z_{AT} given by Equation (117) has been used and $k = 2\pi\ f/c$. If the acoustical load impedance at the open end of the line can be neglected, this equation can be written

$$Z_{E2} = \frac{(B\ell)^2}{S_D^2} \frac{S_T}{j\rho_0 c \tan(2\pi\ f L_T/c)}. \tag{237}$$

For short line lengths or low frequencies, the tangent in this equation can be approximated by its argument, which results in

$$Z_{E2} = \frac{(B\ell)^2\ S_T}{j\omega S_D^2 \rho_0 L_T}. \tag{238}$$

Thus, for these conditions, Z_{E2} has the form of an electrical impedance that results from a capacitor having the value

$$C_E = \frac{S_D^2 \rho_0 L_T}{(B\ell)^2\ S_T}. \tag{239}$$

Figure 47 shows a plot of the magnitude of two impedance components, their parallel combination, and the loudspeaker input impedance. The loudspeaker input impedance Z_{VC} is obtained by adding the voice-coil resistance and the impedance of the voice-coil inductance to the parallel combination of Z_{E1} and Z_{E2}. As expected from Equation (238), at low frequencies, the plot of Z_{E2} has the form of the impedance of a capacitor. It is a straight line of slope -1 decades per decade.

It can be seen that the variations in Z_{VC} cannot be attributed solely to the physical structure of the transmission line. The variations are the result of resonances between the electrical tube impedance Z_{E2} and the electrical suspension impedance Z_{E1}. If the effect of the voice-coil inductance is neglected, the peaks in Z_{VC} occur at the frequencies where $(Z_{E1} \| Z_{E2} + R_E)$ is a maximum, and the minima in Z_{VC} occur at the frequencies where it is a minimum.

In terms of the phase, the peaks occur where the phase of $(Z_{E1} \| Z_{E2} + R_E)$ is zero and its sign is changing from positive to negative. The minima occur where its phase is zero, but its sign is changing from negative to positive.

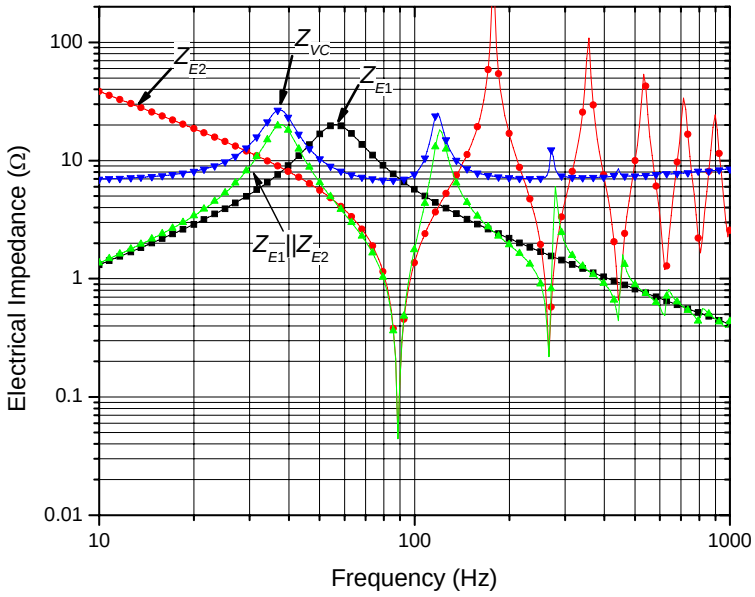

Figure 47. Illustration of how the suspension and transmission-line impedance components affect the driver input impedance.

The addition of the real quantity R_E to $Z_{E1}\|Z_{E2}$ causes the phase of the sum move nearer to zero. Thus at frequencies where the phase of $Z_{E1}\|Z_{E2}$ is zero, the addition of R_E has no effect. Therefore, the locations of the maxima and minima in the loudspeaker input impedance are the same as the frequencies where the phase of $Z_{E1}\|Z_{E2}$ is zero. For the lower frequency peaks of Z_{VC}, this condition occurs near crossings of the Z_{E1} and Z_{E2} curves where the slopes of the two curves are of opposite sign. Reflections in the tube result in multiple frequency locations where the phase of $Z_{E1}\|Z_{E2}$ is zero, and thus cause multiple peaks in the input impedance curve.

4.4 Acoustical Impedance of the Filled Line

Figures 48 and 49 show plots of the measured acoustical input impedance for the 925 mm length line filled with two, four, six, eight, and ten cylindrical fiberglass samples. These quantities of samples result in packing densities of 2.6, 5.2, 7.9, 10.5, and 14.2 $\mathrm{kg\,m^{-3}}$, respectively. The attenuation of reflections in the tube with increased packing densities is evident from the figure. A mechanical resonance of the fiberglass fibers introduces a

minimum in the filled-tube plots that is not present in the empty-tube plot. This minimum increases in frequency as the packing density increases. The impedance at zero frequency is equal to the acoustical flow resistance of the fiberglass. As expected, the flow resistance can be seen to increase with increasing packing density.

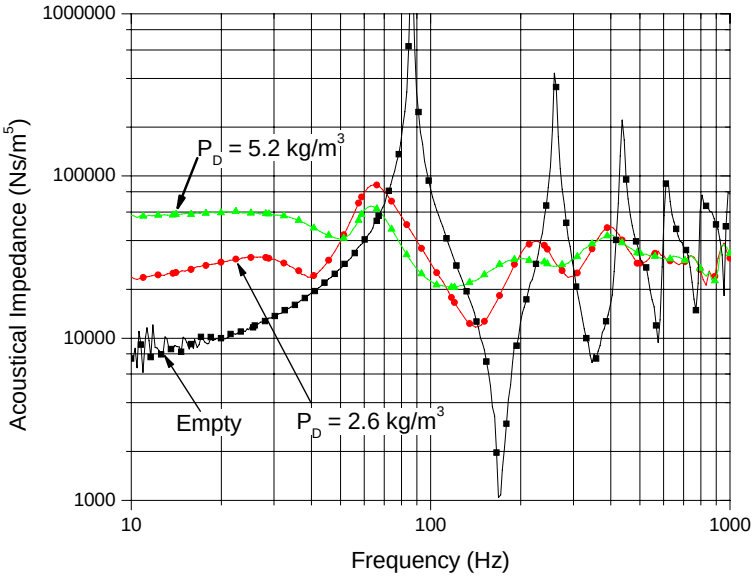

Figure 48. Acoustical input impedance for tube stuffed to various packing densities.

As the packing density is increased, the low-frequency acoustical input impedance of the line changes from a mass reactance to a compliant reactance, that is the slope of the curve changes from positive to negative, approaching a slope of approximately -0.5 decades per decade for large packing density P_D. The low-frequency input impedance is nearly a pure resistance for $P_D = 5.2\,\mathrm{kg\,m^{-3}}$. If the variations that result from the fiber resonance are ignored, this behavior suggests that for large values of P_D the line appears to be a lossy filled closed box system that can be modeled as an acoustical resistor that models the flow resistance in parallel with a frequency dependent acoustical compliance.

The peak near 400 Hz that is evident in all of the filled-tube plots is not a result of the transmission line. Rather, it corresponds to a mechanical diaphragm resonance in the loudspeaker that can be seen in the measured loudspeaker input impedance plot of Figure

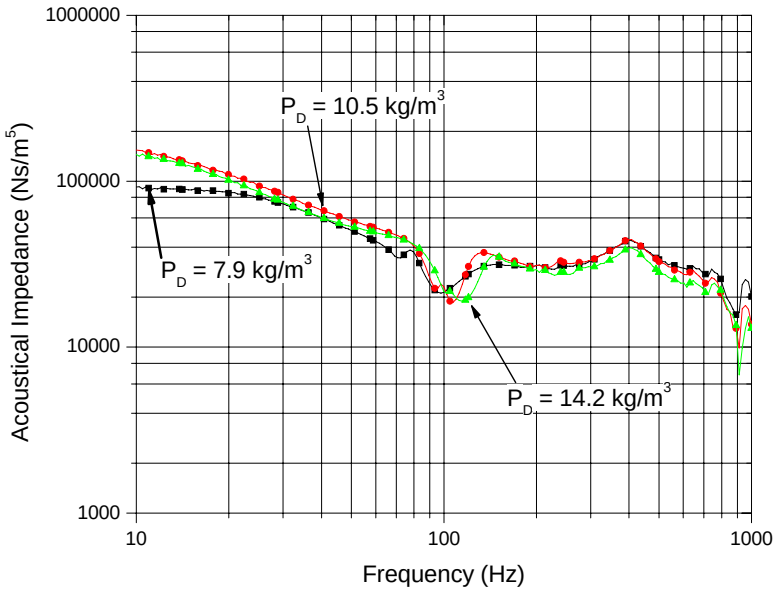

Figure 49. Acoustical input impedance for line stuffed to various packing densities.

22.

4.4.1 Determination of the Line Parameters

To calculate the modeled acoustical input impedance curves, numerical values for the fiber parameters m_{af}, c_{af}, r_{afr}, and R_f and the acoustical parameters m_{aa} and c_{aa} must be determined. Once reasonable values are obtained, they can be refined by curve fitting to the measured data.

The value of the flow resistance R_f can be determined from the low-frequency asymptote of the measured acoustical impedance plots. The lower frequency limit of 10 Hz that was imposed by the measurement equipment does not allow the asymptote to be clearly seen. However, a good estimate can still be made. If the measured impedance plots level off at low frequencies at a value of R_{fa}, the flow resistance can be calculated from

$$R_f = \frac{R_{fa}}{S_T L_T}. \tag{240}$$

A more accurate determination of R_f can be made by using a dedicated flow resistance measurement apparatus, such as the one described in [12]. However, the determination of

R_f from the measured impedance data is convenient because it can be obtained from the one automated measurement discussed in Section 2.8.

In the derivation of the transmission line model, the distribution of fibers in each incremental length of the line was considered to be uniform in a cross section of the line. However, the fibers in the tube are not actually uniformly distributed, and the parameters can vary over a cross section. For example, the fibers are fixed at the tube walls and the range of motion of a fiber near the tube walls is less than that of the fiber near the center. Thus all of the parameters are average or bulk values.

An estimate of the acoustical mass m_{af} can be obtained from the measured mechanical mass of the fiberglass. However, the effective acoustical mass may be different from that calculated from the measured mass. This primarily is because not all of the fibers can move. The acoustical mass m_{af} is related to the packing density P_D by the equation

$$m_{af} = \frac{P_D}{S_T}. \tag{241}$$

where S_T is the cross-sectional area of the tube.

Similarly, the a measured value of the fiber compliance may not be the same as the effective compliance of the fibers. In [20], the compliance of the fibers was measured by placing the fiberglass on a horizontal surface and placing a known mass of cross-sectional area nearly equal to that of the fiberglass on top of a layer of it. The displacement x_f of the fiberglass was measured and the mechanical compliance was calculated from

$$c_{mf\ell} = \frac{x_f}{m_{mp}g} \tag{242}$$

where m_{mp} is the mass of the plate and g is the gravitational constant.

Because the fiberglass samples used in [20] had a large surface area and were not inside a tube, this measurement would give a good estimate for the mechanical compliance among fibers $c_{mf\ell}$. Although the fibers of the transmission line system could slip along the tube walls, this is unlikely for the forces applied to them in a typical application. Because the fibers are effectively fixed at the tube walls, the compliance at the walls is zero. It increases

toward the center of the tube in any cross section. For a tube of large radius, the compliance between the fibers and tube wall c_{mf} is less significant than for a tube of smaller radius. The compliance among fibers can be significant in determining the tube characteristics. A measurement of the compliance of the fibers in a tube of small diameter can give some indication of the value of c_{mf}.

A direct measurement of r_{afr} would be difficult. For this investigation, r_{afr} was considered to be a general parameter that models losses and was estimated by curve fitting to measured data.

The acoustical compliance c_{aa} changes when a filling is placed in the transmission line. Its value is dependant on the thermodynamic properties of the fiberglass [3]. For an unfilled line,c_{aa} is given by

$$c_{aa} = \frac{S_T}{\gamma_a P_0} \tag{243}$$

where γ_a is the ratio of the specific heat of air at constant pressure to that of air at constant temperature and $P_0 = 1.013 \times 10^5\,\mathrm{Pa}$ is the static atmospheric pressure. For an unfilled tube, the sound pressure wave is an adiabatic process, where the compressions and rarefactions of the air occur fast enough that there is no exchange of heat to the surrounding air. For an adiabatic process, $\gamma_a = 1.4$. For this value of γ_a, Equation (6) for the velocity of sound gives $c = 345\,\mathrm{m\,s^{-1}}$. This is the velocity of sound at standard temperature and pressure.

In an adiabatic wave, the temperature of the air varies with the acoustic pressure. When filling is added to the tube, heat transfer can occur between the air and the filling. This tends to reduce the temperature variations in the air, causing the acoustic pressure wave to be an isothermal process. This occurs at low frequencies where the period of the wave is long compared to the thermal time constant of the filling. If the temperature of the air does not change with pressure, the specific heat ratio is decreased to the value $\gamma_a = 1$. In practice, the temperature of the air does vary somewhat so that it would be expected that the specific heat ratio lies in the range $1 \leq \gamma_a \leq 1.4$. At higher frequencies the thermal

time constant of the filling is much greater than the period of the wave and this effect does not occur. Thus the acoustical compliance for a filled tube is in the range

$$\frac{S_T}{1.4P_0} \leq c_{aa} \leq \frac{S_T}{P_0}. \tag{244}$$

Because γ_a is a function of frequency, c_{aa} cannot be represented by a frequency independent circuit element as it does in the model of the filled line. However, at the low frequencies of operation of a transmission line system, it was found in this work that the assumption of a constant value for c_{aa} in the range given in Equation (244) gives acceptable results.

As is the case with screens discussed in Section 2.3.3 that are used as acoustical resistances, it would be expected that the fiberglass increases the value of the acoustical mass m_{aa} from its value for an unfilled line. This was found to be true in this research.

If $r_{afr}\Delta z << R_f \Delta z/S_T$ in the model of Figure 35, it follows by current division that that the fiber and air velocities are approximately equal when the fibers are near their resonance frequency. This is because the series resonant circuit that models the fibers has an impedance minimum of $r_{afr}\Delta z$ at the fiber resonance frequency. Because the fibrous structure and the air tend to move together at that frequency, the acoustical mass is not increased by the fiber. It follows that any additional acoustical mass that is a result of the fibers must be added to the model in series with the flow resistance R_f in Figure 35. This conclusion was borne out by a comparison of the modeled and measured acoustical input impedances presented in the following section. Thus the flow resistance R_f in the model can be thought of as having a complex impedance given by

$$Z_f = R_f + (j\omega m_{aa2}) \,\|\, r_{aa2} \tag{245}$$

where m_{aa2} models the additional acoustical mass introduced by the fiberglass, and r_{aa2} models the acoustical losses in this mass.

In [24], the fiber impedance was also determined to introduce a mass component which was referred to as "dynamic resistivity." From the data presented in [24], its impedance

could be approximated as a lossy inductor having an impedance of the form of Equation (31). However, it was found in this work that modeling the losses in the mass by a parallel resistor gave acceptable results.

It was found from the experimental data measured in this work that the values of the acoustical mass m_{aa2} and the acoustical resistance r_{aa2} varied little for the different packing densities and tube areas used. For a given fiber orientation and transmission line diameter, it was found that a higher packing density resulted in a larger value of the flow resistance R_f, a larger value of the acoustical compliance c_{aa}, and smaller values of the acoustical compliances c_{af} and $c_{mf\ell}$.

4.4.2 The Modeled Impedances

The model of the filled transmission line described here contains ten parameters. These are the length L_T and radius a_T of the transmission line, the acoustical mass of air in the unfilled line m_{aa}, the additional acoustical mass m_{aa2} and its associated acoustical resistance r_{aa2} added by the fibers, the acoustical compliance of the air in the line c_{aa}, and the packing density P_D, flow resistance R_f, acoustical compliance c_{af}, and acoustical resistance r_{afr} for the fiberglass.

The parameters L_T, a_T, and P_D can be measured directly. The acoustical mass m_{aa} can be calculated from $m_{aa} = \rho_0/S_T$. The range of expected values for the acoustical compliance c_{aa} can be calculated from Equations (244). R_f can be determined from the low frequency values of the measured acoustical impedance. Values for c_{af} and r_{afr} can be determined from the location and magnitude of the fiber resonance minimum in the acoustical impedance plots.

The resonance frequency of the series resonant circuit consisting of the elements $m_{af}\Delta z$, $c_{af}\Delta z$, and $r_{afr}\Delta z$ that model the fibers in Figure 35 is approximately given by

$$f_r = \frac{1}{2\pi}\sqrt{\frac{S_T}{P_D c_{af}}}. \tag{246}$$

Because f_r, S_T, and P_D can be measured, an initial value for c_{af} can be calculated from

this relation. It can then be refined by curve fitting to obtain the best fit of the experimental data to the model. The acoustical resistor r_{afr} can be adjusted for the proper depth and width of the minimum at f_r.

The values of m_{aa2} and r_{aa2} can be adjusted to give good agreement at low and high frequencies. It was found in this work that the values of these two parameters vary little with changes in packing density. It was also found that these parameters have little effect and can be set to zero to eliminate them from the model for packing densities having values $P_D \geq 10.5\,\mathrm{kg\,m^{-3}}$. This is because the flow resistance becomes large compared to the impedance of the lossy mass at high packing densities.

Figures 50 through 54 show the modeled and measured acoustical input impedances of the line for packing densities of 2.6, 5.2, 7.9, 10.5, and 14.2 $\mathrm{kg\,m^{-3}}$. The parameter values used in Equation (212) to calculate the modeled responses are given in Table 2.

Table 2. Parameter values for transmission line filled to various packing densities.

P_D	L_T	a_T	R_f	m_{aa}	c_{aa}	c_{af}	r_{afr}	m_{aa2}	r_{aa2}
2.6	0.925	0.075	407	67	1.37×10^{-7}	6.65×10^{-8}	20000	90	60000
5.2	0.925	0.075	1089	67	1.37×10^{-7}	2.15×10^{-8}	54000	120	60000
7.9	0.925	0.075	1767	67	1.57×10^{-7}	0.84×10^{-8}	60000	120	60000
10.5	0.925	0.075	3681	67	1.67×10^{-7}	0.39×10^{-8}	48000	130	60000
14.2	0.925	0.075	3276	67	1.67×10^{-7}	0.26×10^{-8}	55000	130	60000

Figures 55 and 56 show plots of the real and imaginary parts of the propagation constant given by Equation 214 for the $a_T = 7.5\,\mathrm{cm}$ line for various packing densities. Figure 55 indicates that, although the attenuation per meter of the sound wave in the line generally increases with frequency, there is a minimum in the attenuation because of the fiber resonance frequency.

The phase shift between the driver and the tube outputs at a given frequency can be determined from Figure 56. At higher frequencies, the phase shift per meter becomes linear with frequency indicating that the line is dispersionless and that the speed of sound is a constant. At lower frequencies, this is not the case.

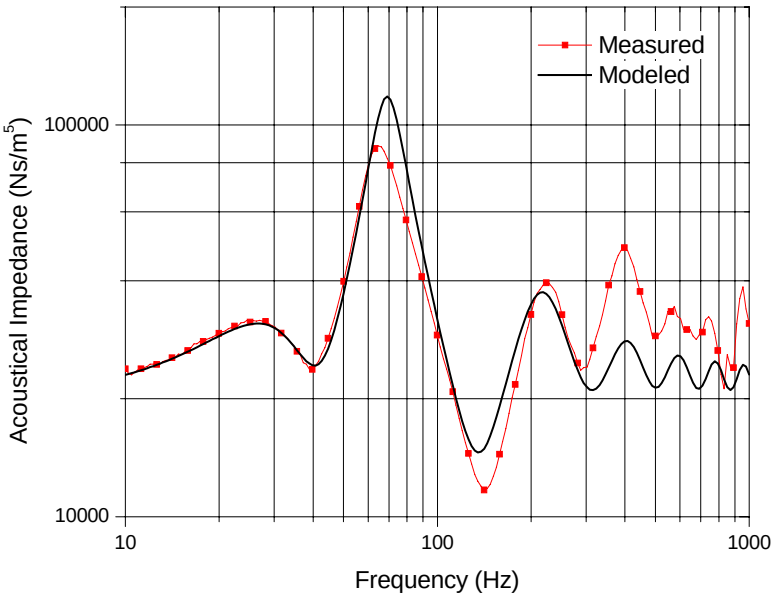

Figure 50. Measured and modeled input impedance for $P_D = 2.6\,\mathrm{kg\,m^{-3}}$.

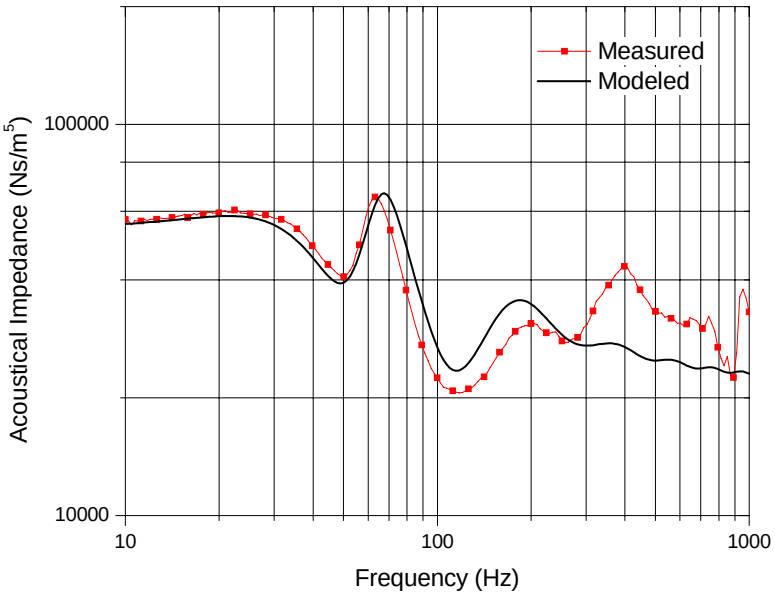

Figure 51. Measured and modeled input impedance for $P_D = 5.2\,\mathrm{kg\,m^{-3}}$.

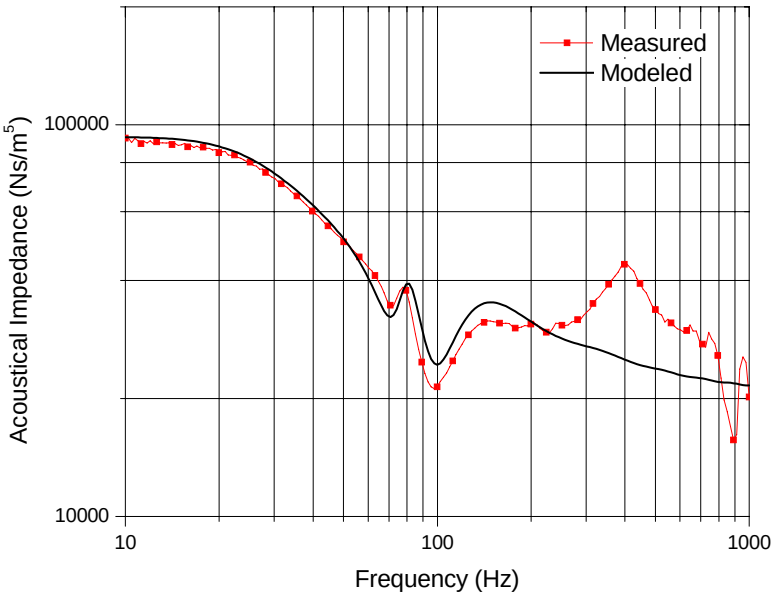

Figure 52. Measured and modeled input impedance for $P_D = 7.9\,\mathrm{kg\,m^{-3}}$.

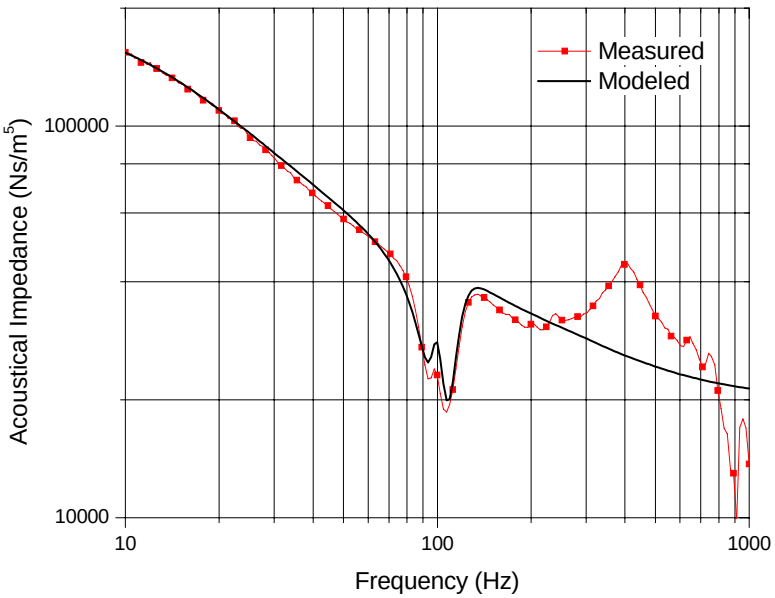

Figure 53. Measured and modeled input impedance for $P_D = 10.5\,\mathrm{kg\,m^{-3}}$.

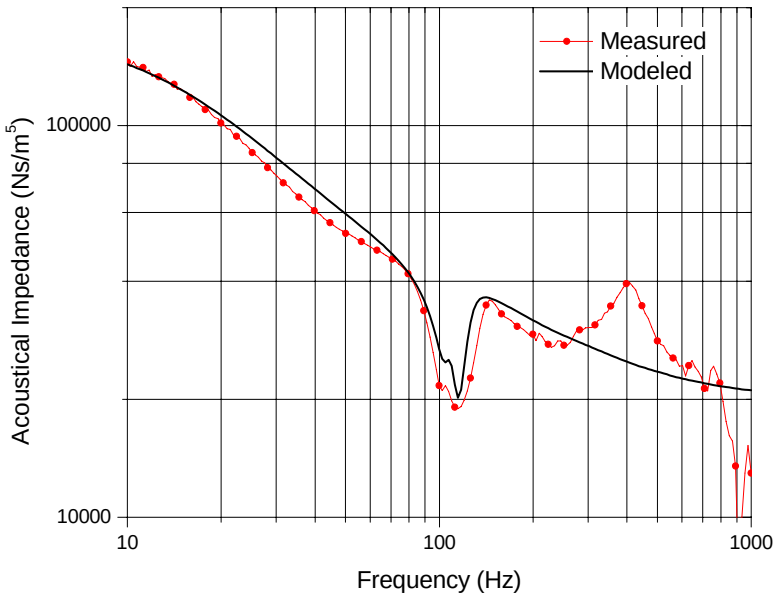

Figure 54. Measured and modeled input impedance for $P_D = 14.2\,\mathrm{kg\,m^{-3}}$.

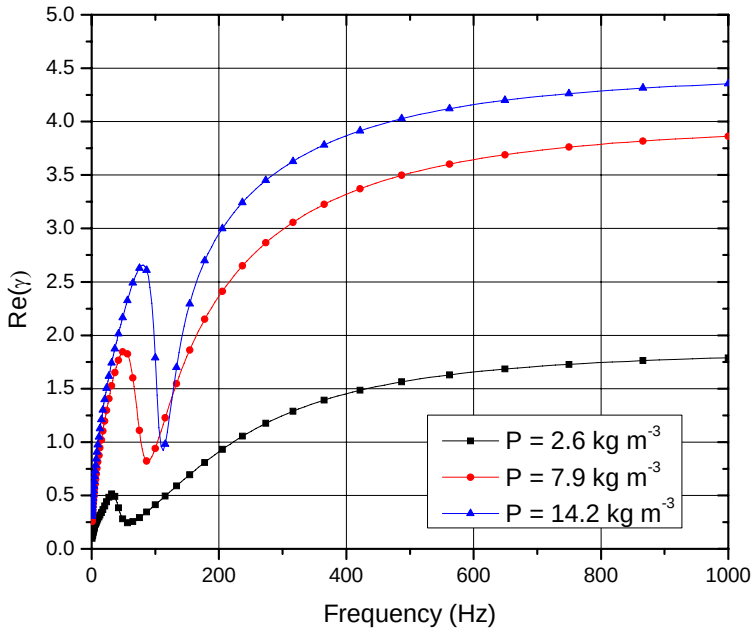

Figure 55. Real part of the propagation constant vs. frequency for the $a_T = 7.5\,\mathrm{cm}$ line for various packing densities.

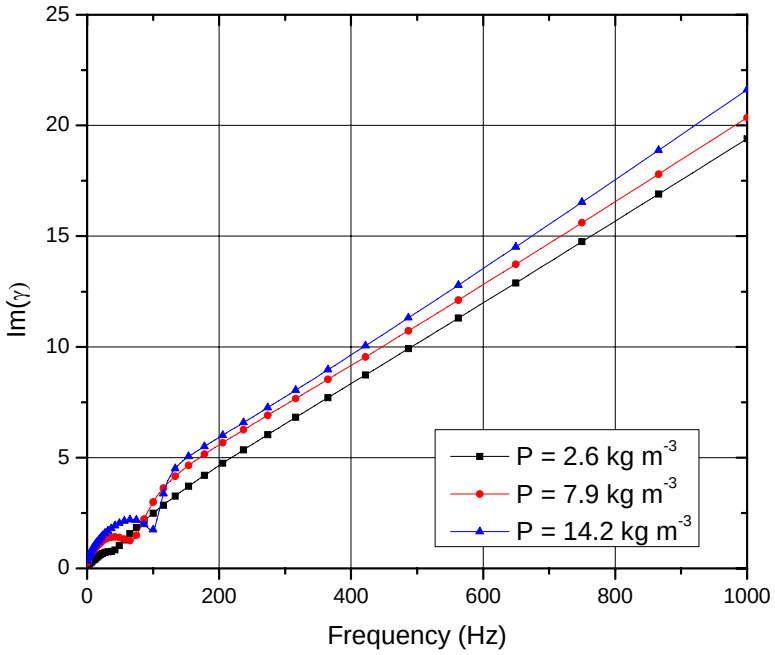

Figure 56. Imaginary part of the propagation constant vs. frequency for the $a_T = 7.5\,\mathrm{cm}$ line for various packing densities.

4.4.3 Comparison to Other Models

To determine how the performance of the transmission line model given in Figure 35 compares with that of other models, plots of measured acoustical input impedance were compared to those predicted by the models of Augspurger (model A) and Bradbury (model B) and of the model derived in this work. These models can be obtained from the transmission line model of Figure 35 by appropriately varying the parameters. Figures 57 through 59 show a comparison of the acoustical input impedance predicted by these models to measured data for packing densities of 2.6, 7.9, and $14.2\,\mathrm{kg\,m^{-3}}$. The parameters used in the model are shown in Table 3.

For both models, $c_{af} = \infty$, $r_{aa2} = 0$, and $m_{aa2} = 0$. For model A, r_{afr} is set to infinity to eliminate the fiber motion. For model B, r_{afr} is set to zero, so that only the fiber mass determines the characteristics of the fiber motion.

All of the features of the measured impedance curves are not predicted by either of these two other models. In plotting the impedance predicted by Augspurger's model, the

Table 3. Parameter values that reduce the simplified transmission-line model to those of Augspurger and Bradbury for various packing densities.

Model	P_D	L_T	a_T	R_f	m_{aa}	c_{aa}	r_{afr}
A	2.6	0.925	0.075	407	67	1.67×10^{-7}	∞
B	2.6	0.925	0.075	1089	67	1.67×10^{-7}	0
A	7.9	0.925	0.075	1767	67	1.67×10^{-7}	∞
B	7.9	0.925	0.075	3681	67	1.67×10^{-7}	0
A	14.2	0.925	0.075	3276	67	1.67×10^{-7}	∞
B	14.2	0.925	0.075	3276	67	1.67×10^{-7}	0

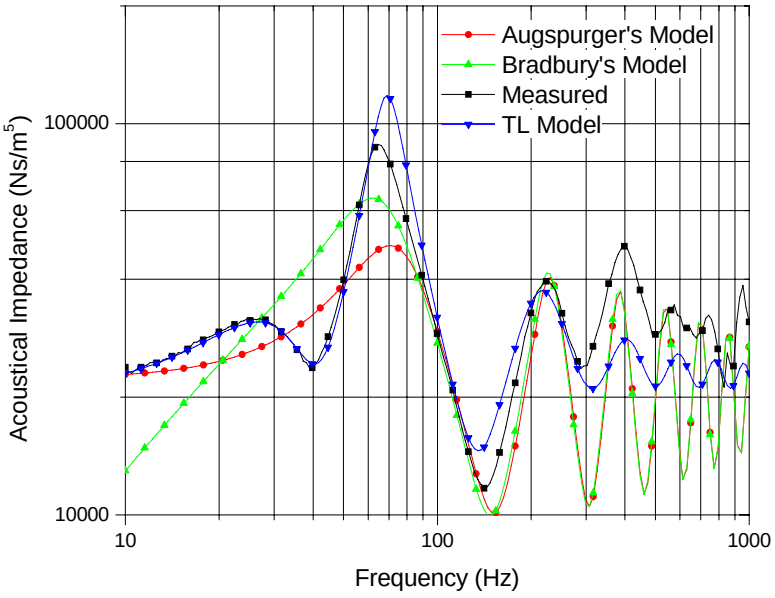

Figure 57. Comparison of measured acoustical input impedance to Augspurger's and Bradbury's models and to the simplified transmission line model developed in this work for $P_D = 2.6\,\mathrm{kg\,m^{-3}}$.

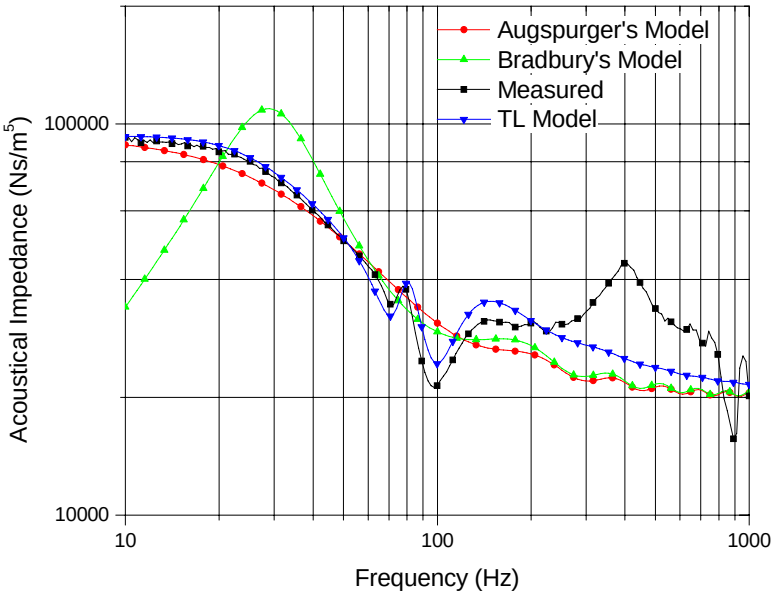

Figure 58. Comparison of measured acoustical input impedance to Augspurger's and Bradbury's models and to the simplified transmission line model developed in this work for $P_D = 8.5\ \mathrm{kg\,m^{-3}}$.

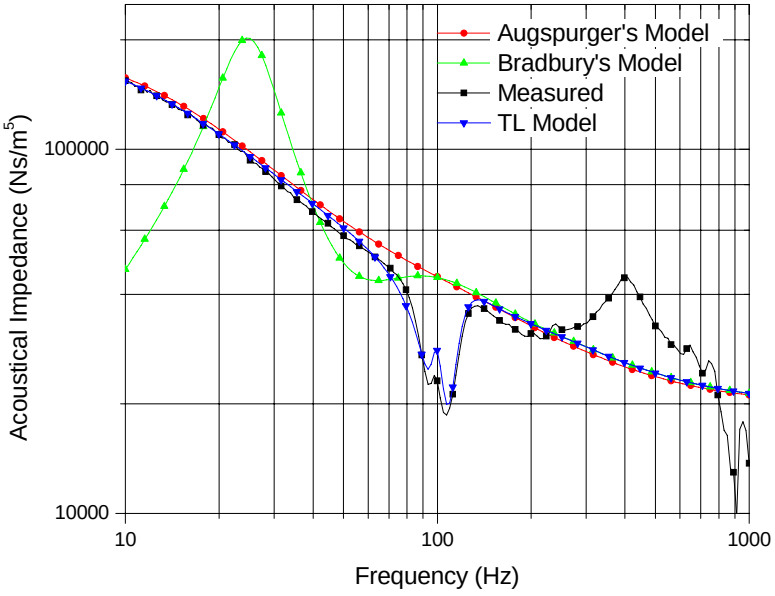

Figure 59. Comparison of measured acoustical input impedance to Augspurger's and Bradbury's models and to the simplified transmission line model developed in this work for $P_D = 11.3\,\mathrm{kg\ m^{-3}}$.

flow resistance was held constant with frequency. Augspurger stated that he varied the resistance with frequency, but it is unclear how he did this or what values he used. The resonances that result from fiber motion are not predicted by his model. In it, the mass of the air is fixed by the tube dimensions and the flow resistance is chosen to give the correct value at low frequencies. Therefore, only the air compliance is unknown. It was found that the maximum value of compliance given by Equation (244) resulted in the best fit of Augspurger's model to the measured data.

Bradbury's model permits the fibers to move, but only at the lowest frequencies. This does not agree with measured data where the fibers exhibit a resonance that occurs at increasingly higher frequencies as the packing density is increased. As in Augspurger's model, the maximum value of air compliance given by Equation (244) gave the best fit between Bradbury's model and the measured data. The value for the acoustical mass per unit length of the fibers was calculated from $m_{af} = P_D/S_T$. By significantly reducing this mass, the fiber resonance minimum in the modeled response using Bradbury's model could be made to occur at the same frequency as the measured minimum frequency, but there is a large peak in the modeled impedance that is not present in the measured data.

4.4.4 Characterization of the Fiberglass

From Table 2, it can be seen that the parameters R_f, c_{af}, and r_{afr} all vary significantly with packing density. Figures 60 through 62 show plots of each parameter versus packing density. The measured parameter values were obtained for six values of P_D by fitting the parameters of the simplified transmission line model given by Equation (212) to measured data for the tube filled with three to eight fiberglass samples. The tube used had length $L_T = 925\,\text{mm}$ and radius $a_T = 7.5\,\text{cm}$.

The smooth curve in Fig 60 is a plot of the equation

$$R_f(P_D) = 27.3 P_D^{2.3}. \tag{247}$$

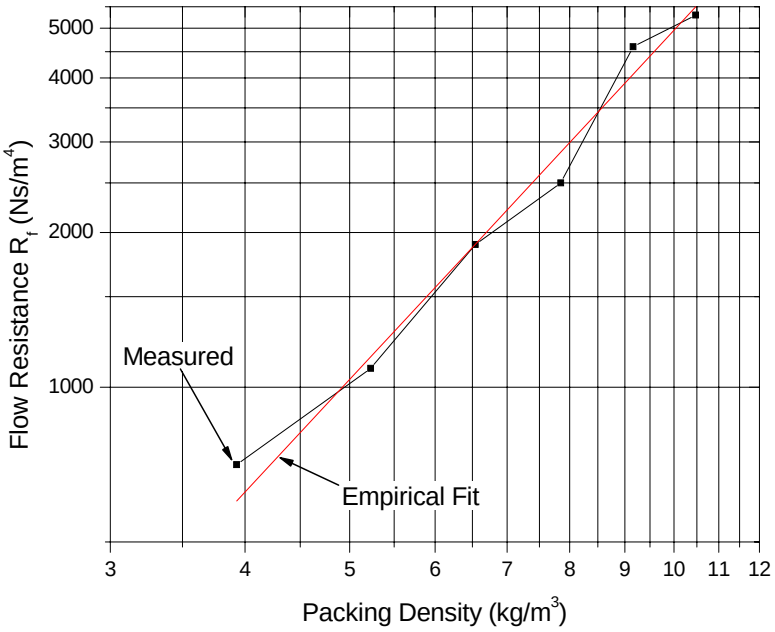

Figure 60. Measured and modeled flow resistance versus packing density.

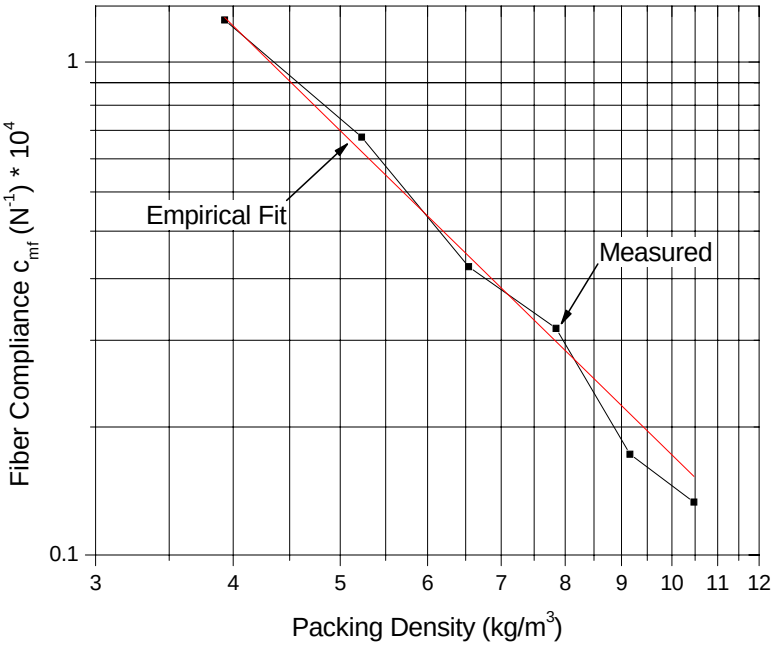

Figure 61. Measured and modeled compliance versus packing density.

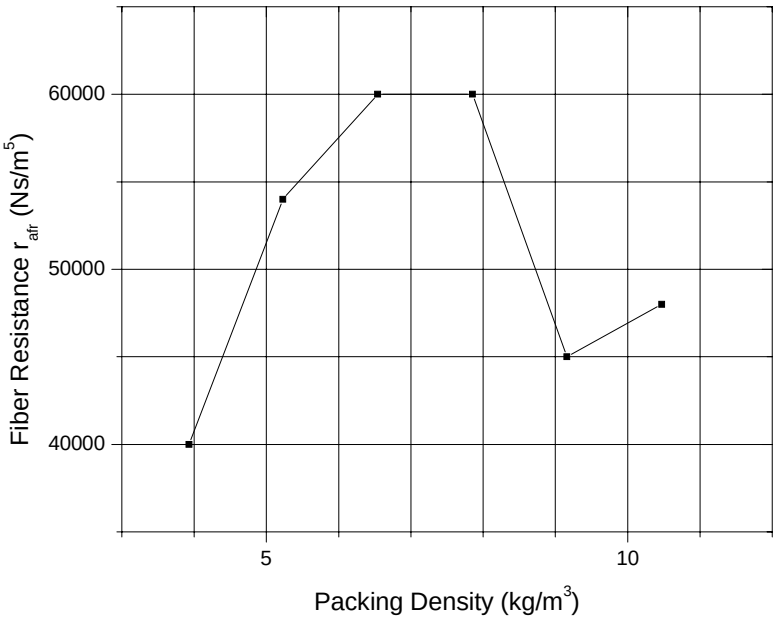

Figure 62. Measured fiber resistance versus frequency.

The numerical values in this equation were obtained using a least square curve fitting routine to the data for $P_D \leq 10.5\,\mathrm{kg\,m^{-3}}$. This equation is of the same form as Bradbury's equation for $R_f\,(P_D)$ given in Equation (26). It is also of the same form as are the formulas for flow resistance given in [14] and [16]. However, the numerical values are different. Bradbury found the exponent to be 1.4. In [14], the exponent is 1.53, and in [16], the exponent is 1.404.

The experimentally obtained compliance is plotted as a function of the packing density in Figure 61. The red curve in the figure shows the compliance calculated from the empirical equation

$$c_{mf}(P_D) = \frac{1}{407 P_D^{2.2}}. \tag{248}$$

The coefficients in this equation were obtained by a least-squares curve fit to the experimental data.

4.4.5 Parameter Scaling

To design a transmission line loudspeaker system using the transmission line model developed here, the change in model parameters with changes in the physical dimensions of

the line must be addressed. The impedance data was measured for filled transmission lines having the radii $a_T = 7.5\,\text{cm}$ and $a_T = 10\,\text{cm}$. From this data, the required relationships can be obtained.

The model parameters obtained are per unit length parameters, permitting the parameters to be used in modeling any line length L_T. To investigate this, the parameters determined for the 925 mm line that are given in Table 2 were used in calculating the acoustical input impedance for a 1.6 m line. In addition, a line having this length and a packing density $P_D = 3.9\,\text{kg}\,\text{m}^{-3}$ was measured. A comparison of the the calculated and the measured data is shown in Figure 63. The two curves match well at low frequencies, in that the prominent features of the curves are at the same frequencies. The peaks of the modeled impedance are more prominent than are those of the measured response. The discrepancy above 200 Hz results from the measurement technique as discussed in Section 4.3.

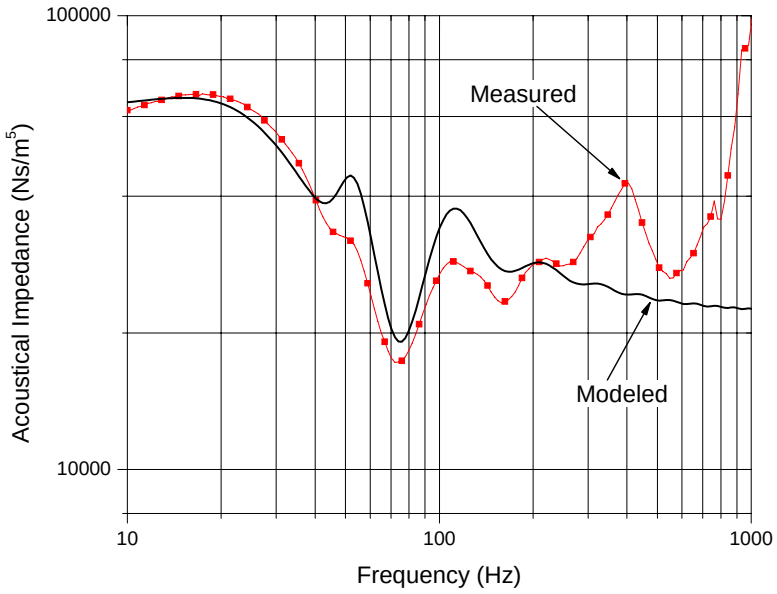

Figure 63. Comparison of measured and modeled input impedance for filled tube of length $L_T = 1.6\,\text{m}$.

Conceptually, it is possible to model a change in diameter of the tube by appropriately scaling the model parameters. The acoustical parameters that model the airflow, namely $m_{aa} = \rho_0/S_T$ and $c_{aa} = S_T/\rho_0 c^2$, correctly scale with area, as was verified experimentally

by measuring the input impedance of unfilled tubes of different diameters. However, the variation of the mechanical properties of the fiberglass with tube diameter is less straightforward.

Figure 64 shows plots of measured acoustical input impedance for two filled tubes, one having radius $a_T = 7.5\,\text{cm}$ and the other having radius $a_T = 10\,\text{cm}$. For both tubes, the packing density and length were $P_D = 3.9\,\text{kg}\,\text{m}^{-3}$. and $L_T = 925\,\text{mm}$. Because the acoustical input impedance of the unfilled tube is inversely proportional to the square of the tube area, the larger diameter tube has an overall lower input impedance. The variations in the impedance that result from reflections or cone resonances occur at the nearly the same frequencies for both tubes, but the resonance attributed to the presence of the fibers occurs at a lower frequency for the larger-diameter tube. The ratio of the fiber resonance frequency for the larger-diameter tube to that for the smaller-diameter tube is 0.75, which is also the ratio of the tube radii. Although the locations of the resonance frequencies change with packing density, the measured ratio of the resonance frequencies for these two tubes remains nearly constant for packing densities ranging from $3.9\,\text{kg}\,\text{m}^{-3}$ to $10.5\,\text{kg}\,\text{m}^{-3}$. This implies that the fiber resonance frequency varies inversely with the tube radius.

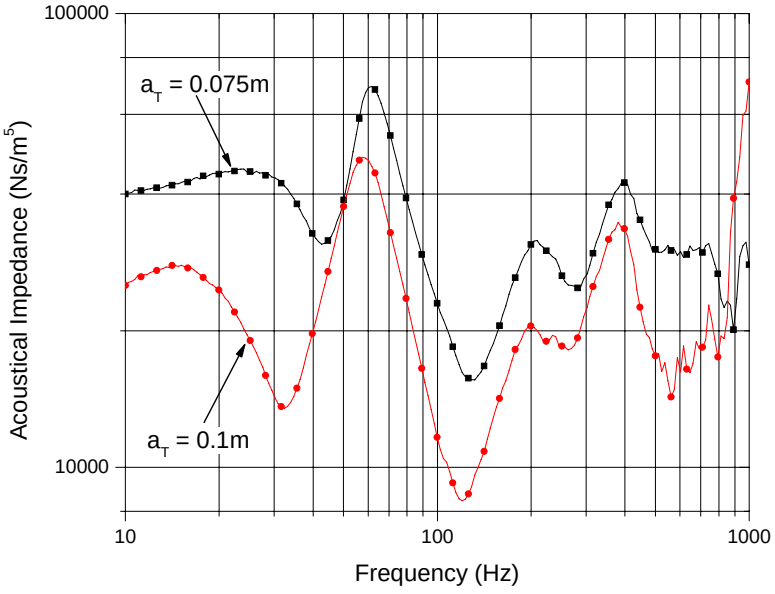

Figure 64. Comparison of input impedance for lines of same length but different radii.

For the fiber-resonance modeled by the series resonance of the mass m_{mf} and compliance c_{mf} in Figure 35, the resonance frequency is given by

$$f = \frac{1}{2\pi\sqrt{m_{mf}c_{mf}}}. \tag{249}$$

As the tube radius is increased, the fiber mass per unit length given by $m_{mf} = P_D S_T$ increases as the radius squared. For two tubes having radii a_1 and a_2 and having the same packing densities, the ratio of their fiber-resonance frequencies is given by

$$\frac{f_1}{f_2} = \sqrt{\frac{a_2^2 c_{mf2}}{a_1^2 c_{mf1}}}. \tag{250}$$

For this equation to agree with the experimentally observed ratio, which was a_2/a_1, the mechanical compliance c_{mf} must be constant with changes in tube diameter. If the fiber layers resonate as do stretched elastic diaphragms [35], where the fundamental resonance frequency is inversely proportional to the radius, the observed behavior is explained. If a single fiber in a tube attached at its ends to the tube wall and stretched along a diameter is considered, the resonance frequency also varies inversely with the radius, and the observed behavior is also explained. If the length of this fiber is doubled, both the mass and the compliance double, which results in a resonance frequency that is halved.

In scaling the parameters determined with a particular diameter tube in order to predict the behavior of a tube of different diameter, the moving fiber mechanical mass is calculated from $m_{mf} = P_D S_T$. The mechanical compliance c_{mf} of the fibers can be assumed to vary only with packing density (as shown in Figure 61) and not with tube area. This assumption gives good agreement between predicted and measured depths of the resonance minimum in the acoustical impedance of the tube.

The mechanical resistance of the fibers r_{mfr} is an experimentally determined parameter. Plots of experimentally determined values for r_{mfr} versus the packing density P_D for both the $a_T = 7.5\,\text{cm}$ and the $a_T = 10\,\text{cm}$ tubes are shown in Figure 65. There are insufficient data to predict any empirical relation that predicts r_{mfr}. In the range $5 \leq P_D \leq 7$, it is approximately constant and has the same value for both tubes.

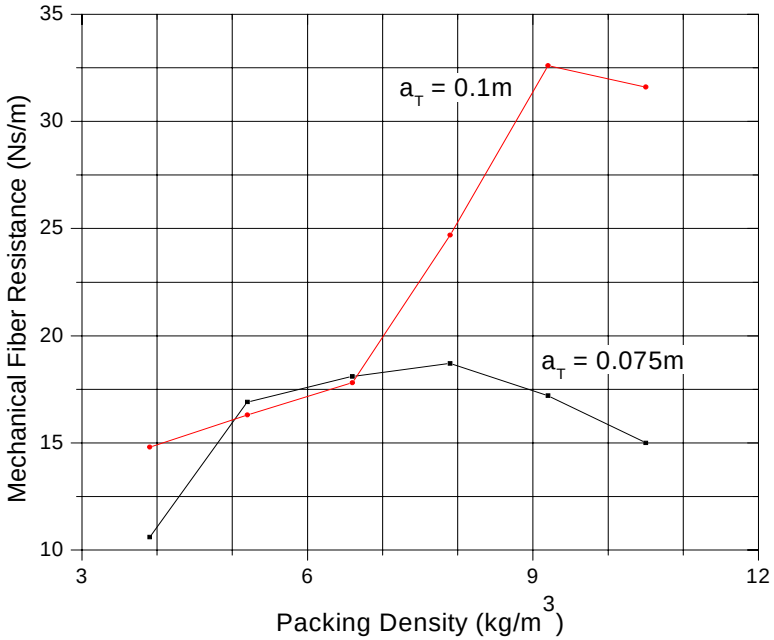

Figure 65. Measured mechanical fiber resistance for two tubes of different diameter having various packing densities.

Let the ratio of two tube radii be written

$$A = \frac{a_2}{a_1} \tag{251}$$

The parameters for a tube of radius a_2 can be obtained from those of the $a_1 = 7.5\,\text{cm}$ tube by multiplying c_{aa} by A^2, dividing m_{aa} by A^2, multiplying c_{af} by A^4, and adjusting r_{afr} according to Figure 65.

Figure 66 shows the measured and modeled input impedances for a tube having $a_T = 0.1\,\text{m}$, $P_D = 3.9\,\text{kg}\,\text{m}^{-3}$, and $L_T = 925\,\text{mm}$. The modeled response was obtained by adjusting the measured parameters for the $a_T = 7.5\,\text{cm}$ tube.

With the relationships of this section and the empirical relationships of Section 4.4.4, the input impedance of a transmission line filled with fiberglass can be written as a function of P_D, a, and L_T. For the simplified model of Figure 35, the model parameters in terms of packing density P_D and tube radius a_T are given by

$$R_f = 27.3 P_D^{2.3} \tag{252}$$

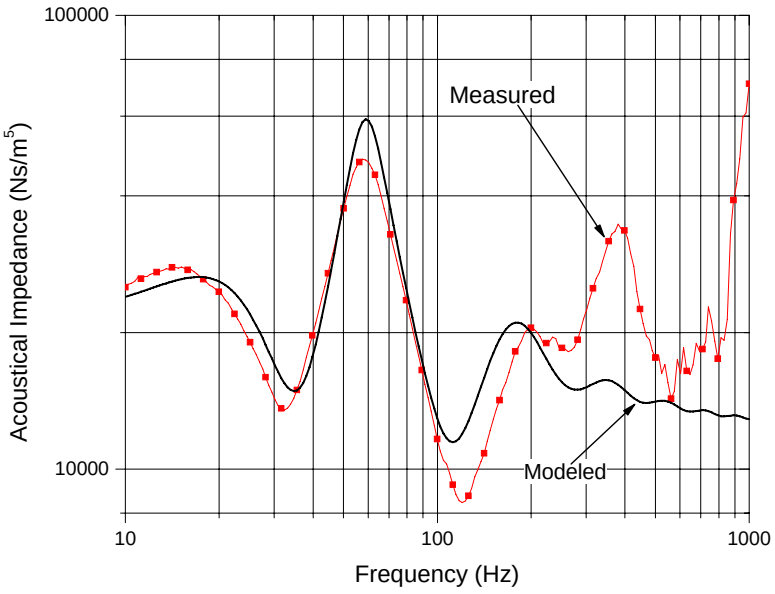

Figure 66. Comparison of measured response to that obtained from using scaled parameters in the model.

$$c_{aa} = \frac{S_T}{\gamma_a P_0} \tag{253}$$

$$m_{aa} = \frac{\rho_0}{S_T} \tag{254}$$

$$c_{af} = \frac{S_T^2}{407 P_D^{2.2}} \tag{255}$$

$$m_{aa2} = 120 \tag{256}$$

$$r_{aa2} = 50000 \tag{257}$$

where $S_T = \pi a_T^2\ \mathrm{m}^2$, $P_0 = 1.013 \times 10^5\ \mathrm{N\,m^{-2}}$, $\rho_0 = 1.18\ \mathrm{kg\,m^{-3}}$, and γ_a is chosen to be 1.1, a value that indicates that the sound wave is approaching a purely isothermal process. An estimate for the value of r_{afr} can be found by an interpolation of the data in Figure 65.

The values for m_{aa2} and r_{aa2} do vary slightly with packing density, but the above values result in good agreement with measured data.

A comparison of measured acoustical input impedances to those predicted by Equation 212 using the parameters given by Equations (252) - (257) indicates that a filled transmission can be modeled accurately in this way. These expressions can be used to predict the input impedance of lines of various packing densities, radii, and lengths. With the transmission line characterized in terms of these three parameters, the performance of a transmission line loudspeaker system can be predicted.

4.4.6 Nonlinear Behavior of the Fiberglass

It was found in this research that the measured electrical input impedance of a filled transmission line changes with the source voltage, thus indicating a nonlinear behavior. Because this did not occur when the loudspeaker was measured in free air or on an unfilled tube, it is a nonlinearity in the fibers. Figure 67 shows measured electrical input impedance curves for a line having a radii $a_T = 7.5\,\text{cm}$, a length $L_T = 925\,\text{mm}$, and the packing density $P_D = 14.2\,\text{kg}\,\text{m}^{-3}$ for various values of source voltage. The measurement setup is as shown in Figure 36. The loudspeaker is the unit having the parameters given in Table 1.

The figure shows that the peak in the response moves to lower frequencies and its amplitude decreases as the generator voltage is increased. Figure 68 shows a magnified view of the responses near the peaks.

Because the loudspeaker is not a source of constant volume velocity, the volume velocity emitted by the diaphragm is a function of the acoustical input impedance to the transmission line. The electrical impedance data presented in Figures 67 and 68 were made by holding the source voltage constant with frequency. Thus the volume velocity emitted was a function of frequency. Because the fiberglass parameters may vary with the volume velocity, it is desirable to hold the volume velocity constant with frequency during a measurement when it is desired to determine parameters from measured data. To do this, the generator voltage must be varied with frequency. A method of accomplishing this is

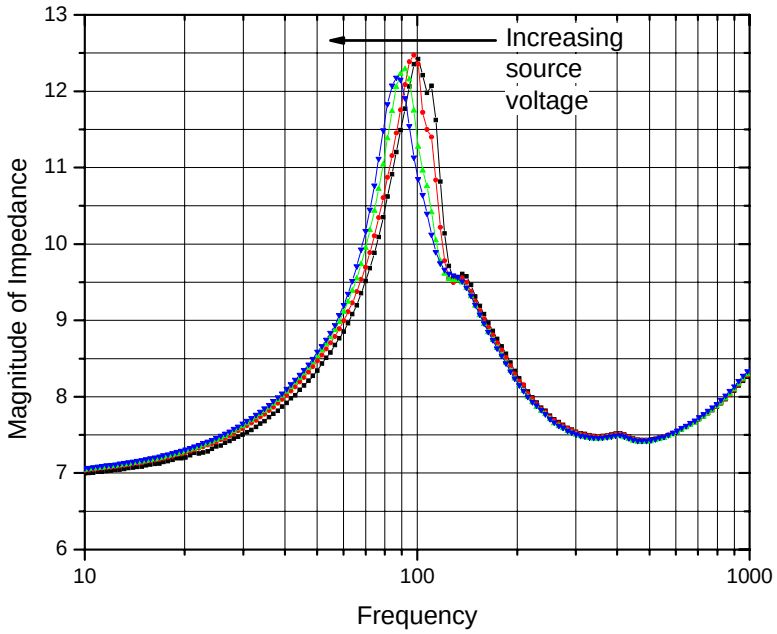

Figure 67. Electrical input impedance of driver on line having $P_D = 14.2\,\mathrm{kg\,m^{-3}}$ for input source voltage varying from $300\,\mathrm{mV}$pp to $5\,\mathrm{V}$pp.

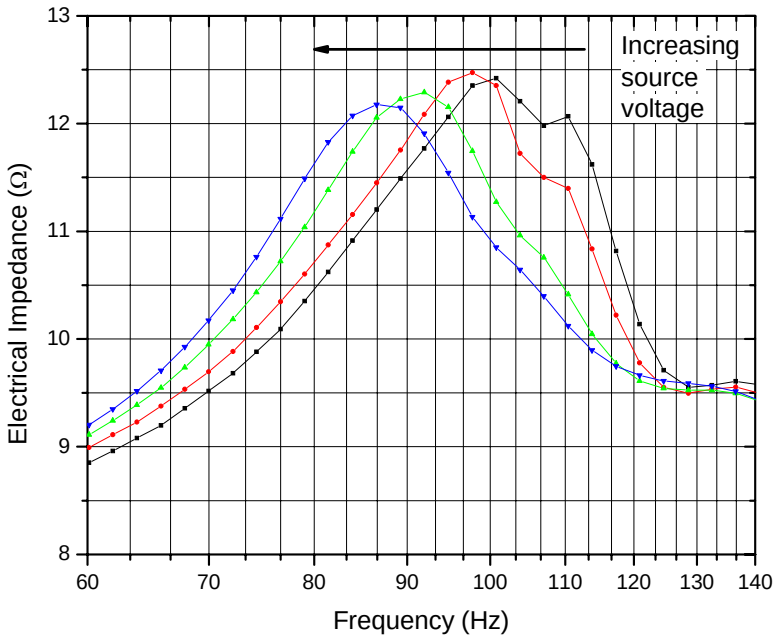

Figure 68. Magnified view of electrical input impedance of driver on line having $P_D = 14.2\,\mathrm{kg\,m^{-3}}$ for four values of input source voltage from $300\,\mathrm{mV}$pp to $5\,\mathrm{V}$pp.

described below.

Figure 69 is a diagram of a test setup that was used to determine the relationship between volume velocity and input voltage. The Audio Precision System Two Analyzer generates a sinusoidal test signal. The signal is applied to a variable attenuator. Its output is then applied to a power amplifier having a voltage gain of 21. Without the attenuator the Audio Precision output voltage would have to be set to a small value. Because its output is noisy at low levels, the attenuator was used. Thus by keeping the output level of the Audio Precision system large and attenuating it to the desired level, signal-to-noise ratio is improved. A closed box was placed on the rear of the driver and a calibrated microphone was used to measure the acoustic pressure inside the box. The frequency analyzer is used to provide power for the microphone preamp and to monitor the output pressure. The AP System Two records the driver voltage, the input voltage, and the microphone voltage.

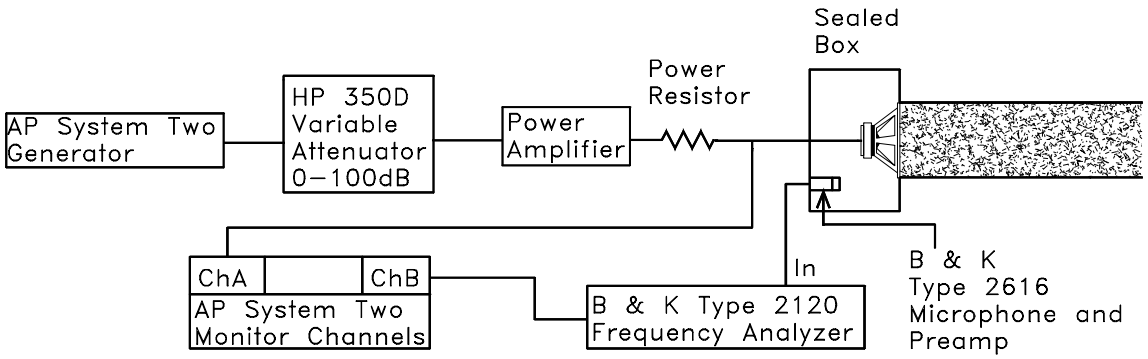

Figure 69. Pressure measurement test setup.

As in Figure 36, the front of the driver radiates into a filled transmission line having a radius $a_T = 7.5\,\text{cm}$, a length $L_T = 925\,\text{mm}$, and a packing density $P_D = 14.2\,\text{kg}\,\text{m}^{-3}$. At wavelengths much greater than the box dimensions, the box can be considered to be an acoustical compliance having the acoustical impedance $Z_A = (j\omega C_A)^{-1}$, where $C_A = V/\rho_0 c^2$ and V is the volume of air in the box. The volume velocity emitted by the front of the diaphragm can be written as

$$U_D = -p_D j\omega C_A. \tag{258}$$

It can be seen that if the box pressure p_D is varied inversely with frequency, the volume velocity is constant with frequency.

Box acoustic pressure versus frequency data were measured for source voltages ranging from 0.1 V to 2.9 V rms to generate the family of curves shown in Figure 70. The first eleven curves, from bottom to top, correspond to source voltages of 0.1 V to 1.1 V rms in steps of 0.1 V. The remainder of the curves step in 0.2 V increments to a final voltage of 2.9 V rms. On the graph, the box pressure would vary inversely with frequency if the measured pressure variation with frequency lies on a line with a slope of -20 dB/decade. By drawing a line on the graph having the equation $20\log(p_0/f)$, where p_0 is a desired acoustic pressure in the box at $f = 1$ Hz, an interpolation of the curves can be used to solve for how the input voltage must be varied with frequency to maintain the pressure on the chosen line.

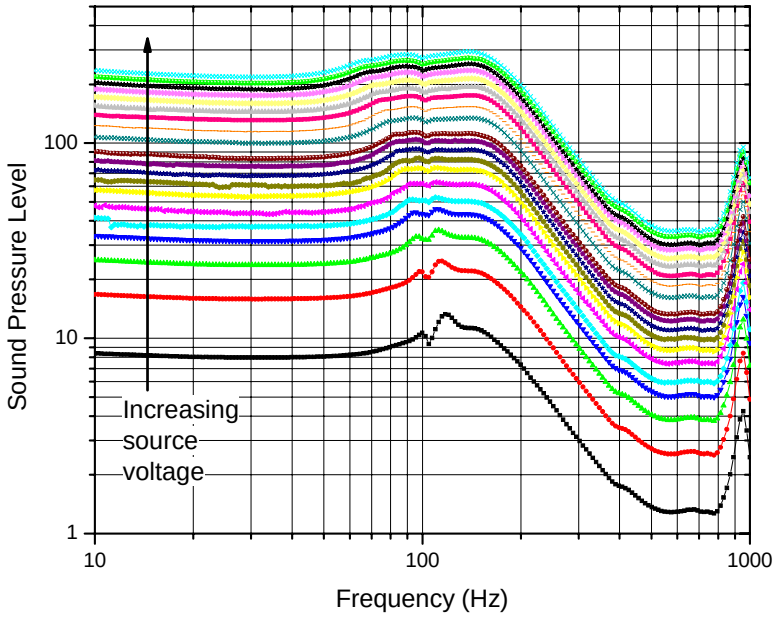

Figure 70. Variation of box pressure with source voltage and frequency.

In making impedance measurements, either the voice-coil voltage or the volume velocity can be held constant with frequency. It was found that the non-linear effects measured with a constant volume velocity excitation were less than those measured with constant

voltage excitation. However, the impedance measured for low levels of constant voice-coil voltage closely matched those measured for constant volume velocity. It was determined that the parameters determined from impedance measurements with a voice-coil voltage of 0.1 V rms were reasonably free from the non-linear effects.

CHAPTER 5

THE TRANSMISSION LINE LOUDSPEAKER SYSTEM

The model for the filled transmission line derived in Chapter 3 allows the output of the entire transmission line system to be determined. An illustration of the transmission line system is shown in Figure 71.

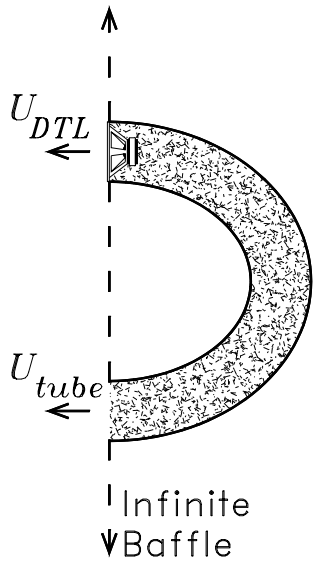

Figure 71. Transmission line on an infinite baffle.

It is assumed that the filled line is mounted on an infinite baffle such that the driver and the open end are in the same plane, preferably close together. The volume velocity U_D in the figure is the volume velocity emitted by the driver on the transmission line and U_{tube} is the volume velocity emitted from the open end of the line. The total volume velocity output of the system is the complex sum of the two volume velocities.

5.1 The Acoustic Pressure Radiated by the Loudspeaker Diaphragm

Figure 72 shows the Norton form of the low-frequency combination acoustical analogous circuit [36] for a loudspeaker mounted so that the front of the driver radiates from an infinite baffle. At low frequencies, the impedance that results from the air load on the front side

of the driver is modeled as a mass acoustical mass. This mass adds in series with the diaphragm acoustical mass to give the mass M_{AFS} in the model. The acoustical compliance C_{AS} is the acoustical compliance of the driver suspension. The acoustical resistor R_{AS} models mechanical losses in the suspension. The acoustical resistance R_{AE} models losses resulting from the electrical resistance of the loudspeaker voice coil.

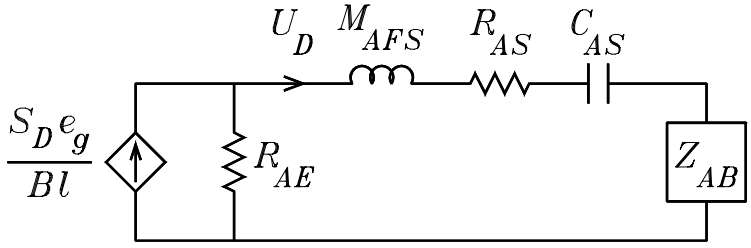

Figure 72. Combination analogous circuit for driver in an infinite baffle with arbitrary back load.

The circuit shown in Figure 72 differs from the circuit of Figure 12 in that the series combination of Z_{AD} and Z_{AF} in Figure 12 is replaced by the series circuit elements M_{AFS}, R_{AS}, and C_{AS}. Also, the impedance $(B\ell)^2 / \left(Z_{ET} S_D^2\right)$ is replaced by its low-frequency value R_{AE}. The element values are given by

$$R_{AE} = \frac{(B\ell)^2}{S_D^2 R_E} \tag{259}$$

$$R_{AS} = \frac{R_{MS}}{S_D^2} \tag{260}$$

$$C_{AS} = S_D^2 C_{MS} \tag{261}$$

$$M_{AFS} = \frac{M_{MD}}{S_D^2} + M_{A1} \tag{262}$$

where B is the magnetic flux density in the air gap of the magnet, ℓ is the effective length of the voice-coil wire that cuts this flux, S_D is the area of the driver diaphragm, R_E is the electrical resistance of the voice coil, C_{MS} is the mechanical compliance of the loudspeaker suspension, M_{MD} is the mechanical mass of the loudspeaker diaphragm and voice coil, and M_{A1} is the acoustical mass of the air load on the front side of the diaphragm given by

Equation (54). The acoustical impedance seen by the back of the loudspeaker Z_{AB} is the acoustical impedance presented by the air load behind the diaphragm.

The circuit of Figure 72 can be used to calculate the volume velocity U_D emitted by the diaphragm for a given electrical voice-coil voltage e_g and back acoustical impedance Z_{AB}. To facilitate this calculation, the Norton acoustical equivalent circuit seen by the impedance Z_{AB} can be formed. This circuit is shown in Figure 73.

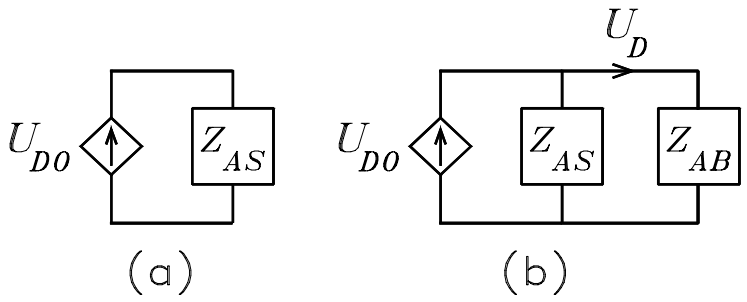

Figure 73. (a) Norton acoustical equivalent circuit with respect to the back air load Z_{AB}. (b) Circuit showing the addition of an arbitrary back load Z_{AB} and the volume velocity emitted from the front of the loudspeaker driver U_D.

The volume velocity U_{D0} in the figure is the volume velocity that flows through Z_{AB} in Figure 72 with $Z_{AB} = 0$. By current division, it is given by

$$U_{D0} = \frac{S_D e_g}{B\ell} \frac{R_{AE}}{Z_{AS}} \tag{263}$$

where Z_{AS} is the total acoustical impedance given by

$$Z_{AS} = j\omega M_{AFS} + R_{AE} + R_{AS} + \frac{1}{j\omega C_{AS}}. \tag{264}$$

The transfer function for the volume velocity U_D emitted by the loudspeaker diaphragm for any arbitrary Z_{AB} can be calculated by applying current division to the circuit of Figure 73(b). The transfer function is given by

$$U_D = U_{D0} \frac{Z_{AS}}{Z_{AS} + Z_{AB}}. \tag{265}$$

For example, the volume velocity of a loudspeaker mounted in an infinite baffle is given by

$$U_D = U_{D0} \frac{Z_{AS}}{Z_{AS} + j\omega M_{A1}} \tag{266}$$

where M_{A1} is the acoustical mass given in Equation (54). When the loudspeaker is mounted on a filled transmission line terminated in an infinite baffle, the volume velocity emitted by the diaphragm is given by

$$U_D = U_{D0} \frac{Z_{AS}}{Z_{AS} + Z_{AT}} \tag{267}$$

where Z_{AT} is the acoustical impedance calculated from Equation (211).

The pressure radiated by a flat circular piston in an infinite baffle at a distance z along its axis is given by

$$p(z) = j\omega\rho_0 U_D \frac{e^{-jkz}}{2\pi z} \tag{268}$$

where U_D is the volume velocity emitted by the piston. For a loudspeaker on an infinite baffle with an arbitrary back acoustical load impedance Z_{AB}, the pressure transfer function can be written

$$p(z) = j\omega\rho_0 U_{D0} \frac{Z_{AS}}{Z_{AS} + Z_{AB}} \frac{e^{-jkz}}{2\pi z}. \tag{269}$$

where U_{D0} is the volume velocity given by Equation 265.

The on-axis pressure sensitivity is given by the magnitude of Equation 269 at a distance $z = 1\,\text{m}$ for an input voltage $e_g = 1\,\text{V}$ rms. It is given by

$$p_{\text{rms}} = \rho_0 f \left| U_{D0} \frac{Z_{AS}}{Z_{AS} + Z_{AB}} \right|. \tag{270}$$

The corresponding sound pressure level is then given by

$$SPL = 20 \log \left(\frac{p_{\text{rms}}}{p_{\text{ref}}} \right) \tag{271}$$

where $p_{\text{ref}} = 2 \times 10^{-5}\,\text{Pa}$. The sound pressure level corresponding to the rms pressure given by Equation (270) is given by

$$\begin{aligned} SPL_{\text{driver}} &= 20 \log \left(\frac{\rho_0 f}{p_{\text{ref}}} \left| \frac{U_{D0} Z_{AS}}{Z_{AS} + Z_{AB}} \right| \right) \\ &= 20 \log \left(\frac{\rho_0 f}{p_{\text{ref}}} \frac{B\ell}{S_D R_E} \frac{1}{|Z_{AS} + Z_{AB}|} \right) \\ &= 20 \log \left(\frac{\rho_0 f}{p_{\text{ref}}} \right) + 20 \log \left(\frac{B\ell}{S_D R_E} \right) - 20 \log |Z_{AS} + Z_{AB}| \end{aligned} \tag{272}$$

where Z_{AB} is chosen appropriately as discussed above.

5.2 The Acoustic Pressure Radiated by the Transmission Line System

The sound pressure level found using Equation (272) with $Z_{AB} = Z_{AT}$ results from the loudspeaker output only. It does not include the output from the open end of the transmission line. The volume velocity emitted from the line combines with that emitted by the loudspeaker to produce the total sound pressure level of the transmission line loudspeaker system. An expression for the total sound pressure level is derived in the following.

The volume velocity emitted from the load end of the tube is equal to the volume velocity given by Equation (198) with $z = 0$. It is

$$\begin{aligned} U_{\text{tube}} &= 2U_{01} + 2U_{02} \\ &= \frac{U_T \gamma_2 M_2}{\gamma_2 M_2 \cosh(\gamma_1 L_T) - \gamma_1 M_1 \coth(\gamma_2 L_T) \sinh(\gamma_1 L_T)} \\ &\quad + \frac{U_T \gamma_1 M_1}{\gamma_1 M_1 \cosh(\gamma_2 L_T) - \gamma_2 M_2 \coth(\gamma_1 L_T) \sinh(\gamma_2 L_T)} \end{aligned} \tag{273}$$

where M_1 and M_2 are given by Equation (210) and U_T is the volume velocity emitted by the loudspeaker into the tube.

This equation can be simplified to obtain

$$U_{\text{tube}} = U_T D \tag{274}$$

where D is given by

$$D = \frac{\gamma_2 M_2 \sinh(\gamma_2 L_T) - \gamma_1 M_1 \sinh(\gamma_1 L_T)}{2\gamma_2 M_2 \sinh(\gamma_2 L_T) \cosh(\gamma_1 L_T) - 2\gamma_1 M_1 \sinh(\gamma_1 L_T) \cosh(\gamma_2 L_T)} \tag{275}$$

If the total volume velocity of the system is measured at a point equidistant from each end of the transmission line, the volume velocities will add in phase. Under this condition, the total volume velocity U_{total}^{TL} of the transmission line system is given by

$$U_{\text{total}}^{TL} = U_D + U_{\text{tube}}. \tag{276}$$

The volume velocity emitted by the loudspeaker into the tube U_T is the negative of the volume velocity emitted outward by the loudspeaker. That is

$$U_T = -U_D. \tag{277}$$

When Equations (274), (276), and (277) are combined, a relationship between the total volume velocity and the loudspeaker volume velocity is obtained. It is given by

$$U_{\text{total}}^{TL} = U_D\,[1 - D]\,. \tag{278}$$

This equation can be solved to obtain a transfer function between the loudspeaker volume velocity and the total volume velocity to obtain

$$\begin{aligned} H_{TL}\,(j\omega) &= \frac{U_{\text{total}}^{TL}}{U_D} \\ &= 1 - D. \end{aligned} \tag{279}$$

From Equation (279), the total volume velocity of the system can be determined if the loudspeaker volume velocity is known. It is given by

$$U_{\text{total}}^{TL} = U_D H_{TL}\,(j\omega)\,. \tag{280}$$

For the simplified transmission line model with the boundary condition that the acoustic pressure at the open end of the line is zero, which is equivalent to setting $Z_{AL} = 0$, U_{tube} is given by

$$\begin{aligned} U_{\text{tube}} &= \frac{U_T}{\cosh(\gamma\, L_T)} \\ &= \frac{-U_D}{\cosh(\gamma\, L_T)}. \end{aligned} \tag{281}$$

In this case, the transfer function $H_{TL}\,(j\omega)$ is given by

$$H_{TL}\,(j\omega) = 1 - \frac{1}{\cosh(\gamma\, L_T)} \tag{282}$$

where γ is the complex propagation constant given in Equation (214). For the general case for an arbitrary load impedance Z_{AL} on the line, the expression for $H_{TL}\,(j\omega)$ is given by

$$H_{TL}\,(j\omega) = 1 - \frac{Z_C}{Z_C \cosh(\gamma\, L_T) + Z_{AL} \sinh(\gamma\, L_T)} \tag{283}$$

where Z_C is the acoustical characteristic impedance of the line given in Equation (213) and Z_{AL} is the acoustical impedance of the external air load.

Thus the total sound pressure level that results from the combination of the tube output and the loudspeaker output together can be written

$$\begin{aligned} SPL_{\text{total}} &= 20\log\left|\frac{\rho_0 f}{p_{\text{ref}}}U_{\text{total}}^{TL}\right| \\ &= 20\log\left|\frac{\rho_0 f}{p_{\text{ref}}}\frac{H_{TL}(j\omega)\,U_{D0}Z_{AS}}{Z_{AS}+Z_{AT}}\right| \end{aligned} \tag{284}$$

where the voice-coil voltage is assumed to be $e_g = 1\,\text{V}$ rms and Z_{AS} is given by Equation (264).

It can be observed that if Z_{AB} in Equation (272) is replaced by the impedance Z_{AQ}^{TL} defined by

$$Z_{AQ}^{TL} = \frac{Z_{AS}+Z_{AT}}{H_{TL}(j\omega)} - Z_{AS}$$

then Equation (272) becomes identical to Equation (284).

Conceptually, the impedance Z_{AQ}^{TL} is a back-load impedance that, when placed on the loudspeaker, causes the loudspeaker volume velocity output to be equal to the total volume velocity output of the transmission line system. It is possible to define other impedances Z_{AQ} that replace Z_{AB} in Equation (284) that cause the sound pressure level predicted by that equation to predict the total sound pressure level output of the infinite-baffle system, the closed-box system, and the vented-box system. These impedances are defined in the following.

5.3 The Acoustic Pressure Radiated by the Alternate Systems

To find expressions for Z_{AQ} for the infinite-baffle, closed-box, and vented-box systems, the low-frequency acoustical analogous circuits [36] shown in Figure 74 are used to solve for the total output volume velocity. In these circuits, it is assumed that the front of the loudspeaker radiates from an infinite baffle so that the front air-load impedance can be modeled by the acoustical mass M_{A1} given in Equation (54).

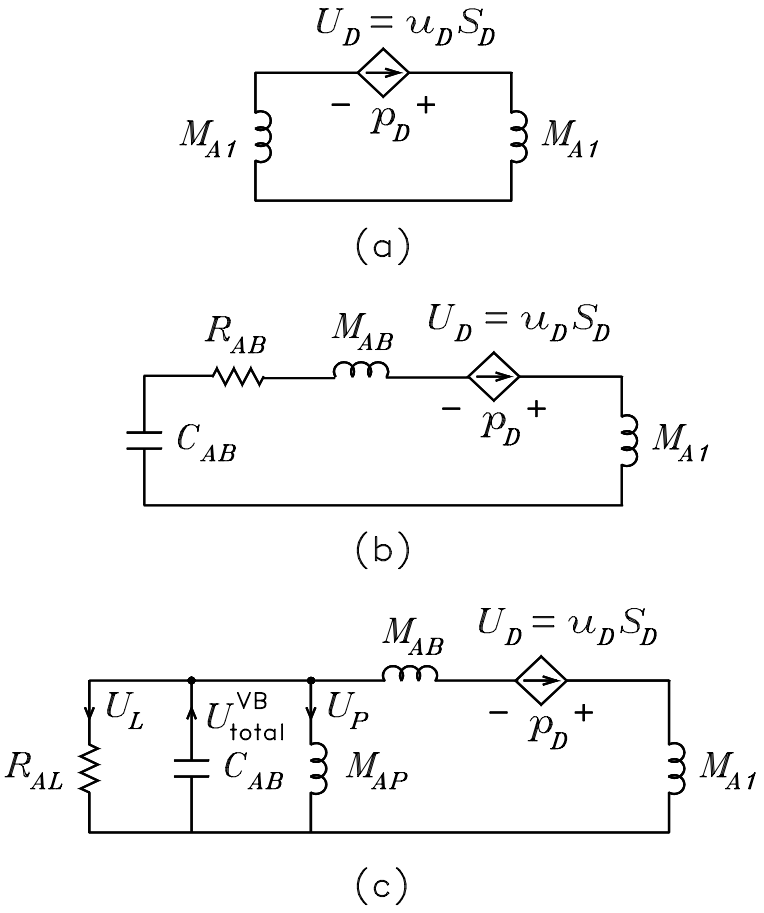

Figure 74. Acoustical analogous circuits of a driver on (a) an infinite baffle, (b) a closed box, and (c) a vented box.

The infinite-baffle circuit in Figure 74(a) shows a back air load modeled by the acoustical mass M_{A1}, which is the same as the front air-load mass. The impedance Z_{AQ}^{IB} corresponds to the back acoustical air-load impedance for the infinite-baffle system and is given by

$$Z_{AQ}^{IB} = j\omega M_{A1}. \tag{285}$$

When this impedance replaces Z_{AB} in Equation (284), sound pressure level predicted by that equation to predict the total sound pressure level output of the infinite-baffle system.

The closed-box circuit in Figure 74(b) shows a back air load modeled by the series circuit elements M_{AB}, R_{AB}, and C_{AB}. The acoustical mass M_{AB} is the equivalent acoustical mass of the air load in the box, the acoustical compliance C_{AB} is the acoustical compliance of the air in the box, and the acoustical resistor R_{AB} models losses in the box. The impedance Z_{AQ}^{CB} corresponds to the back acoustical air-load impedance for the closed-box system and is given by

$$Z_{AQ}^{CB} = j\omega M_{AB} + R_{AB} + \frac{1}{j\omega C_{AB}}. \tag{286}$$

When this impedance replaces Z_{AB} in Equation (284), sound pressure level predicted by that equation to predict the total sound pressure level output of the closed-box system.

For the vented-box system in Figure 74(c), M_{AB} and C_{AB} represent the same quantities as in the figure for the closed box, M_{AP} is the acoustical mass of air in the port or the vent, and the acoustical resistor R_{AL} models air leaks in the system. It follows from the figure that the acoustical impedance presented to the back of the loudspeaker diaphragm is given by

$$Z_{AB}^{VB} = j\omega M_{AB} + (j\omega M_{AP}) \,\|\, R_{AL} \,\|\, \frac{1}{j\omega C_{AB}}. \tag{287}$$

In Figure 74(c), the volume velocity U_P is that emitted by the port and the volume velocity U_L is that emitted by the air leaks. The total volume velocity emitted by the system is

$$U_{\text{total}}^{VB} = U_D + U_P + U_L$$

which is the volume velocity that flows through the acoustical compliance C_{AB} in the figure. By current division, it follows from the figure that U_{total}^{VB} is given by

$$U_{\text{total}}^{VB} = U_D \frac{R_{AL} \| (j\omega M_{AP})}{R_{AL} \| (j\omega M_{AP}) + (j\omega C_{AB})^{-1}}. \tag{288}$$

Thus the transfer function for the total volume velocity output is given by

$$\begin{aligned} H_{VB}(j\omega) &= \frac{U_{\text{total}}^{VB}}{U_D} \\ &= \frac{R_{AL} \| (j\omega M_{AP})}{R_{AL} \| (j\omega M_{AP}) + (j\omega C_{AB})^{-1}}. \end{aligned} \tag{289}$$

This transfer function appears in the impedance Z_{AQ}^{VB} described above. It follows that Z_{AQ}^{VB} is given by

$$Z_{AQ}^{VB} = \frac{Z_{AS} + Z_{AB}^{VB}}{H_{VB}(j\omega)} - Z_{AS}.$$

When this impedance replaces Z_{AB} in Equation (272), that equation can be used to predict the total sound pressure level output of the vented-box system.

5.4 Modeled System Outputs

For reference, Equation (272) is repeated below with Z_{AB} replaced with Z_{AQ} as discussed above.

$$SPL_{\text{total}} = 20\log(f) + 20\log\left(\frac{\rho_0}{2\pi}\frac{B\ell}{S_D R_E}\right) - 20\log\left|Z_{AS} + Z_{AQ}\right|. \tag{290}$$

The total sound pressure level output of a system can be calculated with the aid of this equation after Z_{AQ} is replaced with any of the four acoustical impedances Z_{AQ}^{TL}, Z_{AQ}^{IB}, Z_{AQ}^{CB}, or Z_{AQ}^{VB} defined above. Note that the first term in this equation is independent of the loudspeaker system. The second term is dependent on the driver alone. The third term is dependent on both the driver and the system in which it is used. The acoustical impedance Z_{AS} is defined in Equation (264).

Figures 75 through 79 show plots of the system sound pressure level calculated from Equation (290) for the six-inch test loudspeaker having the parameters given in Table 1 on

transmission lines of length $L_T = 925\,\text{mm}$ and radius $a_T = 75\,\text{mm}$ for packing densities $P_D = 2.6$, 5.2, 7.9, 10.5, and 14.2 $\text{kg}\,\text{m}^{-3}$. The sound pressure outputs of the loudspeaker diaphragm only and the tube only are also shown plotted. In addition, plotted on each graph is the response of the loudspeaker on an infinite baffle so that the transmission line system responses can be compared to this reference response. It can be seen that the infinite-baffle system gives the best low-frequency response for all cases. It can be concluded that each one of these figures seems to contradict much of the "conventional wisdom" concerning the transmission-line loudspeaker system. The performance of a different driver in a transmission line system is investigated in the next section where the transmission line system response is compared to that of the infinite baffle system, the closed-box system, and the vented-box system.

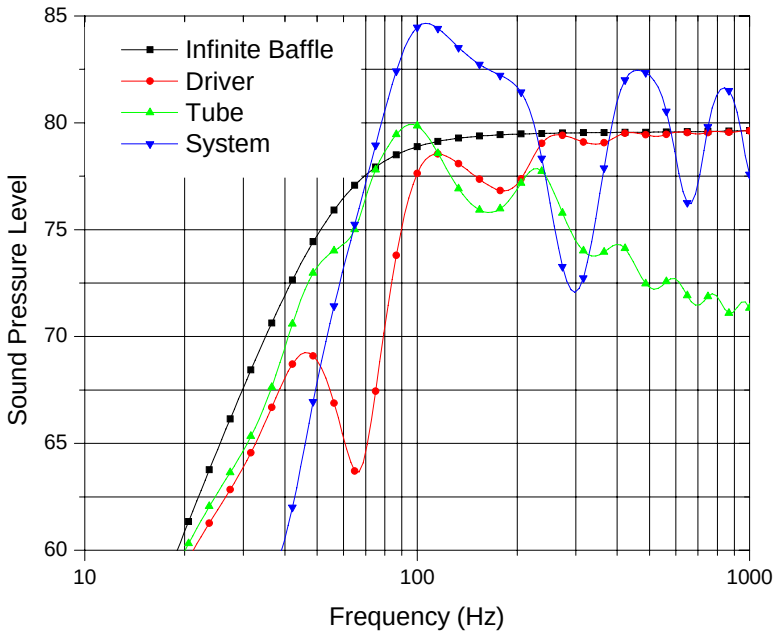

Figure 75. Comparison of SPL for driver on an infinite baffle to that of driver on the transmission line for a packing density of $P_D = 2.6\,\text{kg}\,\text{m}^{-3}$.

For the smallest packing density, the -3 dB frequency of the transmission line system is close to that of the infinite baffle, but a large 13 dB variation in the pass-band is present in the transmission line system. As the packing density is increased, the magnitude of the

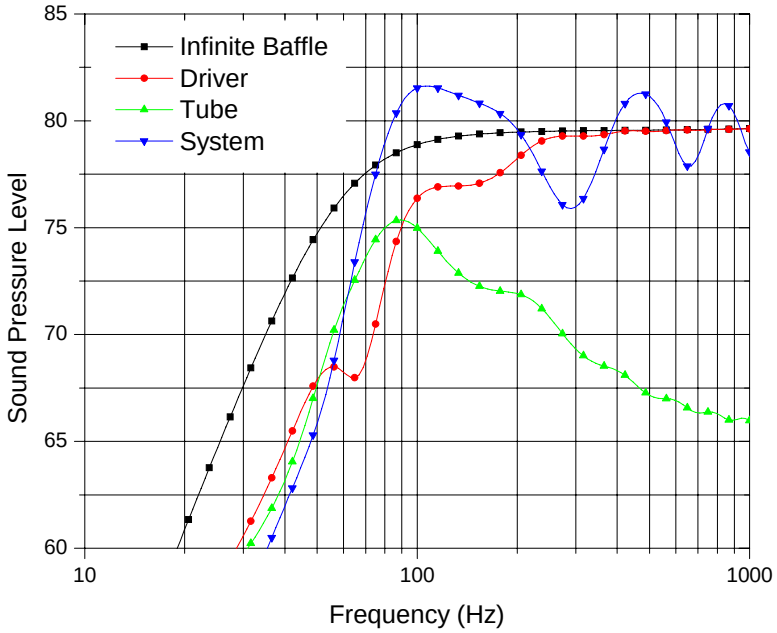

Figure 76. Comparison of SPL for driver on an infinite baffle to that of driver on the transmission line for a packing density of $P_D = 5.2\,\mathrm{kg\,m^{-3}}$.

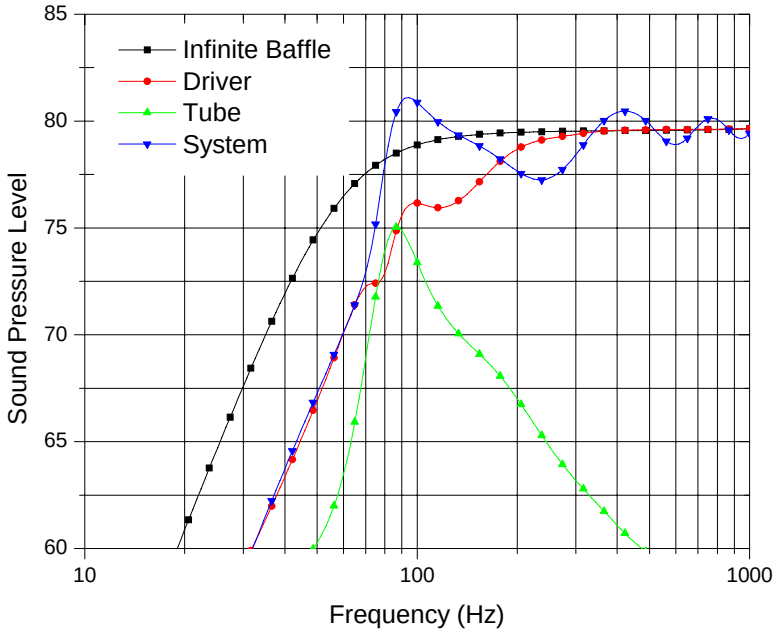

Figure 77. Comparison of SPL for driver on an infinite baffle to that of driver on the transmission line for a packing density of $P_D = 8.5\,\mathrm{kg\,m^{-3}}$.

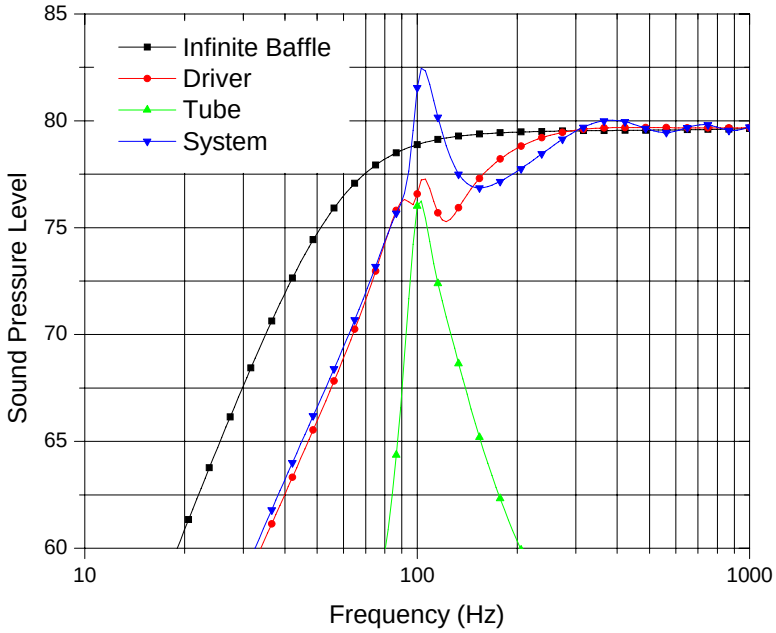

Figure 78. Comparison of SPL for driver on an infinite baffle to that of driver on the transmission line for a packing density of $P_D = 11.3\,\mathrm{kg\,m^{-3}}$.

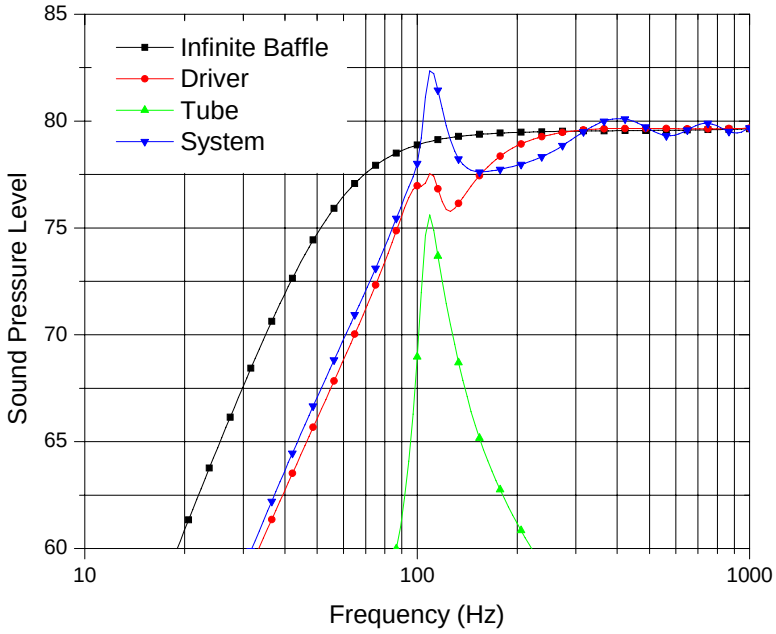

Figure 79. Comparison of SPL for driver on an infinite baffle to that of driver on the transmission line for a packing density of $P_D = 14.2\,\mathrm{kg\,m^{-3}}$.

pass-band ripple decreases, but the -3 dB frequency increases as the load on the loudspeaker increases. It can be seen for this loudspeaker on this length of transmission line that the system response is never better than that of the infinite baffle. The tube output does provide a boost in bass frequencies, but it also introduces an undesirable null that can be deep.

For packing densities greater than $P_D = 5.7\,\mathrm{kg\,m^{-3}}$, the reflections from the open end of the line are damped and do not appear as ripples in the loudspeaker diaphragm output as they do in the plots for lower packing densities. Only near the fiber resonance, where the damping is reduced, do the reflections have an effect. The ripples in the pass-band result from phase differences between the tube and loudspeaker outputs.

Figure 80 shows the responses for $P_D = 7.9\,\mathrm{kg\,m^{-3}}$ for the special case of stationary fibers, which is the assumption that Augspurger made in deriving his model. When the fibers do not move, the tube output is smaller in magnitude and broader. The bass frequency boost is thus smaller and the large variations in the pass-band are reduced. This figure can be compared to Figure 77 which is based on the model derived in this work where fiber motion is accounted for.

The system sound pressure level in the above figures is calculated from Equation (290) with $Z_{AQ} = Z_{AQ}^{TL}$. There are three terms in Equation (290). The frequency dependent first term is not a function of the loudspeaker driver or the loudspeaker system. The second term is a function of the loudspeaker driver only. For a given loudspeaker driver, only the third term is a function of the transmission line and its filling. The parameters in this term can be manipulated to investigate the change in these parameters on the system response. The overall shape of the system sound pressure level is, for the most part, determined by the last term. The first term increases the slope of the sound pressure level plot by adding $+20$ dB per decade to the slope of the plot when it is plotted versus frequency on a log frequency axis. The second term adds a vertical offset to the sound pressure level curve. Thus changes in the system parameters can be investigated by examining only the last term.

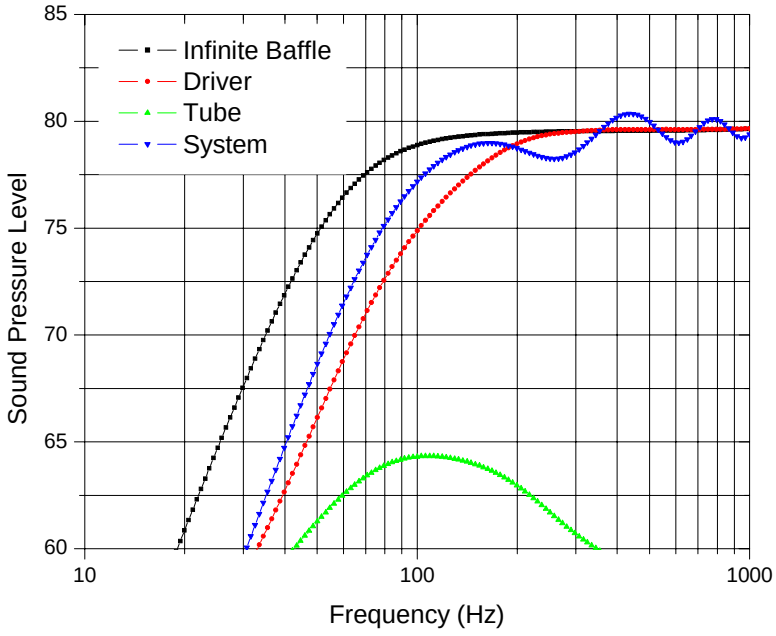

Figure 80. System sound pressure level for transmission line with stationary fibers and $P_D = 7.9\,\mathrm{kg\,m^{-3}}$.

Figure 81 contains a number of plots that illustrate the relationships between the system impedances and the system outputs. The figure shows a plot of $20\log\left|Z_{AS}+Z_{AQ}\right|$ for the loudspeaker mounted both in an infinite baffle and on the transmission line for $P_D = 8.50\,\mathrm{kg\,m^{-3}}$. The frequency at which the minimum of this load-dependent term occurs can be directly related to the extent of the system low-frequency response. When this term is combined with the other terms of Equation (290), the portions of the curve to the right of the minima translate into the pass-band regions of the system sound pressure level curves. The portions to the left of the minima translate into the cutoff regions of the system sound pressure level curves.

The graphs also show the acoustical output of each system. It can be seen from the figure that there is a close relationship between the $20\log\left|Z_{AS}+Z_{AQ}\right|$ term and the system sound pressure level. The shape of the output sound pressure level is the inverted and rotated $20\log\left|Z_{AS}+Z_{AQ}\right|$ term. The shape of the output of any system is determined by the magnitude of the complex sum of the acoustical loudspeaker impedance Z_{AS} and the

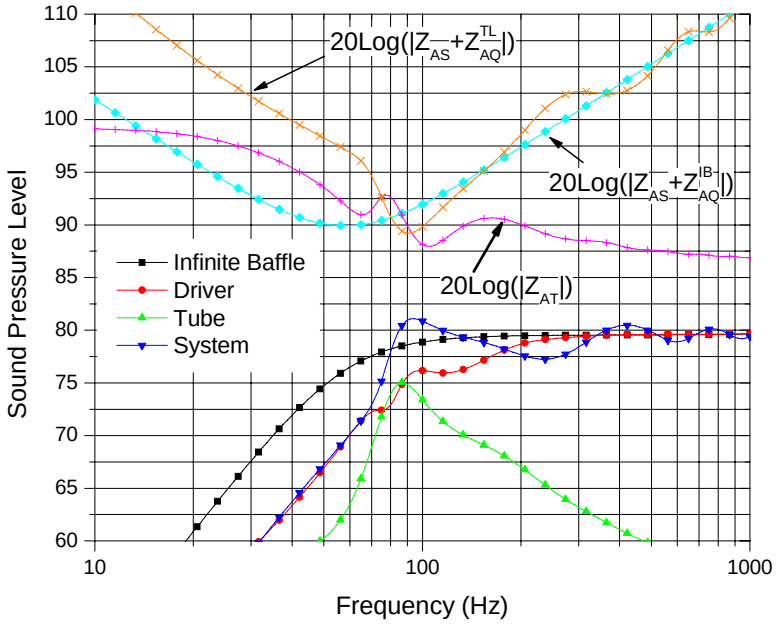

Figure 81. Relationship between system impedances and sound pressure levels.

acoustical loudspeaker load impedance Z_{AQ}. The shape of the transmission line system output can be seen to result from the inverted and rotated $20\log\left|Z_{AS}+Z_{AQ}^{IB}\right|$ term. The output of the driver on the transmission line results from the $20\log|Z_{AS}+Z_{AT}|$ term. This "rotation" is the result of the $20\log(f)$ term in Equation (290), which adds a slope of one decade per decade to the inverted impedance term.

The inverted infinite baffle impedance $\left(20\log\left|Z_{AS}+Z_{AQ}^{IB}\right|\right)^{-1}$ has asymptotic slopes of $+1$ decade per decade for frequencies to the left of the maximum and -1 decade per decade for frequencies to the right of the maximum. When a slope of $+1$ is added to it, the infinite baffle sound pressure level response is obtained, where the response has a slope of $+2$ decades/decade below the cutoff frequency and a slope of 0 above the cutoff frequency.

When the line input impedance $20\log|Z_{AT}|$ curve lies above that of the infinite baffle curve, the loudspeaker output on the transmission line is reduced from that of the loudspeaker on an infinite baffle. However, it is still possible to improve the system response by including the tube output. To achieve a transmission line system that is an improvement over the infinite baffle system, the plot of $20\log\left|Z_{AS}+Z_{AQ}^{TL}\right|$ must cross the plot of

Table 4. Parameter values for CTS 12W54C twelve inch driver.

M_{AD}	R_{AS}	C_{AS}	$B\ell$	a_D	R_E	L_e	n_e	L_{E2}
31.1	1977	8.055×10^{-7}	16.0	0.1275	5.3	0.0539	0.6079	0.00582

$20\log\left|Z_{AS}+Z_{AQ}^{IB}\right|$ to the left of the minimum of $20\log\left|Z_{AS}+Z_{AQ}^{IB}\right|$. For the case shown in Figure 81, the $20\log\left|Z_{AS}+Z_{AQ}^{TL}\right|$ curve crosses the $20\log\left|Z_{AS}+Z_{AQ}^{IB}\right|$ curve to the right of the minimum, and the transmission line system has a significantly higher -3 dB frequency than does the infinite-baffle system.

5.5 Comparisons of System with a Given Driver

The design of a transmission line system having a line of constant line area involves choosing the loudspeaker, the packing density of the fiberglass, the length of the line, and the diameter of the line. For a given loudspeaker, only the line characteristics must be determined.

In Section 5.4, it is shown that the system response of the six-inch test loudspeaker on a 925 mm long tube of radius 7.5 cm for any packing density is never better than the response of the loudspeaker on an infinite baffle. In an attempt to design an acceptable system, the length, diameter, and packing density of the modeled system are varied and their effects are observed on a plot like that of Figure 81. As an example, a system designed around a loudspeaker manufactured by CTS having the parameters given in Table 4 is investigated.

The simplified transmission line model is used along with the empirical expressions of Sections 4.4.4 and 4.4.5 to determine the line input impedance. Equation (290) is used to generate the sound pressure level curves. Figures 82 through 90 show a plots of the system sound pressure level for three tube lengths and three fiberglass packing densities. For each graph, the tube radius is equal to the loudspeaker diaphragm radius of $a_D = 127.5$ mm. Also on each graph are plots of the same loudspeaker on a closed box, a vented box, and an infinite baffle. The closed and vented box systems were designed [36] for Butterworth alignments.

Figures 91 through 93 directly compare the system sound pressure levels for each line length for different values of packing density. It can be seen that for all line lengths, an increase in packing density reduces the amplitude of the variations in the passband, but it also increases the lower -3 dB frequency for the two larger line lengths. There is no change in the lower -3 dB frequency for the shortest line, because the frequency of the tube output maximum occurs well above the -3 dB frequency of the driver output. Thus, in this case, the system -3 dB frequency is determined by the driver alone.

For the tube of length $L_T = 1\,\text{m}$, the frequency of the tube output maximum is too large, so there is no improvement of the system -3 dB frequency over that of the other systems. This frequency is greater than the -3 dB frequency of the driver, so the driver output is large. This causes a large peak when the tube and driver outputs combine to form the system output. For the $L_T = 3\,\text{m}$ tube, the frequency of the tube output maximum is too low. It occurs where the driver output is rolling off, so the system response, while improved slightly over that of the other systems, is not optimal. The tube length of $L_T = 2\,\text{m}$ is nearly optimal. This length causes the tube output maximum to be near the -3 dB frequency of the driver. For this tube length, the lowest packing density gives the best low-frequency response of the system. However, there is a large minimum in the response. If this configuration were used as a subwoofer for frequencies below approximately 100 Hz, this minimum would be of no consequence.

The size of the transmission line loudspeaker systems compared to that of the other systems should be noted. The closed-box system and the vented-box system have enclosure volumes of $0.8\,\text{ft}^3$ and $1.7\,\text{ft}^3$, respectively. The $L_T = 2\,\text{m}$ transmission line system has a volume of $3.6\,\text{ft}^3$.

In determining the values for P_D, L_T, and S_T from the model, the line diameter is first set to the diameter of the loudspeaker. Then, P_D and L_T are adjusted to obtain an acceptable response. Changes in S_T can also be investigated by varying the tube radius, but the model was derived assuming that the tube and driver had the same diameter. An

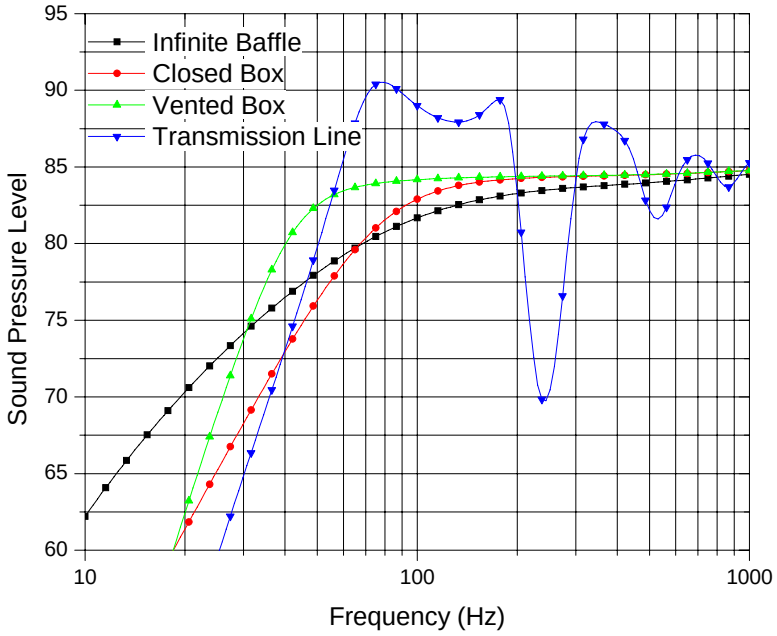

Figure 82. Comparison of system designs for $L_T = 1\,\mathrm{m}$ and $P_D = 1\,\mathrm{kg\,m^{-3}}$.

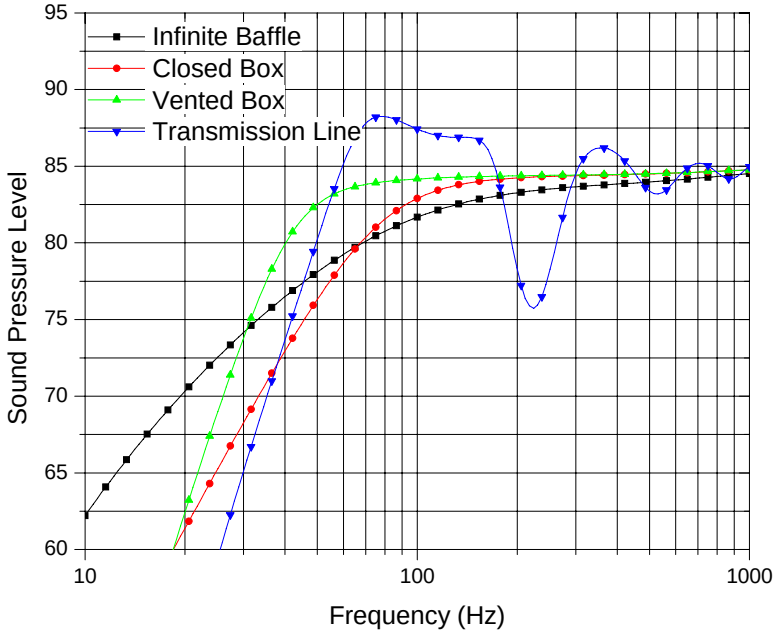

Figure 83. Comparison of system designs for $L_T = 1\,\mathrm{m}$ and $P_D = 4\,\mathrm{kg\,m^{-3}}$.

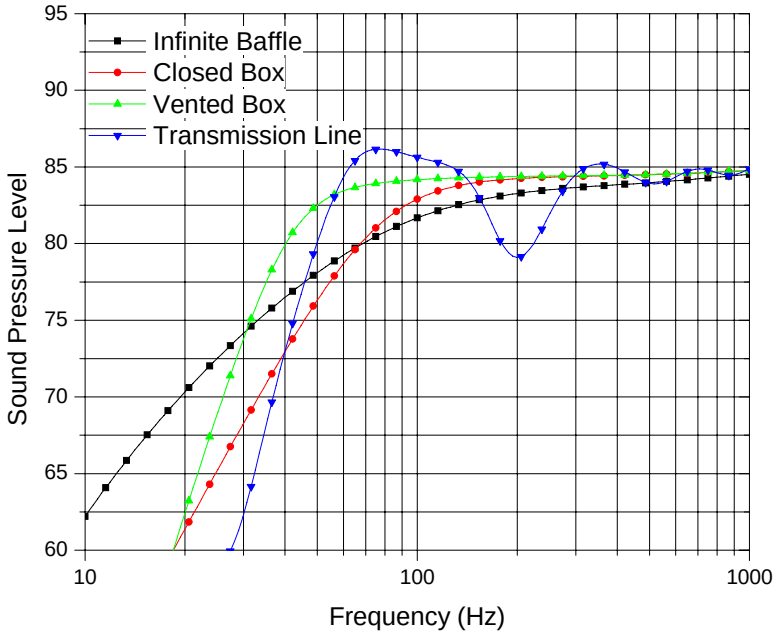

Figure 84. Comparison of system designs for $L_T = 1\,\mathrm{m}$ and $P_D = 8\,\mathrm{kg\,m^{-3}}$.

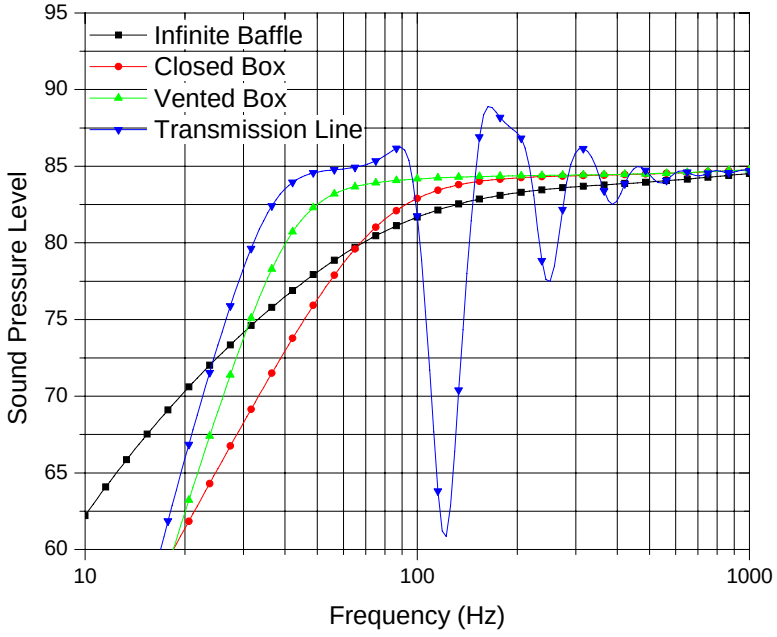

Figure 85. Comparison of system designs for $L_T = 2\,\mathrm{m}$ and $P_D = 1\,\mathrm{kg\,m^{-3}}$.

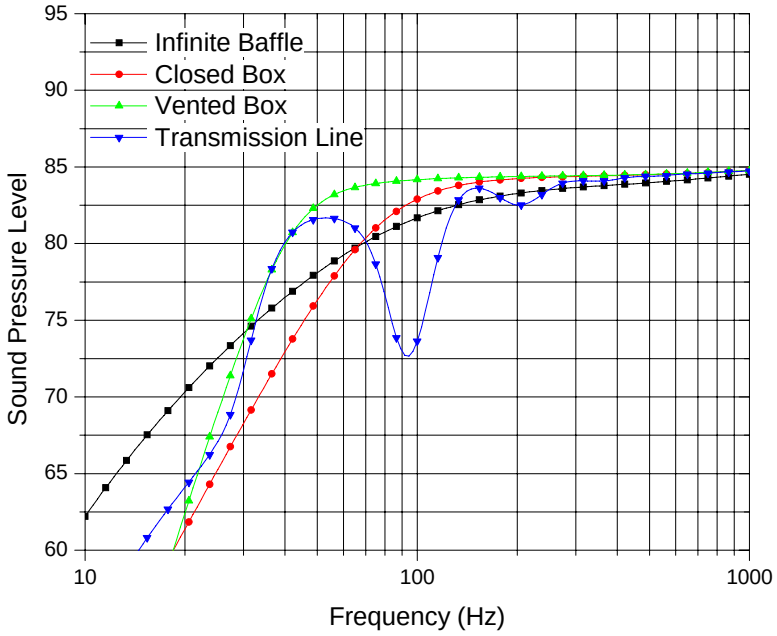

Figure 86. Comparison of system designs for $L_T = 2\,\mathrm{m}$ and $P_D = 4\,\mathrm{kg\,m^{-3}}$.

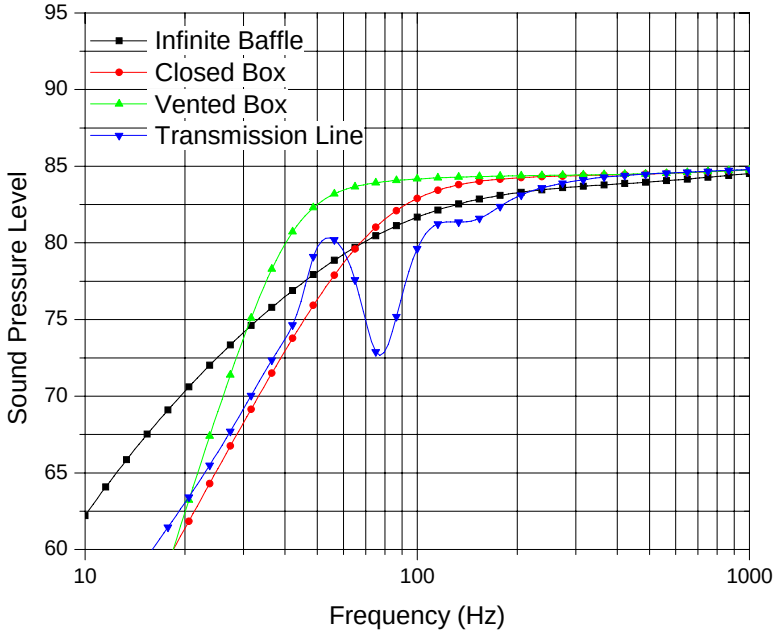

Figure 87. Comparison of system designs for $L_T = 2\,\mathrm{m}$ and $P_D = 8\,\mathrm{kg\,m^{-3}}$.

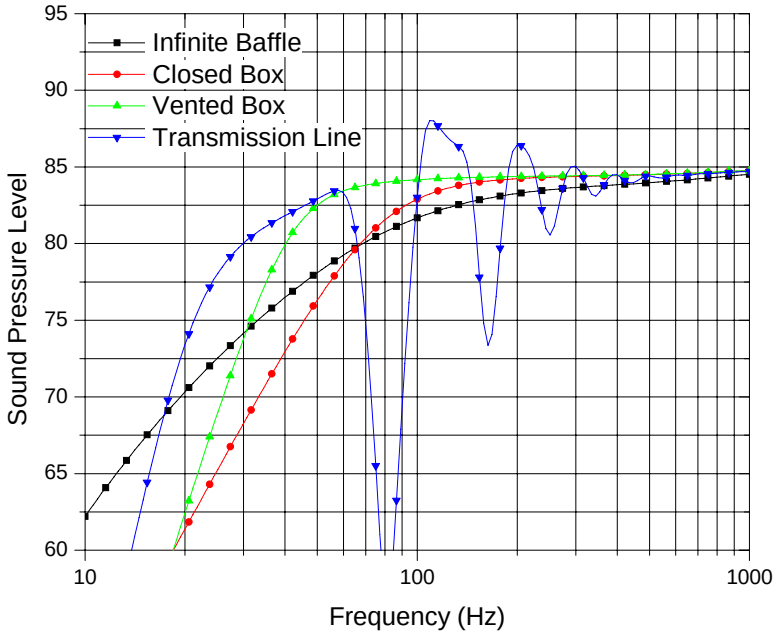

Figure 88. Comparison of system designs for $L_T = 3\,\mathrm{m}$ and $P_D = 1\,\mathrm{kg\,m^{-3}}$.

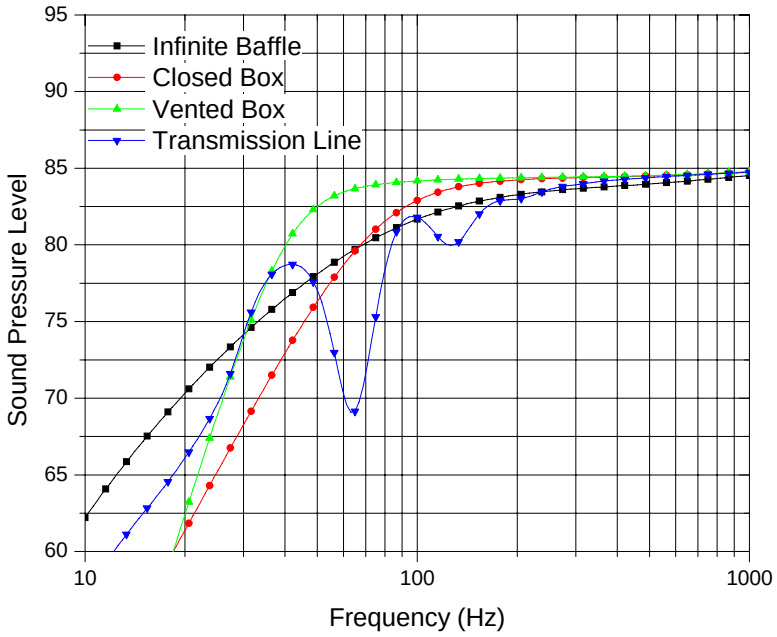

Figure 89. Comparison of system designs for $L_T = 3\,\mathrm{m}$ and $P_D = 4\,\mathrm{kg\,m^{-3}}$.

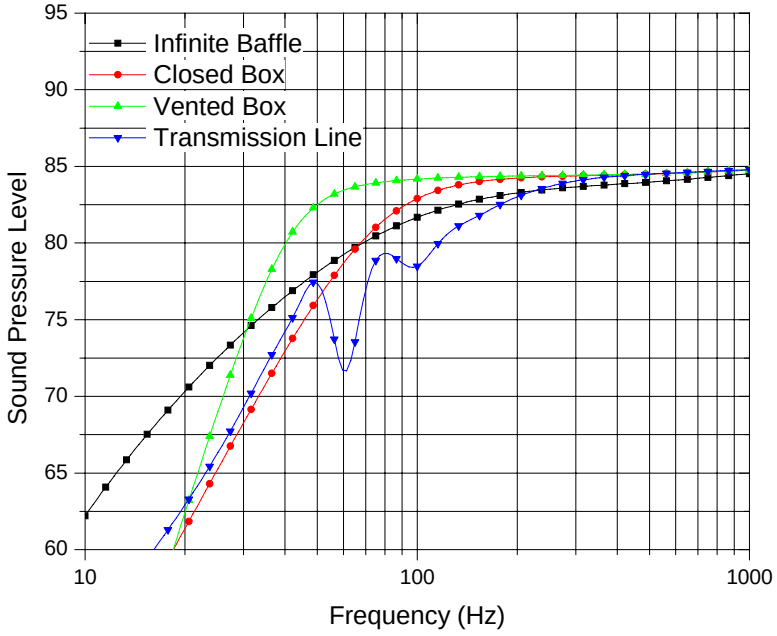

Figure 90. Comparison of system designs for $L_T = 3\,\mathrm{m}$ and $P_D = 8\,\mathrm{kg\,m^{-3}}$.

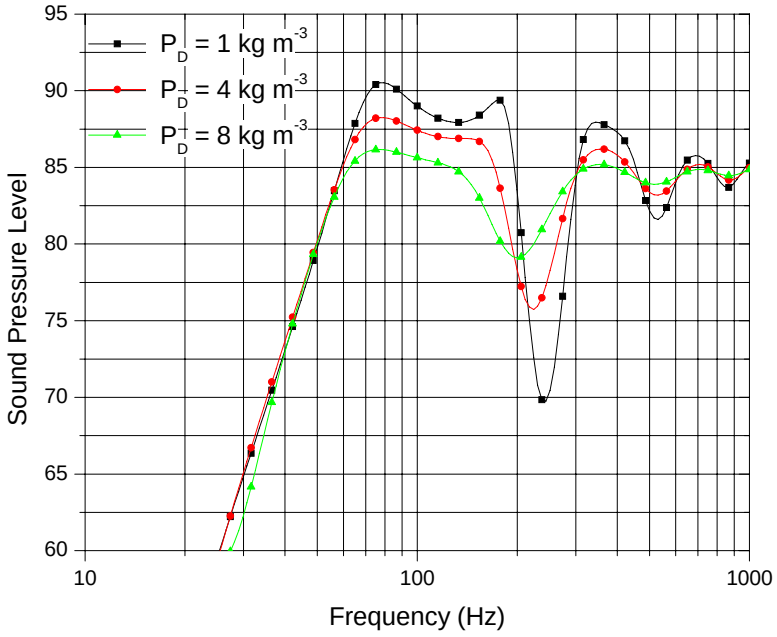

Figure 91. Variation in system sound pressure level with changes in packing density for the $L_T = 1\,\mathrm{m}$ tube.

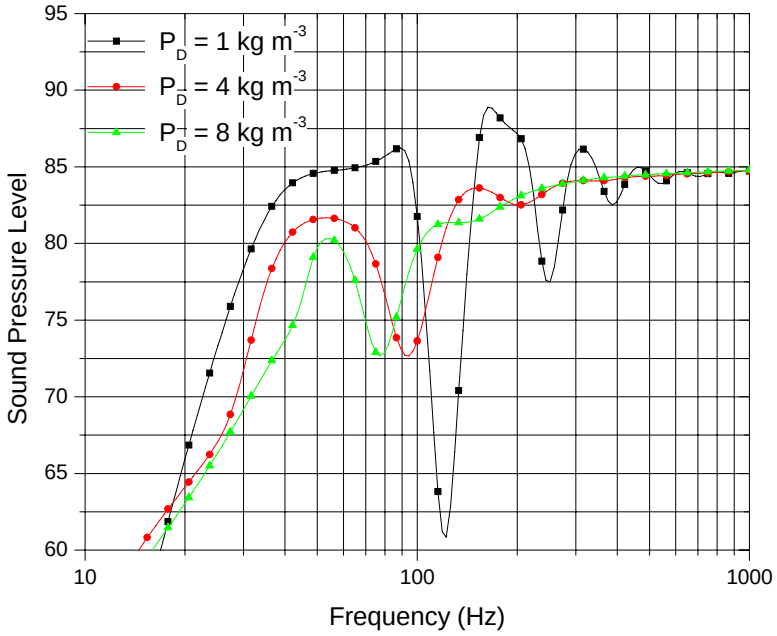

Figure 92. Variation in system sound pressure level with changes in packing density for the $L_T = 2\,\mathrm{m}$ tube.

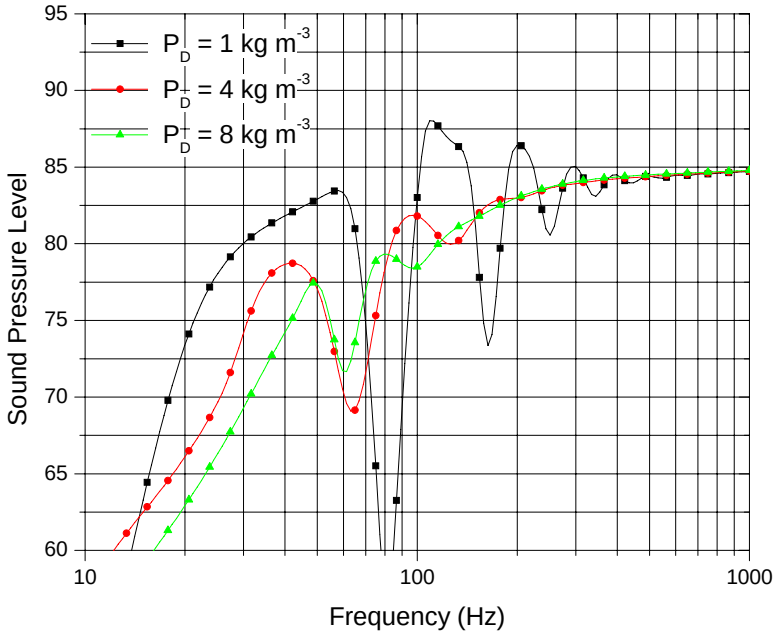

Figure 93. Variation in system sound pressure level with changes in packing density for the $L_T = 3\,\mathrm{m}$ tube.

increase in P_D results in a more distinct tube output peak, but its level is decreased because of the fiber attenuation. An increase in P_D also dampens reflections, which decreases the ripples in the loudspeaker output. A decrease in P_D results in a broad tube output with numerous ripples that result from reflections and more distinct minima in the loudspeaker output. The choice of P_D is a trade off between tube output level and passband ripple.

Decreasing the tube length decreases the peak output frequency of the tube and the frequency of the quarter-wavelength minimum in the loudspeaker output. It also increases the tube output, because there is less distance over which the fibers can attenuate the sound wave. As the frequency of the tube output maximum is decreased by increasing the line length, the system response is improved until the boost from the tube output cannot compensate for the decrease in loudspeaker output as the frequency decreases.

CHAPTER 6

CONCLUSIONS

It has been shown that a fiber-filled acoustical transmission line in transmission line loudspeakers can be modeled by two separate lines, a mechanical line and an acoustical line. The mechanical line models the mechanical motion of the fibers and the acoustical line models the motion of the air. The two lines are linked by the acoustical flow resistance that models the aerodynamic drag on the fibers caused by the air flow in the acoustical wave.

The model derived from this representation has an exact solution that includes the effects of fiberglass motion. Solutions for the system output can be readily calculated. In addition, the circuit models that are developed can be analyzed with very powerful electrical circuit analysis computer programs such as SPICE. If the coupling among fibers is neglected, a simplified model results that gives good agreement to measured data. This model is believed to be an improvement over Augspurger's model described above. His model is composed of a finite number of lumped-element resistor, inductor, and capacitor (RLC) sections that must be analyzed with circuit simulation software. A major problem with his model is that he does not give empirical or analytical expressions for all of the line parameters. From the experimental data taken in this research, it has been found that a fiberglass filling does not behave as Bailey and Bradbury believed that long-fibered wool behaved in their model of the transmission line loudspeaker. It has been found in this research that the coupling among fiberglass fibers and the air flow at low frequencies is determined by a mechanical resonance phenomenon. The model derived here simplifies to either Augspurger's model or Bradbury's model if certain assumptions are made. However, neither Augspurger's model or Bradbury's model agrees well with the measured data presented here.

The empirical formulas for the line parameters given in Sections 4.4.4 and 4.4.5 allow the design of a fiberglass-filled line to be evaluated by adjusting three parameters: the

line length, the line diameter, and the fiber packing density. In further applications, more detailed experimental data is required to better characterize the fiberglass and its associated parameters over a wider range of tube diameters and packing densities. The empirical equation obtained for the flow resistance has the same form as those given in [9], [16], and [14]. By varying the line length, the line diameter, and the fiber packing density, the effects of each parameter on sound pressure level radiated by the driver, the tube, and system can be easily studied using mathematical software. The evaluation can also be performed with electrical circuit simulator software.

In addition to modeling the simple transmission line system that has the loudspeaker mounted at one end of the line, the model can be adapted to model two other popular types of transmission line systems. By placing a transmission line load on both the front and back sides of the loudspeaker, a transmission line system having a recessed loudspeaker can be analyzed. An acoustical compliance in parallel with the line can be used to model a coupling chamber between the loudspeaker and the line. It is believed that the model can be extended to account for tapered or flared lines by using techniques found in [38] that apply to acoustical horns.

APPENDIX A

APWIN IMPEDANCE MEASUREMENT PROCEDURE

The control procedure for the Audio Precision System Two is given below.

```
'procedure name: Zin.apb
'purpose: To measure the loudspeaker impedance curve
Dim Ro As Double                          'Generator resistance
Dim Vgen As Double                        'Specified open circuit generator voltage
Dim Size As Integer                       'Number of measurement steps
Dim Zm()                                  'Measured impedance magnitude
Dim Zp()                                  'Measured impedance phase
Dim f                                     'Sweep Frequency
Dim L As String
Const Pi = 3.14159265359
Const R = Pi/180
Const D = 180/Pi
Sub Main
    AP.Application.NewTest
    Ro = 40                               'Generator resistance
    Vgen = 1.0                            'Open circuit generator voltage
    'InitializeSettings                   'Initialize settings when not using test file
    AP.File.OpenTest("zinml2.at2")        'Open System Two test
    AP.Sweep.CreateTable = True
    AP.Sweep.CreateGraph = True
    InputFilename
    ObtainData
    CalculateImpedance
```

```
    DisplayResults
    SaveData
End Sub
Sub InitializeSettings
    AP.Application.Page = 1
    AP.Application.PanelOpen apbPanelAnalogGenLarge
    AP.Application.PanelOpen apbPanelAnlrLarge
    AP.Gen.ChAAmpl("Vrms") = Vgen
    AP.Gen.Freq("Hz") = 20
    AP.Gen.Config = 0                          'Set to 0 for balanced floating
    AP.Gen.Impedance = 0                       'Set to 0 for 40 ohms balanced floating
    AP.Gen.ChBTrackA = True
    AP.Anlr.ChAInput = 2                                    'Set to GenMon
    AP.Anlr.ChBInput = 2                                    'Set to GenMon
    AP.Application.Page = 2
    AP.Application.PanelOpen apbPanelSweepSmall
    AP.Sweep.Data1.Id = 5903          'Set data column 1 to be Analyzer Amplitude
    AP.Sweep.Data1.LogLin = 0                               'Log y-axis
    AP.Sweep.Data1.Top("V") = 60
    AP.Sweep.Data1.Bottom("V") = 0.001
    AP.Sweep.Data1.Autoscale = True
    AP.Sweep.Data2.Id = 5905                   'Set data column 2 to be Vp
    AP.Sweep.Data2.Top("deg") = 90
    AP.Sweep.Data2.Bottom("deg") = -90
    AP.Sweep.Data2.Autoscale = True
    AP.Sweep.Data3.Id = 5904   'Set data column 3 to be measured generator voltage
    AP.Sweep.Source1.Id = 5051                 'Source 1 = Generator Frequency
```

```
    AP.Sweep.Source1.Start("Hz") = 20.0
    AP.Sweep.Source1.Stop("Hz") = 20000.0
    AP.Sweep.Source1.Steps = Size
    AP.Sweep.Data4.Id = 5901          'Set data column 4 to be measured frequency
    AP.Sweep.CreateTable = True
    AP.Sweep.CreateGraph = False
End Sub
Sub ObtainData
    AP.Gen.ChAAmpl("Vrms") = Vgen
    AP.Gen.Output = True
    AP.Anlr.FuncInput = 1
    AP.Anlr.ChBInput = 2                          'Set ch B input to Genmon
    Vgen = AP.Anlr.FuncRdg("V")                   'Read rms generator voltage
    AP.Sweep.Start
    AP.Gen.Freq("Hz") = 20
End Sub
Sub CalculateImpedance
    Vm = AP.Data.XferToArray(0, 1, "V")     'Assign sweep data to array variables
    Vp = AP.Data.XferToArray(0, 2, "deg")
    Vg = AP.Data.XferToArray(0, 3, "V")
    f = AP.Data.XferToArray(0, 4, "Hz")
    Size = AP.Sweep.Source1.Steps             'Set array length to number of steps
    ReDim Zm(Size)                                'defined by test (.at2) file
    ReDim Zp(Size)
    Dim K As Double
    For i = 0 To Size Step 1                      'Calculate magnitude and phase
        K = Vg(i)/Vm(i)
```

```
            P = Vp(i)*R
            C = Cos(P)
            S = Sin(P)
            Zp(i) = -D*Atn(K*S/(K*C-1))  'Minus sign added to make phase referenced
to Vg
            Zm(i) = Ro/Sqr((K*C-1)^2+(K*S)^2)
        Next i
    End Sub
    Sub DisplayResults
        AP.Data.XferToArray(0, 1, "V") = Zm          'Load Zm into first data column
        AP.Data.XferToArray(0, 2, "deg") = Zp        'Load Zp into second data column
        AP.Sweep.Data3.Id = 5049
        AP.Sweep.Data4.Id = 5049
        AP.Graph.OptimizeIndividually                'Optimize the graph
        'AP.Data.UpdateDisplay(0)                    'Show updated impedance curve
    End Sub
    Sub SaveData
    Open L$ For Output As #1
    Print #1, Date;" ";Time
    Print #1,"Vgen = ";Format(Vgen,"000.000");" Vrms"
    Print #1,"Frequency";Chr$(9);"Magnitude";Chr$(9);" Phase"
        For i = 0 To Size Step 1
            If Zp(i) < 0 Then
                Print #1,Format(f(i),"00000.00000");Chr$(9);
    Format(Zm(i),"000.00000");Chr$(9);Format(Zp(i),"00.00000")          'linewrap
            Else
                Print #1,Format(f(i),"00000.00000");Chr$(9);
```

```
Format(Zm(i),"000.00000"); Chr$(9);" ";Format(Zp(i),"00.00000")          'linewrap
        End If
    Next i
Close #1
End Sub
Sub InputFilename
    Do
    L$ = InputBox$("Enter a filename (without an extension)
for saving your impedance data:", _ "Zin Filename","ZinBox")              'linewrap
        If L$ = "" Then
            Begin Dialog UserDialog 200,120
                Text 10,10,180,15,"You must enter a filename."
                OKButton 80,90,40,20
            End Dialog
            Dim dlg As UserDialog
            Dialog dlg                                  'show dialog (wait for ok)
        End If
Loop Until L <> ""
L$ = "C:\ImpedanceCurves\" & L$ & ".txt"                'Set location of saved data
End Sub
```

REFERENCES

[1] B. Olney, "A method of eliminating cavity resonance, extending low frequency response and increasing acoustical damping in cabinet type loudspeakers," *J. Acoust. Soc. Amer.*, vol. 8, October 1936.

[2] R. Schultz, "Alpha transmission lines," *AudioXpress*, pp. 34-45, August 2003.

[3] R. H. Small, "Direct-radiator loudspeaker system analysis," *J. Audio Eng. Soc.*, vol. 20, pp. 383-395, June 1972.

[4] R. H. Small, "Closed-box loudspeaker systems, parts I and II," *J. Audio Eng. Soc.*, vol. 20, pp. 798-808, Dec. 1972; vol. 21, pp. 11-18, Jan./Feb. 1973.

[5] R. H. Small, "Vented-box loudspeaker systems, parts I-IV," *J. Audio Eng. Soc.*, vol. 21, pp. 363-372, June 1973; pp. 438-444, July/Aug. 1973; pp. 549-554, Sept. 1973; pp. 635-639, Oct. 1973.

[6] A. N. Thiele, "Loudspeakers in vented boxes, parts I and II," *J. Audio Eng. Soc.*, vol 19, pp. 382-392, May 1971; pp. 471-483, June 1971.

[7] A. R. Bailey, "A non-resonant loudspeaker enclosure," *Wireless World*, October 1965.

[8] A. R. Bailey, "The transmission line loudspeaker enclosure," *Wireless World*, May 1972.

[9] L. J. S. Bradbury, "The use of fibrous materials in loudspeaker enclosures," *J. Audio Eng. Soc.*, pp. 390-398, Apr. 1976.

[10] G. L. Augspurger, "Loudspeakers on damped pipes," *J. Audio Eng. Soc.*, vol. 48, pp. 424-436, May 2000.

[11] B. N. Locanthi, "Application of electric circuit analogies to loudspeaker design problems," *J. Audio Eng. Soc.*, vol 19, pp. 778-785, Oct. 1971.

[12] R. H. Nichols, Jr., "Flow-resistance characteristics of fibrous acoustical materials," *J. Acoust. Soc. Amer.*, vol. 19, pp. 866-871, Sep. 1947.

[13] V. Tarnow, "Airflow resistivity of models of fibrous acoustical materials," *J. Acoust. Soc. Amer.*, vol. 100, pp. 3706-3713, Dec. 1996.

[14] D. A. Bies and C. H. Hansen, "Flow resistance information for acoustical design," *Appl. Acoust.*, vol. 13, pp 357-361, 1980.

[15] L. L. Beranek, *Noise and Vibration Control*, New York: McGraw-Hill, 1971.

[16] M. Garai and F. Pompoli, "A simple empirical model of polyester fibre materials for acoustical applications," *Appl. Acoust.*, vol. 66, pp. 1383-1398, 2005.

[17] C. Zwikker and C. W. Kosten, *Sound Absorbing Materials*, Amsterdam: Elsevier, 1949.

[18] M. A. Biot, "Theory of propagation of elastic waves in a fluid-saturated porous solid. I. Low frequency range," *J. Acoust. Soc. Amer.*, vol. 28, pp. 168–178, 1956.

[19] M. A. Biot, "Theory of propagation of elastic waves in a fluid-saturated porous solid. II. Higher frequency range," *J. Acoust. Soc. Amer.*, vol. 28, pp. 179–191, 1956.

[20] V. Tarnow, "Fiber movements and sound attenuation in glass wool," *J. Acoust. Soc. Amer.*, vol. 105, pp. 234-240, Jan. 1999.

[21] J. F. Allard, C. Depollier, P. Guignouard, and P. Rebillard, "Effect of a resonance of the frame on the surface impedance of glass wool of high density and stiffness," *J. Acoust. Soc. Amer.*, vol. 89, pp. 999-1001, 1991.

[22] R. F. Lambert, "The acoustical structure of highly porous open-cell foam," *J. Acoust. Soc. Amer.*, vol. 72, pp. 879–887, 1982.

[23] R. F. Lambert and J. S. Tesar, "Acoustic structure and propagation in highly porous, layered, fibrous materials," *J. Acoust. Soc. Amer.*, vol. 76, pp. 1231–1237, 1984.

[24] V. Tarnow, "Calculation of the dynamic air flow resistivity of fiber materials," *J. Acoust. Soc. Amer.*, vol. 102, pp. 1680-1688, May. 1997.

[25] K. Attenborough, "Acoustical characteristics of rigid fibrous adsorbents," *J. Acoust. Soc. Amer.*, vol. 73, pp. 785–799, 1983.

[26] W. M. Leach, Jr., "Loudspeaker voice-coil inductance losses: circuit models, parameter estimation, and effect on frequency response," *J. Audio Eng. Soc.*, vol. 50, no. 6, pp. 442-450, June 2002.

[27] L. L. Beranek, *Acoustics*, New York: McGraw-Hill, 1954.

[28] F. V. Hunt, *Electroacoustics*, Am. Inst. of Physics for the Acoust. Soc. Am., 1982.

[29] B. B. Bauer, "On the equivalent circuit of a plane wave confronting an acoustical device," *J. Acoust. Soc. Amer. (Letter to the Editor)*, vol. 42, pp. 1095-1097, Nov. 1967.; reprinted in *J. Audio Eng. Soc.*, vol. 24, pp. 653-654, Oct. 1976.

[30] R. A. Dobbins and S. Temkin, "Propagation of sound in a gas-particle mixture," *AIAA J.*, vol. 5, no. 12, 1967.

[31] Audio Precision, Inc., *APWIN System Two User's Manual*, Beaverton, Oregon: Audio Precision, Inc., 1999.

[32] Audio Precision, Inc., Tech Note TN-1A: "Generating impedance vs frequency plots with APWIN," *Audio Precision Tech Notes*, Audio Precision, Inc., 1998.

[33] K. Levenberg, "A method for the solution of certain problems in least squares," *Quart. Appl. Math., vol.* 2, pp. 164-168, 1944.

[34] D. Marquardt, "An algorithm for least-squares estimation of nonlinear parameters," *SIAM J. Appl. Math.*, vol. 11, pp. 431-441, 1963.

[35] Phillip M. Morse and K. Uno Ingard, *Theoretical Acoustics*, New York: McGraw-Hill, 1968.

[36] W. M. Leach, Jr., *Introduction to Electroacoustics and Audio Amplifier Design*, Dubuque, Iowa: Kendall/Hunt, 2001.

[37] W. M. Leach, Jr., "Electroacoustical-analogous circuit models for filled enclosures," *J. Audio Eng. Soc.*, vol. 37, no. 7/8, pp. 586-592, July/Aug. 1989.

[38] W. M. Leach, Jr., "A two-port analogous circuit and SPICE model for Salmon's family of acoustical horns," *J. Acoust. Soc. Amer.*, vol. 99, pp. 1459-1464, Mar. 1996.